THE AMIDATION OF VASCULAR PROTEINS BY NOREPINEPHRINE

By

Kyle B. Johnson

A DISSERTATION

Submitted to
Michigan State University
in partial fulfillment of the requirements
for the degree of

DOCTOR OF PHILOSOPHY

Biochemistry and Molecular Biology

2012

ABSTRACT

THE AMIDATION OF VASCULAR PROTEINS BY NOREPINEPHRINE

By

Kyle B. Johnson

Norepinephrine (NE) is a biogenic monoamine that plays an integral role in the homeostatic maintenance of blood pressure as a neurotransmitter of the sympathetic nervous system. In certain disease states, such as hypertension, sympathetic output is altered. Therefore understanding all the mechanisms by which NE may regulate function is important. Recently, a novel way that monoamines can signal for physiological effect has been described: the transglutaminase (TG)-mediated, covalent modification of proteins by monoamines. Vascular proteins modified in such a manner by serotonin can elicit biologically relevent effects, such as vascular smooth muscle cell (VSMC) migration, growth, and contraction. In these studies, we hypothesized that NE can also serve as a TG substrate, and that the TG-mediated NE-amidation of proteins signaled for a physiologically relevant, biological effect in the vasculature, such as vascular contraction, or VSMC migration and proliferation. We investigated this hypothesis in rat aorta (RA) and vena cava (RVC) tissues.

We found that both RA and RVC tissues express multiple TGs. Moreover, we found that at least two of these TGs, namely TG1 and TG2, were active in the VSMCs of these tissues. These TGs were able to incorporate NE into vascular proteins, as visualized with a NE-biotin conjugate. This incorporation was sensitive to the TG inhibitor cystamine, suggesting that this was a TG-dependent event. Furthermore, NE-

biotin could be competed off with cold, unbiotinylated NE, suggesting that NE and NE-biotin were handled by TGs in a similar fashion. TG protein expression appeared to be downregulated in cell culture. As an intracellular source of NE is necessary for NE-amidation of proteins to occur, we investigated a mechanism by which NE may gain entry into VSMCs. We found that RA and RVC VSMCs expressed the organic cation transporter 3 (OCT3)—a monoamine transporter capable of transporting NE—on their cell surface. The canonical transporter of NE, NET, did not appear to be expressed by VSMCs. Furthermore, in whole RA tissues, NE uptake was found to be sensitive to OCT3 inhibition. Although we also measured NE uptake in the RVC, we were not able to block its uptake with any of the inhibitors used. Interestingly, OCT3 expression and NE uptake appeared to be downregulated in VSMC cultures.

To understand the role the NE-amidation of proteins plays in vascular function, potential NE-amidation substrates were identified with mass-spectrometry and NE-biotin. Several candidate substrates, such as several small GTPases and cytoskeletal proteins such as α-actin, were identified. Confirmation that α-actin served as a TG substrate was done with immunoprecipitation.

We investigated the role that NE-amidation of proteins plays in vascular contraction. The TG inhibitor cystamine inhibited and eventually abolished NE-induced contraction in the RA and the RVC. RVC tissues seemed to be more sensitive to this inhibition. Contraction to the non-receptor mediated contractant, was slightly reduced at concentrations of cystamine that abolished NE-induced contraction. Taken together, these results suggest that the NE-amidation of proteins occurs in the vascular, and may be important in NE-induced contraction.

ACKNOWLEDGEMENTS

It only takes a spark to get a fire going. I would like to acknowledge those people responsible for that spark, as well as those who helped fan the flame.

I would like to start by thanking my parents and family. Mom, Dad, Rachel, Tyler, Tracey, Ryan, Kelly, Paisley, Jaiya, Addysen, Zooey, and Charlotte: I love you. Thank you for molding me into the person I am today.

I would like to thank all my science teachers for instilling in me a fascination with the intricacies of the natural world, and a desire to understand it. Special thanks must go out to Mr. Mueller, my high school chemistry teacher, who both challenged and encouraged me to pursue a scientific career. I would not be here if not for you. To all of my professors at Concordia University, Nebraska, who helped me grow as a citizen and scientist: Dr. J. and K. Jurchen, Dr. Gubanyi, Dr. Hermann, Dr. Royuk, Dr. Herl, Dr. Whitson, and Dr. Callahan. I would like to especially thank Dr. Kregg Einspahr, who is perhaps more responsible for where I am today than anyone else. You were responsible for drawing me to Concordia, getting me my first research position, and played an absolutely essential role in guiding me to graduate school. You have served me as a coach, mentor, professor, and friend. I look forward to soon being able to also call you, and the rest of the faculty at Concordia, a colleague.

I would like to thank Dr. Gautam Sarath, who gave me my first opportunity to work in a lab and introduced to me the world of protein modifications in the form of endogenously biotinylated histones. Additionally, I would like to thank the IN-BRE program for giving me this opportunity.

I would like to thank Michigan State University and the Department of Biochemistry for giving me this opportunity. I am especially grateful for my committee members, Dr. John Wang—who also served me as a liaison when I first contacted MSU about coming for graduate school—Dr. Eric Hegg, who I was fortunate to serve as a teaching assistant and who helped me grow as a teacher—Dr. Zachary Burton, and Dr. John LaPres. You have provided me with valuable feedback that has strengthened and refined my research. Also thank you to the proteomic core, and especially Doug Whitten and Dr. Curtis Wilkerson, who helped me design, run, and interpret my mass-spectrometry experiments.

I am grateful to Department of Pharmacology and Toxicology for letting me work in one of your laboratories. Especially, I am thankful to the members of the PPG and Dr. Dorrance, who have provided me both with guidance and means to perform research.

I would like to thank those with which I collaborated with, namely Dr. Erik Bakker, Dr. Gail Johnson, and Dr. “Kiyo” Hitomi, for the insight and materials they provided.

To the members of the Watt’s lab, especially Janice, Humphrey, Nate, Theo, Patrick, Robert, Cris, Bridget, and Jessie: Thank you all. I couldn’t have done this without you.

Finally, I would like to thank my mentor, Dr. Stephanie Watts. To list all the things that she has done for me would fill another dissertation-sized document. You have helped me grow as a scientist and as a person. There is no way that I could ever hope to repay you for what you’ve done for me. Thank you: I am better for having known you.

TABLE OF CONTENTS

LIST OF TABLES

LIST OF FIGURES

LIST OF ABBREVIATIONS

5-HT	5-hydroxytrytophan; serotonin
ADU	Arbitrary densitometry unit
ALDH	Aldehyde dehydrogenase
ALR	Aldehyde reductase
B2m	β2-microglubulin
BAP	5-(Biotinamido)pentylamine
BCA	Bicinchoninic acid
BSA	Bovine serum albumin
CEO	Chick egg ovalbumin
COMT	Catechol-O-methyltransferase
Cort	Corticosterone
DAB	3,3'-Diaminobenzidine
DAPI	4',6-diamidino-2-phenylindole
DAT	Dopamine transporter
DHMA	3,4-dihydroxymandelic acid

DHPG	3,4-dihydroxyphenolglycol
DTT	Dithiothreitol
FXIII	Factor XIII
HRP	Horseradish peroxidase
IB	Immunoblot
ICC	Immunocytochemistry
IHC	Immunohistochemistry
IP	Immunoprecipitation
KO	Knock out
L-DOPA	L-3,4,-dihydroxyphenylalanine
MA	Mouse aorta
MAO	Monoamine oxidase
MHPG	3-methoxy-4-hydroxy phenylglycol
NE	Norepinephrine
NET	Norepinephrine transporter
Nis	Nisoxetine
OCT	Organic cation transporter

PE	Phenylephrine
PMAT	Plasma membrane monoamine transporter
PNMT	Phenylethanolamine N-methyltransferase
PSS	Physiological salt solution
PVDF	Polyvinylidene difluoride
RA	Rat aorta
Rac1	Ras related 3-botulinum toxin substrate 1
RhoA	Ras homolog gene family, member A
RVC	Rat vena cava
SERT	Serotonin transporter
TBS	Tris-buffered saline
TBST	Tris-buffered saline plus 1% Tween
TG	Transglutaminase
TIG3	Tazarotene-induced gene 3
TRITC	Tetramethyl rhodamine iso-thiocyanate
UCAR	University Committee of Animal Research
VMA	Vanillylmandelic acid

VSMC	Vascular smooth muscle cell
WT	Wild type

Chapter 1: Introduction

1. Norepinephrine

The primary amine norepinephrine (NE) is a member of the organic compounds known as catecholamines. NE mediates a number of physiological functions throughout the body, including perhaps its best known action as one of the stress hormones that act in the “flight or fight” response to increase heart rate, trigger the release of glucose from energy stores, and increase blood flow to skeletal muscles. NE also serves as a neurotransmitter of the sympathetic nervous system, acting in the vasculature to regulate vascular tone. In vascular tissues, NE also stimulates the migration (197) and mitogenesis (191) of vascular smooth muscle cells (VSMCs). This function is most obviously observed *in vitro*; however *in vivo*, VSMC migration and proliferation contributes to neointimal formation (196) and vascular hypertrophy induced by mechanical injury (50), and can stimulate flow-mediated arterial wall remodeling as well (51).

The importance of studying NE’s function in the vasculature is illustrated in a number of vascular disease states. An alteration of sympathetic nervous system activity is observed in several models of hypertension (92, 113). Additionally, in human essential hypertension, an increase in sympathetic nervous system activity is commonly seen (65), suggesting that manipulating NE signaling in the vasculature may result in therapeutic gain. In this thesis I describe a novel signaling mechanism that NE may use to regulate vascular function. Although understanding this mechanism may eventually lead to novel therapeutic strategies, the characterization of this mechanism in disease

states and development of interventional treatments is beyond the scope of these studies.

1.1. NE signaling and metabolism

NE is synthesized from the amino acid tyrosine through a number of enzymatic steps that culminate in the addition of a hydroxyl group to dopamine (**Figure 1**). In nerve terminals, NE is then packed into presynaptic vesicles at very high concentrations (i.e., 100 mM) (163). Classically, NE signaling begins with its release from presynaptic nerve terminals (**Figure 2**). NE rapidly diffuses within the synapse, reaching a concentration of 200-300 μM (164). Binding to low affinity sites can then bring the concentration down to ≤10 μM, concentrations considered within the biological "active" range (164). NE within the intracellular space interacts with post-synaptic adrenergic receptors, which transmit this signal to the inside of the cell leading to a signaling cascade and resulting in a physiological response. Adrenergic receptors are a class of G protein-coupled receptors that were first divided into two main groups based on their excitatory or inhibitory effects in the vasculature: The vasoconstrictive effects of the catecholamines NE and epinephrine are mediated through their interactions with α-adrenergic receptors, while their vasodilatory effects are mediated through their interactions with β-adrenergic receptors (4). In addition to post-synaptic adrenergic receptors, presynaptic adrenergic receptors exist as well, with NE's interaction with them acting as a mechanism for feedback inhibition (99).

Termination of NE's signal requires its removal from the synaptic cleft, either by passive diffusion throughout the extracellular space or via active transport back into a cell. Two uptake systems responsible for the clearance of extracellular monoamines

such as NE have been described: neuronal reuptake ($uptake_1$) and steroid-sensitive, nonneuronal uptake ($uptake_2$) (84). While monoamine transport via $uptake_1$ is mediated through high affinity transporters for dopamine (DAT), serotonin (SERT), and NE (NET), the low affinity, but high capacity, $uptake_2$ system relies on members of the amphiphilic solute facilitator family of transport proteins [organic cation transporter 1 (OCT1) (24), OCT2 (59), and OCT3 (60)], as well as the plasma membrane monoamine transporter (PMAT) (44). Of the OCTs, OCT3, also known as the extraneuronal monoamine transporter, is often viewed as the primary transporter of the $uptake_2$ system due to its widespread expression (199) and much greater efficiency in transporting catecholamines and serotonin (5-hydroxytryptamine; 5-HT) (153). Less is known about PMAT, as it has only been described relatively recently compared to the OCT family of monoamine transporters (49). Although NE has similar affinity for OCT3 and PMAT (K_m: ~920 and ~1080 μM, respectively), OCT3 transports NE faster due to a larger V_{max} (OCT3 = ~30,000; PMAT = ~9,000 pmol*mg $protein^{-1}$*min^{-1}) (44). Thus, many view OCT3 as the most likely candidate for non-NET mediated NE uptake.

Traditionally, NE taken up into cells is thought to await one of two fates. A portion of the NE taken up into adrenergic neurons is recycled into presynaptic vesicles to be reused. Alternatively, NE may be metabolized into noremetanephrine via catechol-o-methyl transferase (COMT), or into NE aldehyde via monoamine oxidase (MAO). Normetanephrine and NE aldehyde can be converted into normetanephrine aldehyde by MAO and COMT, respectively; NE aldehyde and normetanephrine aldehyde are

further metabolized into the final metabolites of NE catabolism by aldehyde reductase or aldehyde dehydrogenase (104) (**Figure 3**). In the central nervous system, the primary metabolite of NE metabolism is 3-methoxy-4-hydroxy phenylglycol; in the peripheral sympathetic nervous system, normetanephrine and vanillylmandelic acid are the two end products that predominate (106). In these studies, however, we propose a possible third fate for NE imported into the cell.

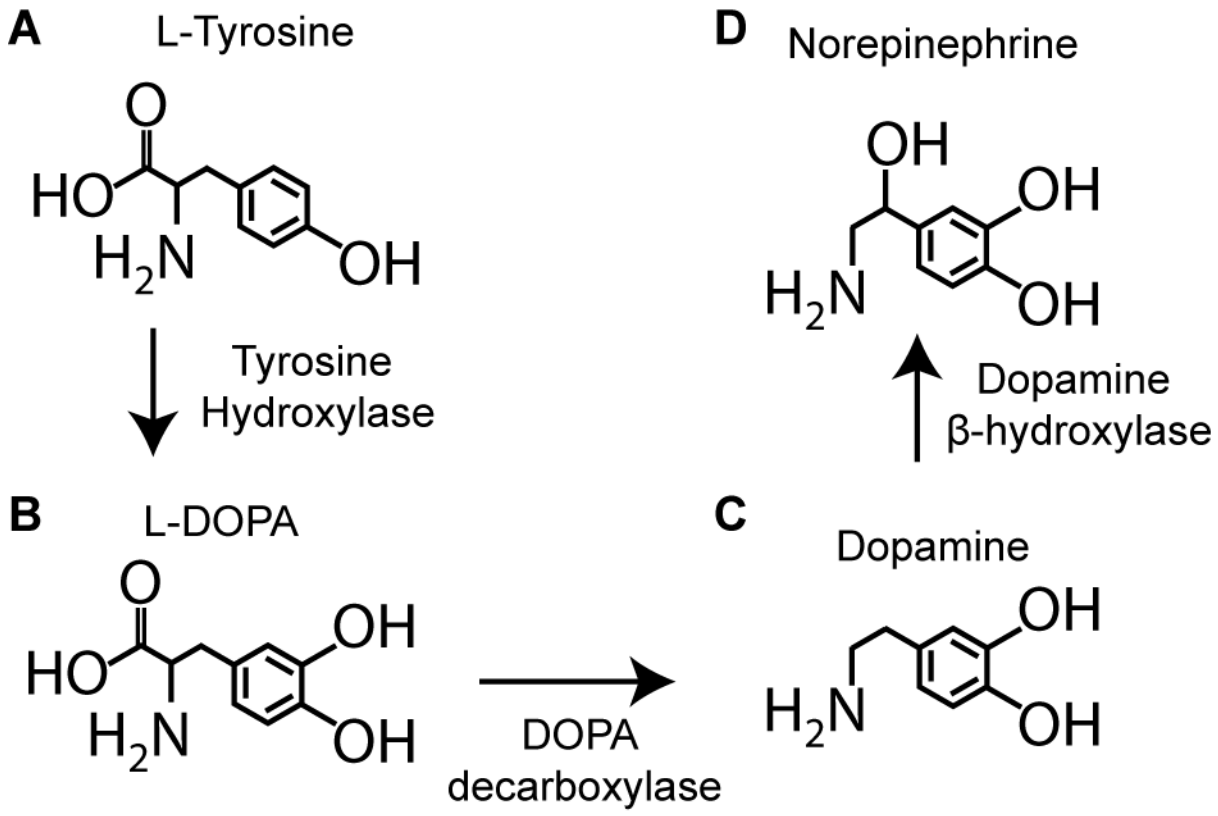

Figure 1. NE synthetic pathway.

Sympathetic neurons—and other NE synthesizing cells—manufacture NE beginning from the amino acid tyrosine (**A**). The first step of NE synthesis involves the hydroxylation of tyrosine (catalyzed by tyrosine hydroxylase) to L-3,4-dihydroxyphenylalanine (L-DOPA) (**B**). L-DOPA, in turn, is converted into dopamine (**C**) by the enzyme DOPA decarboxylase. Finally, dopamine β-hydroxylase converts dopamine to NE (**D**).

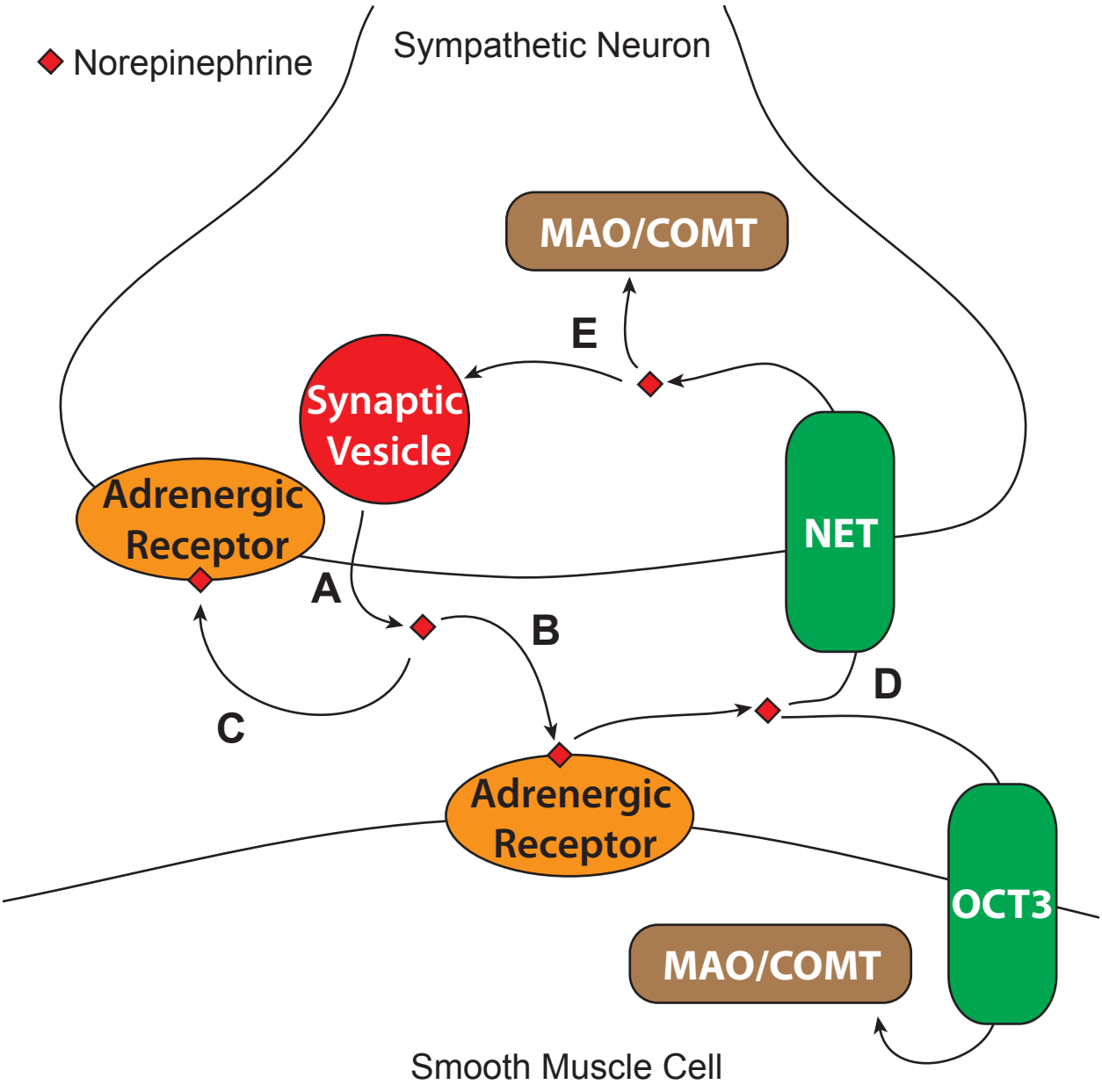

Figure 2. Classical NE signaling.

The canonical pathway for NE signaling is shown. **A**) NE (red diamond), synthesized in synaptic vesicles, is released. **B**) NE in the synaptic cleft interacts with post-synaptic adrenergic receptors, which transmits the signal into the cell. **C**) NE can also interact

Figure 2 (cont'd)

with pre-synaptic adrenergic receptors, acting as a feedback inhibition signal to stop further NE release. **D**) The signal of NE is silenced by its removal from the synaptic space, either by diffusion, or through reuptake into the cell via specific NE transporters, such as NET or OCT3. **E**) NE taken up into the cell can either be metabolized or repackaged into vesicles for recycling. **For the interpretation of colors in this and all other figures, the reader is directed to the electronic version of this dissertation**.

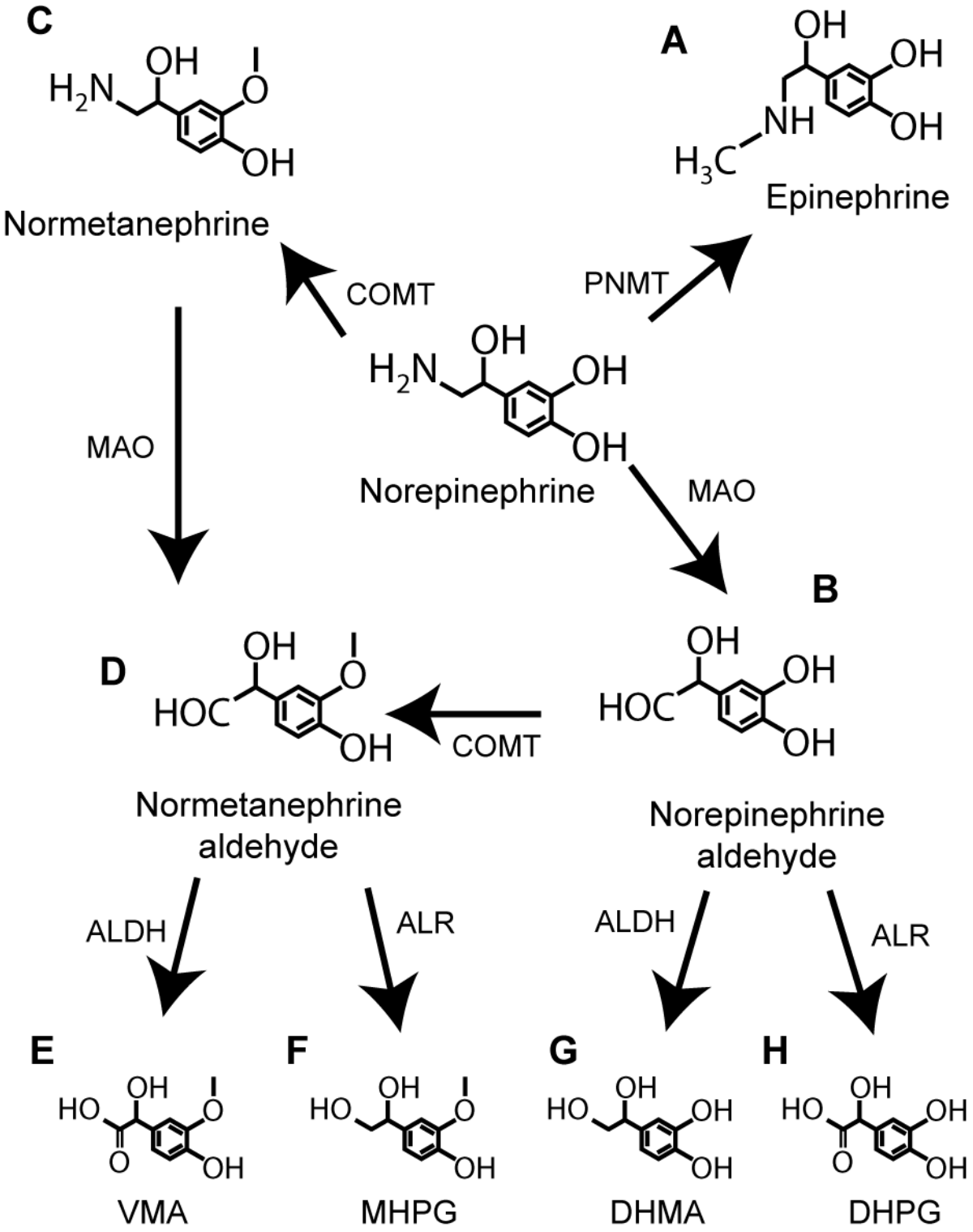

Figure 3. NE metabolism.

Figure 3 (cont'd)

NE can be metabolized in many ways. **A**) NE can be metabolized into epinephrine via phenylethanolamine N-methyltransferase (PNMT). Epinephrine can then act as a signaling molecule itself. **B**) NE metabolized via monoamine oxidase (MAO) is converted to NE aldehyde. **C**) NE can also be metabolized via catechol-O-methyltransferase (COMT) to normetanephrine. **D**) Normetanephrine (via MAO) can be subsequently metabolized to normetanephrine aldehyde. NE aldehyde may undergo further catalysis by aldehyde reductase (ALR) or aldehyde dehydrogenase (ALDH), or may be converted to normetanephrine aldehyde via COMT. The final steps of NE metabolism involve normetanephrine aldehyde metabolism to vanillylmandelic acid (VMA; via ALDH) or 3-methoxy-4-hydroxy phenylglycol (MHPG; via ALR), or NE aldehyde metabolism to 3,4-dihydroxymandelic acid (DHMA; via ALDH) or 3,4-dihydroxyphenylglycol (DHPG; via ALR).

2. Transglutaminases

Recently, a novel mechanism by which primary amines can elicit function via the transglutaminase (TG)-catalyzed amidation of proteins (6, 38, 39, 61, 62, 81, 82, 107, 133, 181, 184, 185, 188, 190) has been described. In this process, primary amines are usually taken up into the cell—although a few studies have demonstrated that phenomenon occurs extracellularly as well—where they serve as intracellular TG substrates to modify proteins. TGs are a family of enzymes that catalyze a Ca^{2+}-dependent acyl-transfer between a γ-carboxamide group of a protein-bound glutamine and a free amine group (58). There are nine members of the mammalian family of TGs: TG1 through TG7, the blood coagulation enzyme Factor XIII (FXIII), and the catalytically-inactive erythrocyte membrane band 4.2 (**Table 1**) (111).

A number of different substrates can act as the free amine donor in this "amidation" reaction (**Figure 4**). Catalysis between a glutamine and the traditionally viewed substrate, the ε-amino group of a protein-bound lysine, results in protein-protein crosslinks via γ-glutamyl-ε-lysine bonds (**Figure 4A**). Other amine donor substrates that have been reported include polyamines such as spermidine, spermine, and putrescine (37), and monoamines (**Figure 4B**) such as 5-HT (108, 184, 188), histamine (181, 185), and dopamine (82, 185). In the absence of free amines, TGs are also capable of deamidating (**Figure 4C**) the glutamine residue (178). In this study, we propose that NE, like other monoamines, may also serve as a substrate for TGs (**Figure 4D**).

TG	Expression*	Regulation**	Disease***
TG1†	Skin (161) Endothelial cells (13)	Zymogen (161)	Ichthyosis lamellaris (145)
TG2†	Ubiquitous, including: VSMCs (172) Endothelial cells (172) Erythrocytes (155) Macrophages/Monocytes (67)	GTP (127)	Celiac disease (154) Huntington's (118) Hypertension (179) Atherosclerosis (68)
TG3	Skin (90)	GTP (5) Zymogen (72)	Possibly esophageal cancer (30, 177) Dermatitis herpetiformis (126)
TG4	Prostate (7)	GTP (160)	Prostate cancer (31)
TG5	Epithelial cells (136)	GTP (26) Zymogen (136)	Acral peeling syndrome (28)
TG6	Brain (171) Central nervous system (171)	GTP (171)	Spinocerebellar ataxia (186) Schizophrenia (27)
TG7	Testes (57) Lung (57)	Unknown	Unknown
FXIII†	Platelets (124) Plasma (124) Macrophages/Monocytes (70)	Zymogen (124)	Hypertension (1) Atherosclerosis (141)

Table 1. Summary of the active mammalian TGs.

Summary of the expression, regulation, and diseases associated with the active members of the mammalian TG family. *The list of expression is not all-inclusive. The tissue and cell types listed are canonical expression sites of the TG where high expression at either the protein or mRNA level has been reported. Additionally, if a TG has been described in the vasculature, the vascular cell types in which it has been observed are also listed. **Regulatory mechanisms listed are in addition to the calcium

Table 1 (cont'd)

dependence and regulation by nitric oxide shared by all active TGs (15). ***The list of diseases is not necessarily all-inclusive. The disease state may be due to an increase, decrease, or loss of the enzymes activity. Additionally, some pathologies, such as celiac disease, are due to autoantibodies directed against the TG. †TG has specifically been described in vascular tissues.

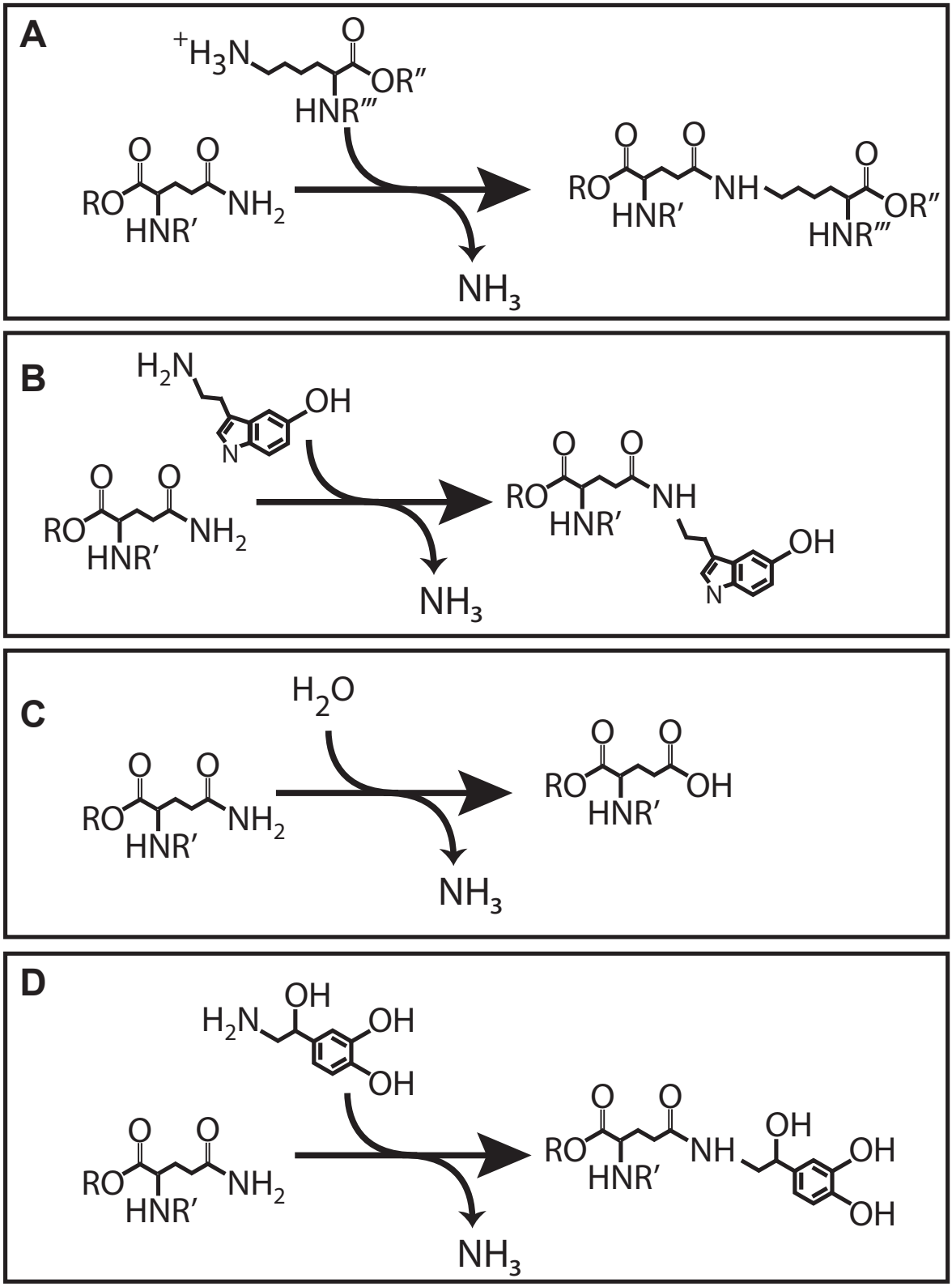

Figure 4. Diagram of TG reactions.

Figure 4 (cont'd)

TGs can catalyze a number of different transamidation reactions. **A**) The traditional view of TGs is that they catalyze protein-protein cross-links via the γ-glutamyl-ε-lysine bonds formed between the γ-amino group of a protein-bound glutamine, and the ε-amino group of a protein bound lysine. **B**) Primary amines, such as 5-HT, can also serve as glutamine acceptors, substituting for the ε-amino group of a protein bound lysine, and resulting in a covalent protein modification. **C**) In the absence of an amine donor, TGs can also catalyze the deamidation of glutamine to glutamate by the hydrolysis of water. **D**) In these experiments, we propose that NE, as a primary amine, can also serve as a TG substrate.

2.1. TG regulation

All TGs require Ca^{2+} for catalytic activity. While the concentration of Ca^{2+} needed to activate TGs was once thought to be supraphysiological and only occur within cells at times of extreme stress, this view has recently been challenged by the observation that non-canonical Ca^{2+}-binding sites may activate some TGs, enabling them to function at physiological conditions (95). This is further supported by some studies that have demonstrated active intracellular TG in living cells (53, 198). Indeed, some of the effects of TG-mediated protein transamidation have been shown to require increased intracellular Ca^{2+} concentrations driven by receptor activation (38, 39, 133, 184).

In addition to their Ca^{2+} requirements, TGs also have several other layers of regulation. Several of the TGs [i.e., TG2 (127), TG3 (5), and TG4 (160)] bind GTP, resulting in inhibition of their transamidation activity. Interestingly, TG2 was demonstrated to act as the G-protein $G_{\alpha h}$ (127), adding another layer of complexity to this protein. Although TG4 (160) is capable of hydrolyzing GTP, to our knowledge it has not been shown to act as a G-protein *in vivo.* It is unclear whether TG3 hydrolyzes GTP, as some reports suggest (5), or whether it is not capable of this function (73). Based on molecular homology, TG6 may also have a GTP-binding site (171). In contrast, GTP has no effect on TG1 activity, demonstrating that GTP binding is not a universal mechanism that regulates TG activity (76).

Proteolytic processing may act as an additional layer of TG regulation, as FXIII (8), TG1 (161), TG3 (74), and TG5 (136), are all zymogens that require proteolytic cleavage for full activation. Proteolytic cleavage of the full-length, 106 kDa form of TG1 gives rise to 67, 33, and 10 kDa fragments, which then form a complex of high TG activity (161). TG3 is initially expressed as a 77 kDa zymogen. Proteolysis cleaves the enzyme into two fragments: a 50 kDa fragment that contains the active site, and a 27 kDa fragment. These two fragments remain associated with one another (90). Interestingly, cleavage at a similar site in TG2 and FXIII leads to inactivation of these enzymes (90), suggesting one way for differential regulation of TG enzymes. Proteolysis of TG5 yield 53 and 28 kDa fragments which remain associated with one another (136). FXIII is well known as a blood-clotting factor. It is activated by thrombin, which cleaves FXIII into 56 and 24 kDa fragments (41). To our knowledge, proteolytic activation of the other TGs has not been described.

Finally, nitric oxide appears to be an important regulator of TG activity, as TG1 (143), TG2 (120), TG3 (143), and FXIII (15) exhibit reduced catalytic activity due to S-nitrosylation by nitric oxide. Because the inhibition by nitric oxide is partially due to S-nitrosylation of the conserved cysteine thiol active center required for TG catalytic activity (15), it is likely that the other TGs are regulated by nitric oxide as well. This regulation may be especially pertinent to vascular function, as nitric oxide is a well known vasodilator (89). Although nitric oxide's effects are largely attributed to the cGMP and PKG, given the observation that vasoconstriction is at least partially mediated by TG activity (189), regulation of TGs by nitric oxide may also play an important role in the regulation of vascular contraction.

2.2. TG-mediated amidation of proteins by monoamines.

As mentioned above, TGs can utilize monoamines as amidation substrates (referred to monoamine-amidation in the remainder of this dissertation). The incorporation of monoamines into glutamine residues was observed as early as 1961 (175, 182), and a functional role for histamine-amidation mast cell proteins was suggested in 1985 (52). Follow-up studies, however, were not performed, and the question of true physiological significance remained unanswered. Furthermore, the observations that TGs supposedly needed concentrations of calcium beyond what is normally encountered intracellularly (discussed above in the TG regulation section) and large concentrations of monoamines were required as well for this modification to occur made the physiological relevance of this modification uncertain. And thus, the field remained relatively unexplored until 2002 when Dale et al. demonstrated that the incorporation of 5-HT into glutamine residues of fibrinogen augmented cell-surface retention of stimulated platelets (40). This modification was later termed serotonylation by Walther, et al. (184). Furthermore, they demonstrated that, although large concentrations of the monoamine 5-HT are needed, these conditions could be met in a physiological setting. For example, immediately after secretion and re-uptake, the concentration of 5-HT can transiently exist at concentrations up to 600 μM (133, 184). The literature on the exact K_m values for the different TGs, monoamines, and protein substrates is sparse. One study that has investigated the different K_m for 5-HT, dopamine, and NE amidation into fibronectin demonstrated the NE had the lowest *Km* (154 nM for NE compared to 448 and 749 nM for dopamine and 5-HT, respectively) (80). It should be noted at this time that the concentration of NE in presynaptic vesicles can

be as high as 100 mM (163), and immediately following its release, concentrations of NE can briefly average about 300 μM in the neuromuscular junction (164). Therefore, if the NE in the neuromuscular junction can be efficiently transported into the cell, it may reach a concentration sufficient for its utilization as a TG substrate.

Serotonylation has subsequently been observed as a physiologically significant event in processes as diverse as insulin secretion from pancreatic β-cells (133), activation of the small G-protein, Ras-related 3 botulinum toxin substrate 1 (Rac1) in neuronal cells (39), and, in the vasculature, proliferation and migration of pulmonary artery VSMCs (107), 5-HT-induced aortic contraction (188), and RhoA degradation leading to decreased aortic contraction (62). **Table 2** summarizes the protein substrates for which monoamine-amidation has been described, and the processes that they mediate.

Some studies have demonstrated differential preference of a TG for monoamines with certain substrates. For example, Qiao et al. showed that histamine is efficiently incorporated into peptides derived from gliadin protein, while 5-HT is not (139). The Walther lab has supposedly found differing efficiencies in monoamine incorporation between different TGs and glutamine-donor substrate proteins [unpublished data cited in (185)]. These results suggest that the covalent modification of proteins by monoamines *in vivo* likely depends on 1) the available monoamine, 2) the TGs expressed, and 3) the potential protein substrates expressed.

One important question that has not fully been elucidated is how signals mediated by protein monoamine-amidation are "switched-off," as the actions of TGs are thought to be irreversible (58). One enzyme, γ-glutamylamine cyclotransferase, was

shown to act in the catabolism of ε-(γ-glutamyl)lysine residues, as well as other similar moieties where the lysine has been replaces with a poly- or monoamine. However, this enzyme is believed to act in the latter stage of TG substrate catabolism, as it is non-reactive towards substrates where the α-amino and/or α-carbonyl groups are occupied, such as when the glutamine residue is in a peptide bond. Furthermore, the reaction catalyzed by this enzyme does not produce as its product the amino acid glutamine, but rather a free amine and 5-oxo-L-proline (55). Thus, if this reaction did occur in proteins, it would still leave the glutamine residue modified. It has been demonstrated that TGs are capable of "back exchanging" with other primary amines (110). For example, the Lorand research group demonstrated that histamine-glutamyl residues in a protein (created by a TG-mediated reaction) can be deamidated by TGs (thus changing the glutamine to a glutamate residue), and that exchange with free histamine occurs quite readily (110, 139). It is conceivable that other monoamines could possibly be exchanged with the monoamine covalently bound in a glutamine residue (e.g., the 5-HT in a serotonylated glutamine residue being exchanged with free NE). Though, to our knowledge, this "cross-exchange", back-exchange, and deamidation of monoamine-amidated proteins has not been shown under *in vivo* conditions, its possibility cannot be ruled out at this time. Several studies have demonstrated the termination of a signal elicited by an activated, monoamine-amidated protein to occur via protein degradation. For example, GTPases that have become constitutively active by serotonylation are also marked for ubiquitination (61, 133), leading to their depletion. Thus, some proteins that become amidated by monoamines may be marked for enhanced degradation.

Finally, it is possible that an as-of-yet not described mechanism exists for the reversal of protein monoamine-amidation.

Monoamine	Cells or Tissue	Substrate	Function
Histamine	Liver (182)	Not identified	Not identified
	Mast cells (52)	Not identified	Suggested regulation of histamine release
	Mast cells (181)	Gαq Gα1 Cdc42	G protein signaling
Dopamine	C6 Glioma cells (82)	Fibronectin	Protein aggregation
5-HT	Platelets (40)	Fibrinogen	Augments binding of adhesive and procoagulation proteins
	Platelets (184)	RhoA Rab4	Small G protein activation and α-granule secretion
	Pulmonary artery and RA VSMCs (62)	RhoA	Small G protein activation and subsequent degradation leading to decreased contraction
	A1A1v cells (a rat corticol neuron cell line) (38, 39)	Rac1	Rac1 activation and platelet aggregation
	Pancreatic β-cells (133)	Rab3a Rab27a	Small G protein activation and insulin secretion
	RA (188)	α-actin β-actin γ-actin Myosin heavy chain Filamin A	5-HT-induced RA contraction and α-actin fiber formation/stability
	C6 Glioma Cells (81)	Fibronectin	Protein aggregation
	Pulmonary artery VSMCs (107, 108, 190)	Fibronectin	Pulmonary artery VSMC proliferation and migration, possibly contributing to pulmonary hypertension
NE*	RA and RVC VSMCs (86)	α-actin	RA and RVC contraction
	C6 Glioma cells (82)	Fibronectin	Protein aggregation

Table 2. Summary of monoamine protein modifications.

Table 2 (cont'd)

Listed in the table are the studies that have observed TG-mediated monoamine-amidation of proteins. The table lists the cell and tissue types where the modification has been observed, the protein targets of monoamine-amidation, and the physiological response the modification induces or regulates. *The studies which reference NE-amidation (and dopamine-amidation) of proteins are publications that either refer to experiments performed in this dissertation, or were published after such studies.

2.3. Receptor-independent NE-effects

Several of the processes that are mediated by serotonylation were discovered when experiments were performed to help explain observations of 5-HT stimulating receptor-independent effects. For example, the discovery that serotonylation was important to pulmonary artery VSMC proliferation and migration (61, 108) was, in part, driven by the observation that pulmonary artery and bovine aorta VSMCs are stimulated by 5-HT to proliferate and migrate via a receptor-independent, SERT-dependent mechanism (18, 47, 100-103).

Similar to 5-HT, there are some examples of NE eliciting an effect in a receptor-independent manner. Examples include the inability of α-adrenergic receptor antagonists to block NE-induced lipolysis in the $\beta_1/\beta_2/\beta_3$-adrenergic receptor knockout mouse (169), as well as the inability of adrenergic antagonists to block the stimulatory effect of NE on Na,K-ATPase activity in rat brain homogenate (3). Additionally, inhibition of NE uptake by tricyclic antidepressants and xylamine was shown to inhibit contraction to NE in the rat vas deferens (79). This suggests that NE may exert receptor-independent effects, and that these effects may require the uptake and actions of NE inside of the cell.

Though those studies discussed above suggest that NE can elicit function in a receptor-independent manner, much of the reported physiological responses to NE in the vasculature are mediated by receptor interaction. However, the amidation of proteins by NE does not necessarily exclude the possibility that NE is also acting *with* adrenergic receptors to stimulate vascular function. Rather, it is possible, and even

likely, that adrenergic receptor stimulation and protein amidation work cooperatively, as activation of adrenergic receptors may be needed to elevate intracellular calcium levels to a concentration that activates TGs so that protein amidation can occur. Evidence that this may be the case can be seen in A1A1v cells (a rat embryonic cortical cell line), where 5-HT(2A) receptor-coupled phospholipase C activation and subsequent intracellular calcium elevation was required for TG-mediated serotonylation of the small G-protein Rac1, resulting in its constitutive activation (38). Thus, there is some precedence in receptor activation coupling to protein amidation to elicit a physiological response.

2.4. TGs in vascular diseases and processes

TGs have been implicated in a variety of disease states. For example, increased TG activity may contribute to vascular diseases such as hypertension (1) and atherosclerosis progression (116), while decreased TG activity is associated with dysfunctional cardiac dilation after myocardial infarction (180). Protein aggregates formed by TG activity are associated with Huntington's disease and vascular dementia (129). A number of disease, including type 1 diabetes (98), celiac disease (154), dermatitis herpetiformis (126), and spinocerebellar ataxias (66), are associated with autoantibodies directed against certain TGs. In some cases of TG autoimmunity, the autoantibodies can have ramifications to vascular functions, such as celiac disease-derived TG2 antibodies that increase the activity of the enzyme leading to angiogenesis inhibition (25).

To date, only TG1, TG2, and FXIII have been reported in the cardiovascular system (12). The literature on cardiovascular TG1 is limited. TG1 has been found in

myocardial endothelial cells [but not pulmonary endothelial cells (13)] where it plays a role in controlling barrier function of endothelial monolayers by stabilizing β-actin (14). In contrast to TG1, vascular TG2 and FXIII have been substantially more studied. FXIII is expressed by platelets and cells of monocyte/macrophage origin (124). In addition to its classical role in the blood coagulation cascade (109), FXIII also promotes fibroblast adhesion (176), healing of the myocardium after infarction (125), and contributes to angiogenesis (41). FXIII expression and activity is altered in a number of vascular disease processes. For example, monocytic expression and activity of FXIII is increased in hypertensive subjects (1).

TG2 is expressed in vascular endothelial and VSMCs of both large (188) and small (10) arteries, as well as fibroblasts and monocytes-macrophages (172). Within the cell, most of the TG2 is located in the cytoplasm, with small amounts located outside the cell membrane and within the nucleus (111). In VSMCs, TG2 colocalizes with stress fibers (33) and may even participate in their formation (156, 192). Evidence that the monoamine transamidating function of TGs may be important to stress fiber formation is provided by the observation that 5-HT colocalizes with α-actin in cultured VSMCs (188). Furthermore, when an inhibitor of TGs, cystamine, is included, colocalization is reduced and α-actin filamentation becomes disrupted (188).

TG2 has been implicated in a number of disease states. For example, TG2 is critical for the calcification of arterial VSMCs (85), a process that decreases artery wall compliance and is linked to increased mortality in atherosclerosis (2). TG2 is also upregulated by shear stress in coronary artery endothelial cells, a process that contributes to the development of atherosclerosis (132). Though TG2 may contribute to

atherosclerotic clot progression, it may also play a beneficial role in the formed atherosclerotic plaque, where TG2 activity helps stabilize the plaque, making it less prone to rupture (68). Reduced red cell deformability, found in pathologic conditions such as hypertension (35), depends on TG2 (138). TG2 is also important for small artery remodeling (10, 11, 138, 179), a process that leads to a reduced lumen diameter and is associated with hypertension (22, 151).

Despite the ubiquitous expression and numerous physiological roles reported for TG2, TG2 knockout (KO) mice show a relatively mild phenotype (43, 128), with no change in blood pressure or heart rate compared to wild-type (WT) mice. FXIII derived from macrophages compensates for some of the vascular functions of TG2 lost in the TG2 KO mice, as evidenced by macrophage-derived FXIII's contribution to the delayed flow-dependent small artery remodeling in these mice (11). However, macrophage recruitment does not explain why the contractile response to adrenergic agonists of the mesenteric artery in TG2 KO mice is not different from WT (11), as TG function is important for amine-stimulated vascular contraction (86, 188). This evidence suggests that other TGs are expressed, either naturally or as a compensating mechanism for the loss of TG2, in the vasculature.

As mentioned above, TG-mediated monoamine-amidation of proteins has significant physiological roles in the vasculature. In addition to a likely role in stress-fiber formation (156, 188, 192), inhibition of TG activity by cystamine in the RA blocked contraction to 5-HT, while the same concentration of cystamine only slightly reduced the contraction to the receptor-independent, depolarization-dependent contractant KCl (188). Interestingly, long-term stimulation of the RA with 5-HT results in the

serotonylation of RhoA (62), constitutively activating the protein and eventually leading to its ubiquitination and proteasomal degradation. Depletion of RhoA in the RA results in reduced contraction to the endoperoxide prostaglandin H_2 analog U46619, which relies on a RhoA/Rho kinase dependent-mechanism for contraction. Thus, while monoamine-amidation may acutely support amine-induced contraction, chronically it can lead to desensitization to some agonists. Additionally, RhoA depletion mediated by serotonylation can have pathological consequences to vascular tissues, as it leads to protein kinase B activation, which in turn contributes to the disease phenotype observed in primary pulmonary hypertension (61, 62). Vascular monoamine-amidation is also important in platelet function. Serotonylation of fibrinogen augmented cell-surface retention of stimulated platelets (40). Additionally, when 5-HT is incorporated into small G-proteins in platelets, they become constitutively active and trigger release of α-granules containing proaggregatory proteins (184). In pulmonary artery VSMCs, serotonylation of fibronectin stimulates their migration and proliferation (107). This, along with increased RhoA activation due to serotonylation (61), may contribute to pulmonary hypertension (190). Thus, there are a number of ways in which monoamine-amidation is important to vascular function and may contribute to vascular disease.

2.5. Protein substrates of vascular TGs.

In these experiments, I propose to identify vascular TG substrates, notably those that are amidated by NE. A number of vascular proteins have been identified as TG substrates. In addition to those mentioned above for serotonylated proteins [i.e., α-actin (188), small GTPases (38, 61, 62, 184), and fibronectin (107, 190)], other proteins substrates have been observed acting as substrates for the cross-linking function of

TGs. For example, vimentin, a class III intermediate filament protein, was identified as a TG substrate in atherosclerotic plaques (64), along with albumin and transferrin. The importance of vascular vimentin is exemplified in that mice lacking this protein have impaired arterial vasodilation in response to altered blood flow (71). Other known substrates of TGs that exist in the vasculature are collagen types I and II (122), apolipoprotein (a) (17), and dermatan sulfate proteoglycan (94). However, many of these substrates were identified as TG substrates using purified proteins. Only a few studies have identified TG substrates in complex mixtures, such as tissue homogenates, in the vasculature (64, 71, 179). Thus, while many candidate proteins have been identified, few of the endogenous TG substrates have been elucidated. Moreover, no one has attempted to identify NE-amidation-specific substrates in the vasculature, as monoamine-amidation as a whole is a relatively novel field. The identification of the true TG substrates is a challenge, in particularly in relation to those that serve as substrates for monoamine-amidation. Unlike other protein modifications, such as phosphorylation which adds a charged group to the protein, monoamine-amidation does not attach a charged group. Thus, the addition of a monoamine does not allow for tracking a protein by a change in native gel electrophoresis, or other biomolecular tool sets that could utilize a change in a proteins charge. Furthermore, antibodies directed towards a *specific* NE-amidation substrate have not been developed—although antibodies directed towards NE conjugated to bovine serum albumin via a glutaraldehyde linker have. Thus, detecting a minor subset of proteins that have a particular monoamine modification remains a challenge to the field in general.

3. Experimental Model

Both an artery (the RA) and a vein (the rat vena cava; RVC) from normal Sprague-Dawley rats were chosen for our model. An artery and a vein were chosen because both may contribute to blood pressure regulations in distinct ways that are reflected in their structures. In arteries, VSMCs and elastin fibers are highly prevalent, while substantially fewer of these components make up the venous vasculature. The most extreme example of these features occurs in the vessels directly responsible for blood coming into and exiting the heart: the aorta and the vena cava (**Figure 5**). These features make arteries low-compliance, high-resistance vessels, while veins are high-compliance and low resistance. These features are well suited for the distinct functions of arteries and veins; while arteries receive oxygen-rich blood from the heart and distribute it to the rest of the body, veins return oxygen-depleted back to the heart for recycling. Arterial vasculature thus needs to be strong and highly resistant to stand up to the shear force generated by blood being pumped out of the heart, while the high-compliance and low resistance of veins enables them to receive deoxygenated blood. The high compliance of veins also makes them more distensible. Because of this, veins can store up to 75% of the body's total blood volume at a given moment (144). Vasoconstriction of veins can mobilize part of this blood volume, while vasodilation increases the volume of blood that can be stored. Thus, both arteries and veins contribute to the regulation of blood pressure: arteries by affecting total peripheral resistance and vascular tone, and veins through the regulation of vascular capacitance.

Although we acknowledge that small resistance vessels are important for the regulation of blood pressure, our choice to use large conductive vessels in these studies is justifiable. Both the aorta and the vena cava reflect the states of the arterial and

venous systems. This is illustrated in aortic stiffening during systolic hypertension (183). Additionally, the vena cava is important in controlling central blood volume, as well as circulatory dynamics (19, 54). Thus, the study of these two vessels has medical relevance. Finally, the use of these tissues was advantageous as they are large enough for experimental manipulation at multiple levels.

The vasculature is an ideal system to test the hypothesis that NE elicits a biological effect via protein amidation by TGs, as both arteries and veins express one or more TG (56). Additionally, not only is NE readily available via the sympathetic nervous system (which innervates both the arterial and venous sides of the vasculature), vascular tissues respond to and depend on NE for homeostatic regulation. Though both arteries and veins respond to NE, the sensitivity and handling of NE is not identical between the two vascular components. For example, the concentration of NE needed to elicit maximum contraction in veins is lower than in arteries (134). Additionally, veins have a lower content of endogenous NE than arteries, which may be a consequence of either the lower cellular content of venous tissues or the denser sympathetic innervation observed in arteries compared to veins (105). **Table 3** lists a number of differences between observed between arteries and veins, particularly in factors related to their contractile kinetics and handling of NE.

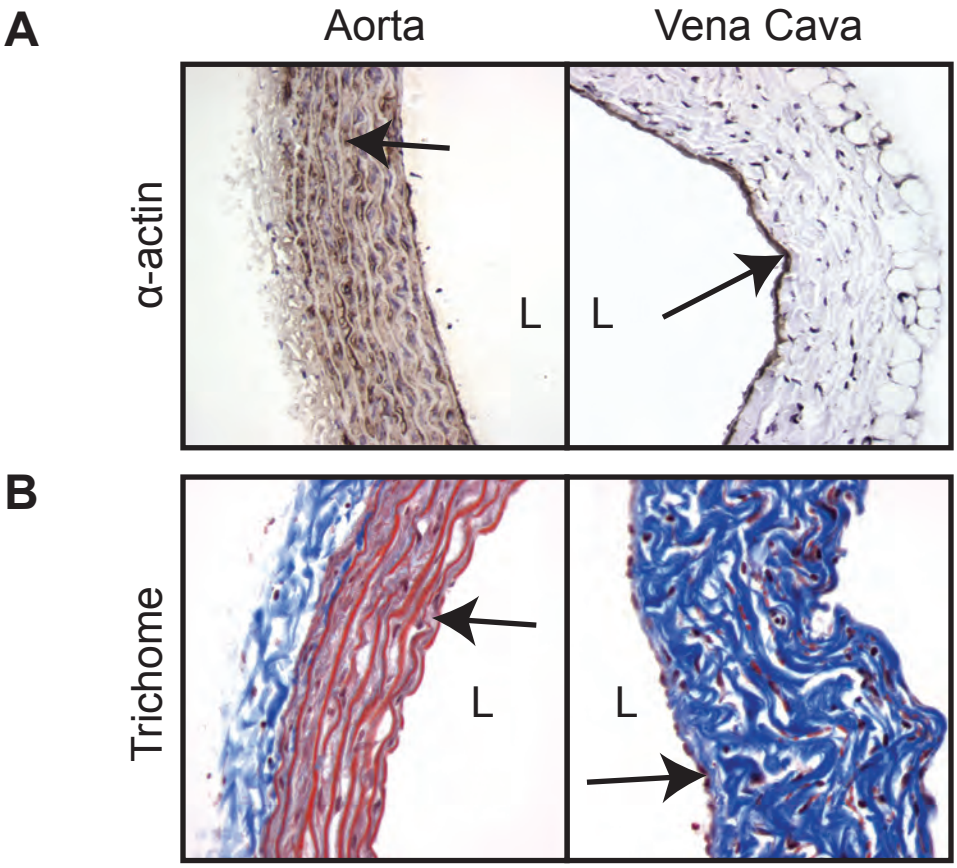

Figure 5. Structure of RA and RVC tissues.

A) Immunohistochemical and **B**) Masson Trichome staining for α-actin in RA (left) and RVC (right) tissue sections. Arrows point to staining in VSMC layers. Brown in A is positive staining. In B: Red stain = elastin; pink = smooth muscle; blue = collagen. L = lumen. Adapted from Rondelli et al. (2007) (142).

Arteries	Veins	Reference
Low α_1 adrenoreceptor expression	High α_1 adrenoreceptor expression	(134)
α_1 adrenoreceptors only	Both α_1 and α_2 adrenoreceptors	(135)
Slow myosin heavy chain expression	Fast myosin heavy chain expression	(142)
Slow contractile kinetics to agonists	Rapid contractile kinetics to agonists	(170)
Contraction less sensitive to NE	Contraction more sensitive to NE	(134)
Contraction desensitizes more rapidly to NE	Contraction desensitizes less rapidly to NE	(134)
NE uptake unchanged in hypertensive arteries	NE uptake increased in hypertensive veins	(112)
Larger endogenous NE content	Smaller endogenous NE content	(105)

Table 3. Notable differences in contraction and NE handling between arteries and veins.

4. Hypothesis

While NE and TGs both have critical functions in the vasculature, a possible interrelationship between the two has not been investigated to date. As a primary amine, it is conceivable that NE acts as a post-translational modifier of proteins via a TG-mediated amidation reaction. Other primary amines, most notably 5-HT, have been shown to modify proteins in a way such as this, with implications in vascular functions and disease states. Because essential hypertension, a widespread pathology with unknown cause, increases one's risk for myocardial infarction, stroke, and other cardiovascular diseases, understanding how blood pressure is regulated is critical to the development of treatment and preventive strategies against hypertension. As such, this study was designed to fill a gap in our understanding of how TGs and NE function regularly in the vasculature. We hypothesized that proteins are amidated with NE via the actions of TGs, resulting in a physiological response (**Figure 6**). This hypothesis is further divided into 4 aims:

Aim 1: Test the hypothesis that TGs present in vascular tissues modify vascular proteins by covalently attaching NE.

Aim 2: Test the hypothesis that NE is taken up into VSMCs (which express TGs).

Aim 3: Identify the protein substrates of TGs, with an emphasis on those that are modified by NE.

Aim 4: Test the hypothesis that the modification of VSMC proteins by NE stimulates a measureable physiological response, such as contraction, migration, and/or growth of VSMCs.

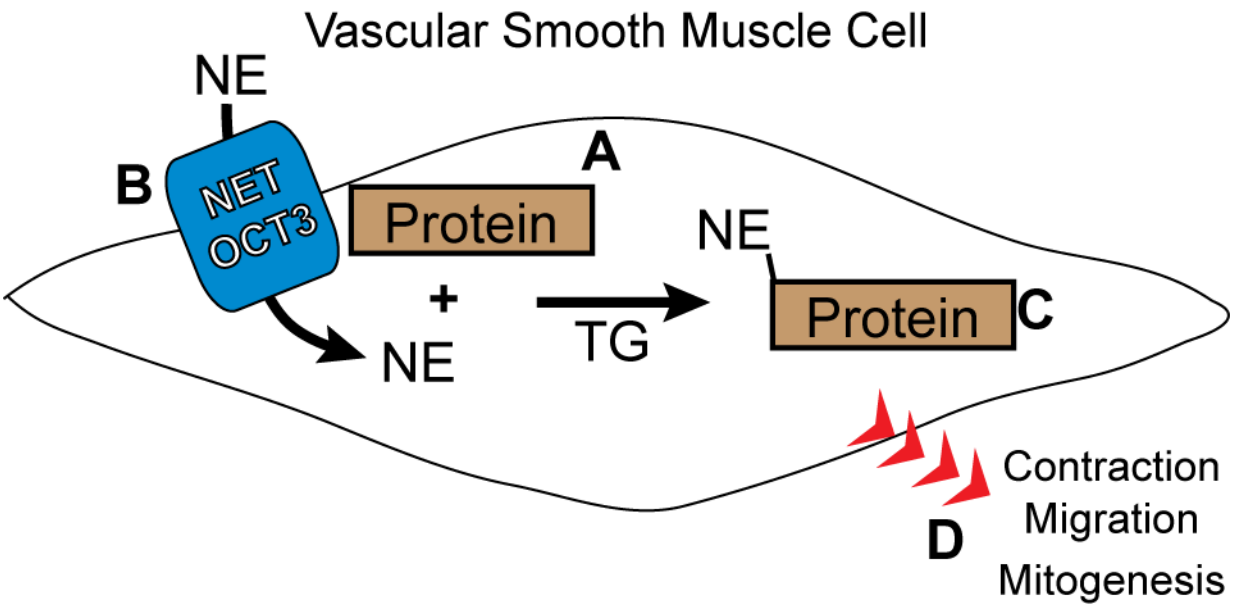

Figure 6. Hypothesis.

NE is taken up by VSMCs and utilized by TGs as a substrate for the covalent modification of vascular proteins, leading to a physiologically relevant response. The main hypothesis is subdivided into 4 sub-hypotheses: **A**) Aim 1: TGs are present, active, and utilize NE as a substrate in VSMCs. **B**) Aim 2: NE is taken up by VSMCs. **C**) Aim 3: Identify the vascular protein substrates of TGs, particularly those that are modified by NE. **D**) Aim 4: The TG-mediated modification of vascular proteins by NE stimulates VSMCs to respond in a measureable, physiologically relevant manner, such as VSMC contraction, growth, or migration.

Chapter 2: Methods

1. Animal Use

Laboratory facilities in which experiments were conducted were located at *Michigan State University*, in the Department of Pharmacology and Toxicology. Procedures involving normal male Sprague-Dawley rats (250-300 g; Charles River Laboratories, Inc., Portage, MI, USA) were performed in accordance with the Institutional Animal Care and Use Committee at Michigan State University, and the Guide for the Care and Use of Laboratory Animals of the National Research Council (USA). Anesthesia and euthanasia were done with a lethal dose of FatalPlus (60 - 100 mg/kg, i.p.) prior to the removal of tissues. The active ingredient in FatalPlus, pentobarbital, is a well-known anesthetic, and its use is consistent with the recommendations put forth by the Panel on Euthanasia of the American Veterinary Medical Association. A concerted effort was made to minimize discomfort and expedite euthanasia of all the animals used in these studies.

Pairs of aortae from two separate colonies of male TG2 KO and WT mice were used in some experiments. The colonies of mice were first established and described by the Melino (43) and Graham (128) lab groups. The Melino WT and TG2 KO mice (25-35 g) are in a mixed Svj129-C57Bl/6 background. The WT and TG2 KO mice were bred separately. Every few generations, the WT and KO mice were crossed and regenotyped to prevent genetic drift. Melino mice were anesthetized with CO_2, and then euthanized by decapitation prior to the removal of tissues. Procedures done with these mice were in accordance with the established *University of Rochester* guidelines on animal care and handling, and approved by the University Committee for Animal Research. The Graham

WT and TG2 KO mice (25-27 g) were backcrossed at least 10x onto a C57Bl/6 background. The TG2 KO mice were maintained as a colony of homozygous TG2 KOs. WT C57Bl/6 non-littermates were used as controls. Graham mice were anesthetized with isoflurane, and then sacrificed by cervical dislocation before tissue collection. Procedures done with these mice were in accordance with the Institutional Animal Use and Care Committee of the *Academic Medical Center*, Amsterdam, the Netherlands. For both the Melino and Graham TG2 WT and KO mouse pairs, whole aortae were sent to *Michigan State University* for experimentation. Tissues were shipped overnight in cold physiological salt solution (PSS; 103 mM NaCl; 4.7 mM KCl; 1.13 mM KH_2PO_4; 1.17 mM $MgSO_4$-$7H_20$; 1.6 mM $CaCl_2$-$2H_2O$; 14.9 mM $NaHCO_3$; 5.5 mM dextrose and 0.03 mM $CaNa_2$ EDTA) and kept cool with dry ice. Upon arrival, tissues were immediately homogenized (Melino) or prepared for sectioning (Graham).

2. Materials

If not otherwise denoted, chemicals and drugs were purchased from Sigma-Aldrich (St. Louis, MO, USA).

3. RT-PCR

Total RNA from ~10 mg sections of RA and RVC was isolated using the MELT total RNA isolation system (Ambion/Applied Biosystems, Austin, TX). The concentration of the RNA isolated was determined using a Nanodrop spectrophotometer. One microgram of the DNase-treated total RNA was reverse transcribed using an oligo$(dT)_{12–18}$ primer, dNTP mix, and SuperScript II reverse transcriptase (Invitrogen, Carlsbad, CA, USA) according to the manufacturer's protocol. Primers for rat TGs and

β2-microglobulin (B2m) were obtained from Real Time Primers, LLC (Elkins Parka, PA, USA). To confirm the uniqueness of each of the primers, Real Time Primers conducted a BLAST search using each primer set biased toward picking “somewhat dissimilar sequences.” Each set was unique to the intended target using this approach. **Table 4** lists the forward and reverse primer sequences used for each target. Expression of the mRNAs of each of the TGs was reported relative to B2m expression and reported as $2^{-\Delta Ct}$.

Primer	Sequence	
B2m	Forward:	5'-TGC TAC GTG TCT CAG TTC CA-3'
	Reverse:	5'-GCT CCT TCA GAG TGA CGT GT-3'
TG1	Forward:	5'-GAC TAC TCT CGA GGC ACC AA-3'
	Reverse:	5'-CGT GTG CAG AGT TGA AGT TG-3'
TG2	Forward:	5'-GGG AAT ACG TCC TCA CAC AG-3'
	Reverse:	5'-GTC ATC ATT GCA GTT GAC CA-3'
TG3	Forward:	5'-GAA CCT GGA ACG GTA GTG TG-3'
	Reverse:	5'-GCT ATC ACT GCC TTT CTC CA-3'
TG4	Forward:	5'-ATA GAA TGC ACC CCA GTG AA-3'
	Reverse:	5'-ACA TGC TTA CCA AGG CTC AG-3'
TG5	Forward:	5'-TAT TTT CAA ACC CCC TCT CG-3'
	Reverse:	5'-TCT GCC TTT GTC CAC TCT TG-3
TG7	Forward:	5'-GGA CAG CCT GTG AAA TAT GG-3'
	Reverse:	5'-GGT GGA AGG TCT TTC CTG AT-3'
FXIII	Forward:	5'-AAA CTG CCC TGA TGT ATG GA-3'
	Reverse:	5'-CCC CAG TGT AGA AGG TGA TG-3'

Table 4. Primer sequences for RT-PCR.

Forward and reverse sequence of the primers used for RT-PCR. The uniqueness of each of the primers was confirmed by a BLAST search using each primer set biased toward picking “somewhat dissimilar sequences.” B2m = β2-microglobulin; used as a “housekeeping” gene to normalize expression.

4. Western Analysis

RA or RVC tissues were cleaned, pulverized in liquid nitrogen, and solubilized in lysis buffer [0.5 M Tris HCl (pH 6.8), 10% SDS, 10% glycerol] with protease inhibitors (0.5 mM PMSF, 10 µg/ml aprotinin and 10 µg/ml leupeptin). Homogenates were briefly sonicated 6 x 1 min, centrifuged (18,000 g for 10 min, 4°C), and the protein concentration of the supernatant was determined using a bicinchoninic acid (BCA) assay (BCA Kit, Sigma, St. Louis, MO, USA). Western blotting procedures were performed using standard SDS-PAGE conditions and transferring proteins to either nitrocellulose or PVDF-FL membranes (130). Unless otherwise noted, 50 µg of protein were loaded in each lane, and 10% SDS gels were used. After transferring, blots were blocked for 3 h at 4°C (while rocking) with either 4% chick egg ovalbumin (CEO) in tris-buffered saline plus 1% tween (TBST) or Li-Cor blocker (Li-Cor Biosciences). Primary antibodies (diluted in blocking solution) were added and allowed to incubate overnight (4°C, rocking). See **Table 5** for primary antibodies used. The next day, primary antibody was removed and blots were washed 5 times with TBST (5-10 min per wash). After the last wash, blots were incubated in secondary antibody (either diluted in TBST or, when Li-Cor secondary antibodies were used, Li-Cor buffer) for 1 h. See **Table 6** for secondary antibodies used. Immunoreactive bands on blots were visualized in one of three ways: Some blots were visualized using horseradish-peroxidase-linked (HRP) secondary antibodies, chemiluminescent ECL reagent (GE Healthcare, Piscataway NJ, USA) and detecting the light produced using film. Alternatively, some blots were visualized with HRP-secondaries, ECL, and visualized using the Li-Cor Odyssey FC (Li-Cor Biosciences, Lincoln, NE, USA). Finally, some blots were visualized using

fluorescently conjugated secondary antibodies and visualized on either the Li-Cor Odyssey FC or the Li-Cor Odyssey Classic. See **Table 7** for the conditions used for each blot. For blots developed using film, the film was subsequently scanned and placed within the figure without gamma modification using Adobe Photoshop (Adobe Systems Incorporated, Mountain View, CA, USA). Densitometric analysis was performed using ImageJ (140).

Antibody Target	Host	Antibody Name	Manufacturer**	Method	Dilution
α-actin	Rabbit	ab5694	Abcam	ICC	1:100
α-actin	Mouse	AB-2	EMD Millipore	IB IP	1:1000 1:21
α-actin*	Mouse	F3777	Sigma	ICC	1:1000
β-actin	Mouse	A2228	Sigma	IB	1:1000
FXIII	Rabbit	ab83895	Abcam	IB ICC IHC	1:1000 1:250 1:1000
NE-BSA	Rabbit	ab8887	Abcam	IB ICC IHC	1:500 1:500 1:500
NET	Mouse	NET05-02	MAb Technologies	IB ICC IHC	1:1000 1:200 1:200
OCT3	Goat	sc-18515	Santa Cruz Biotechnology	IB ICC IHC	1:200 1:50 1:400
OCT3	Rabbit	BS3359	Bioworld	IB	1:500
TG1	Mouse	sc-166467	Santa Cruz Biotechnology	IB ICC IHC***	1:100 1:25 1:100/1:50
TG2	Mouse	TG100	LabVision	IHC	1:1000
TG2	Rabbit	ab421	Abcam	ICC	1:1000
TG2****	Rat		Hybridoma Facility, University of Alabama at Birmingham	IB	1:2000
TG4	Mouse	ATGA0140	ATGEN	IB ICC IHC	1:500 1:25 1:1000

Table 5. Primary Antibodies.

Table 5 (cont'd)

Primary antibodies used in immunoblotting (IB), immunocytochemistry (ICC), immunohistochemistry (IHC), and immunoprecipitation (IP) experiments. The dilution of antibodies used is listed. Dilution of antibodies occurred in the appropriate blocking solution. FXIII = Factor XIII; NE-BSA = NE conjugated to bovine serum albumin; NET = NE transporter; OCT3 = Organic Cation Transporter 3. *FITC-conjugated antibody. Experiments utilizing this antibody were shielded from light. **The following is the company information for the manufacturers: Abcam (Cambridge, MA, USA), EMD Millipore (Billerica, MA, USA), MAb Technologies (Stone Mountain, GA, USA), Santa Cruz Biotechnology (Santa Cruz, CA, USA), Bioworld (St. Louis Park, MN, USA), LabVision (Fremont, CA, USA), Hybridoma Facility (University of Alabama, Birmingham, AL, USA), ATGEN (South Korea). ***IHC experiments utilizing paraffin-embedded RA and RVC tissues used this antibody at a 1:100 dilution, while those that utilized fresh-frozen TG2 WT and KO mouse aortae used the 1:50 dilution. ****This antibody was a generous gift provided to us by Dr. Gail V.W. Johnson from the Department of Anesthesiology at the University of Rochester in Rochester, NY.

Antibody Name	Host Species	Catalog Number	Manufacturer*	Dilution
Immunoblotting				
Anti-Goat IRDye 680	Donkey	926-32224	Li-Cor	1:1000
Anti-mouse HRP	Sheep	NA931V	GE Healthcare	1:2000
anti-mouse IRDye 680LT	Goat	827-11080	Li-Cor	1:1000
anti-mouse IRDye 800	Goat	827-08364	Li-Cor	1:1000
anti-rabbit HRP	Goat	7074	Cell Signaling	1:1000
anti-rabbit IRDye 800	Goat	926-32211	Li-Cor	1:1000
anti-rat HRP	Rabbit	A-5795	Sigma	1:1000
IR dye 680 Streptavidin		926-32231	Li-Cor	1:1000
IR dye 800 Streptavidin		926-32230	Li-Cor	1:5000
Streptavidin-HRP Conjugate		RPN1231V	GE Healthcare	1:2000
Immunocytochemistry**				
anti-goat Alexa Fluor 568	Rabbit	A11079	Invitrogen	1:1000
anti-mouse Alexa Fluor 568	Goat	A11004	Invitrogen	1:1000
anti-rabbit Alexa Fluor 488	Goat	A11008	Invitrogen	1:1000
anti-rabbit Alexa Fluor 568	Goat	A11011	Invitrogen	1:1000
Cy3-conjugated Affini Pure anti-rabbit	Goat	115-165-146	Jackson ImmunoResearch Laboratories Inc.	1:1000
Rhodamine Red-X-conjugated Streptavidin		016-290-084	Jackson ImmunoResearch Laboratories Inc.	1:1000

Table 6. Secondary Antibodies.

Secondary antibodies used in immunoblotting and immunocytochemistry experiments. The dilution of antibodies used is listed. Dilution of antibodies occurred in TBST (immunoblotting) or PBS (immunocytochemistry). HRP = horseradish peroxidase. *The

Table 6 (cont'd)

following is company information for manufacturers: Cell Signaling (Boston, MA, USA), and Jackson ImmunoResearch Laboratories Inc. (West Grove, PA, USA). **Immunocytochemical antibodies were fluorescent, and experiments utilizing these antibodies were shielded from light.

Figure	Antibody Target	Samples	Membrane	Blocker*	Secondary
8A	TG1	RA, RVC	PVDF-FL	CEO	Anti-mouse HRP
8A	TG2	RA, RVC	PVDF-FL	CEO	Anti-rat HRP
8A	TG4	RA, RVC	PVDF-FL	CEO	Anti-mouse HRP
8A	FXIII	RA, RVC	PVDF-FL	CEO	Anti-rabbit HRP
16A	TG1	RA, RAVSMC/RVC, RVCVSMC	PVDF-FL	CEO	anti-mouse HRP
16A	TG2	RA, RAVSMC/RVC, RVCVSMC	PVDF-FL	CEO	Anti-rat HRP
18B	TG1	TG2 WT/KO MA	PVDF-FL	CEO	Anti-mouse HRP
18A	TG2	TG2 WT/KO MA	PVDF-FL	CEO	Anti-rat HRP
18B	TG4	TG2 WT/KO MA	PVDF-FL	CEO	Anti-mouse HRP
18B	FXIII	TG2 WT/KO MA	Nitrocellulose	CEO	Anti-rabbit HRP
19A	BAP	TG2 WT/KO MA ± BAP	PVDF-FL	CEO	Streptavidin-HRP
20	BAP	RA: TG Inhibitors vs BAP	PVDF-FL	CEO	Streptavidin-HRP
24	NE-BSA	RA RVC	PVDF-FL	CEO	Anti-rabbit HRP
25	NE-BSA	RA RVC (NE and NE-BSA competition)	PVDF-FL	CEO	Anti-rabbit IRDye 800
28	Monoamine-Biotin	RA (Monoamine vs cystamine)	PVDF-FL	CEO	Streptavidin-HRP
29A	NE-Biotin	RA/RVC (NE vs NE-biotin)	Nitrocellulose	CEO	Streptavidin-HRP
29A	NE-Biotin	Whole RVC ±NE-biotin	Nitrocellulose	CEO	Streptavidin-HRP
31	NE-Biotin	NE-Biotin uptake in RVC	PVDF-FL	CEO	Streptavidin-HRP

Table 7. Western blot conditions.

Table 7 (cont'd)

32A	OCT3	RA, RVC, RA VSMC, RVC VSMC	PVDF-FL	LiCor	Anti-goat IRDye 800
32B and C	OCT3	RA, RVC, RA VSMC, RVC VSMC	PVDF-FL	LiCor	Anti-rabbit IRDye 800
32D	NET	RA, RVC, RA VSMC, RVC VSMC	Nitrocellulose	CEO	Anti-mouse HRP
39	NE-Biotin	RA (α-actin IP) ±NE-biotin	Nitrocellulose	CEO	Streptavidin-HRP
39	α-actin	RA (α-actin IP) ±NE-biotin	Nitrocellulose	CEO	Anti-mouse IRDye 800

Conditions for the Western blot experiments. The "Figure" column refers to the figure where the blot is shown. Antibody Target refers to the antigen that the primary antibody was raised against. Samples are the proteins that were analyzed in the blot. BAP = 5-(Biotinamido)pentylamine**;** CEO = chick egg ovalbumin; FXIII = Factor XIII; HRP = Horseradish Peroxidase; IP = immunoprecipitation; MA = Mouse aorta; NE-Biotin = NE conjugated to a biotin moiety; NE-BSA = NE conjugated to bovine serum albumin; NET = NE transporter; OCT3 = Organic Cation Transporter 3; vs = Versus; Blocker: CEO is 4% (weight/volume) in TBST; LiCor refers to LiCor's proprietary blocking solution (Part # 927-40000). Secondary refers to the secondary antibody used.

5. Bicinchoninic acid (BCA) assay

The concentration of proteins in tissue homogenates and cell lysates was determined using a BCA assay (BCA Kit, Sigma) following the manufacturer's protocol. BSA protein was used to construct a standard curve of known protein concentration. Samples and standards (5 µL of sample diluted to 100 µl with water) were incubated at 37°C for 30 min with 2 ml of reagent [(50:1 ratio of BCA:copper (II) sulfate (4% w/v)]. Protein concentration was determined by measuring the absorbance at 562 nm.

6. Immunohistochemistry

For immunohistochemical staining experiments, paraffin-embedded sections of RA and RVC tissues were dewaxed and unmasked using Unmasking Reagent (Vector Laboratories, Burlingame, CA, USA). The exception to this was immunohistochemical experiments which utilized the TG2 WT and KO mouse aortae from the Graham colony, and in the RA and RVC sections in which OCT3 or NET were visualized by immunostaining. In these instances, fresh frozen tissue sections were used. Fresh frozen sections were allowed to equilibrate to room temperature before being fixed in cold (4°C) acetone for 10 min. After either fixation or unmasking, the fresh frozen and paraffin-embedded tissues, respectively, were treated identically unless otherwise noted. VECTASTAIN® Elite ABC Kits (Vector Laboratories), which provided the appropriate blocking serum and secondary antibody depending on the species in which the primary antibody was raised, were used according to the manufacturer's instructions. Sections were incubated in 3% hydrogen peroxide dissolved in PBS (plus blocking serum in fresh frozen sections) for 30 min. Sections were rinsed in PBS. For fresh frozen tissues, an avidin-biotin blocking step using an Avidin/Biotin Blocking Kit (Vector Laboratories) was

included. Using this kit, Avidin solution was added to tissue sections for 15 min, after which sections were washed once briefly with PBS and biotin solution was added for an additional 15 min. After the avidin/biotin blocking step, the TG2 WT and KO mouse aorta sections, and fresh frozen RA and RVC tissue sections, the Vector® Mouse on Mouse™ basic kit (Vector laboratories) was utilized according to the manufacture's instructions. This kit was used as preliminary experiments indicated that the horse-anti-mouse secondary antibodies provided in the Elite ABC Kit cross-reacted with endogenous proteins found in these tissues. For all other tissue sections, after either the endogenous biotin/avidin blocking step (fresh frozen tissues) or incubation with hydrogen peroxide (paraffin-embedded sections), sections were blocked in the appropriate serum provided by the VECTASTAIN Elite ABC Kit for 1 h. After blocking, primary antibody, diluted in blocking serum, was added to the tissue sections, and sections were incubated overnight at 4°C in a humidified chamber. The next day, the primary antibody was removed, sections were rinsed briefly with PBS, and secondary antibodies were added for 30 min. Tissues were rinsed with PBS, and ABC Elite Reagent was added for 30 min. Sections were washed with PBS, and developed using either 3,3'-Diaminobenzidine (DAB) Peroxidase substrate (Vector laboratories; paraffin-embedded tissue sections) or ImmPACT™ NovaRED™ Peroxidase Substrate (Vector laboratories; fresh frozen tissue sections). Sections were counterstained with either VECTOR Nuclear Fast Red (Vector Laboratories; for TG2 KO and WT mouse aortae) or haematoxylin (Vector Laboratories; all other sections). See **Table 5** for primary antibodies used. As controls, human skin (for TG1; Cat. No. 12-701-XA1, ProSci Inc., Poway, CA, USA), human prostate (for TG4; Cat. No. 10-635-YA1, ProSci Inc.), human

placenta (for FXIII; AB4360, Abcam) and rat brain (OCT3 and NET; generous gift from Dr. Anne Dorrance, Department of Pharmacology and Toxicology, *Michigan State University*). In all experiments, two tissue sections from the same animal were developed: one with primary antibody included, and one with the primary antibody omitted from the reaction.

7. Enzymatic tissue dissociation

Whole RA and RVC tissues were isolated, cleaned of perivascular fat, and cut into thin rings. Rings were transferred to microcentrifuge tubes and incubated with dissociation solution (80 mM NaCl, 80 mM monosodium glutamate, 5.6 mM KCl, 20 mM $MgCl_2$, 10 mM HEPES, 10 mM glucose, and 1 mg/mL BSA, pH 7.3) with 1 mg/mL DTT and 0.3 mg/mL papain for 18 min in a 37°C water bath. The solution was removed and replaced with fresh dissociation solution containing 100 μM $CaCl_2$ and 1 mg/mL collagenase and incubated 9 min in a 37°C tissue bath. The solution was removed and cells were resuspended in dissociation solution by gentle trituration. Cells were then transferred to coverslips using a Shandon Cytospin 4 Centrifuge (Thermo Scientific, Waltham, MA, USA) before performing immunocytochemical analysis.

8. NE-biotin

In some studies, a NE-biotin conjugate (IBL, Hamburg, Germany) was utilized to visualize NE by taking advantage of the extremely high binding affinity of the streptavidin-biotin interaction (K_d = 10^{-15}). NHS-x-Biotin was used to create NE-biotin. Synthesis took place in dimethylformamide (DMF). Coupling of the amine to biotin was checked through thin layer chromatography and purity verified using HPLC. NE-biotin

stocks were 1 mg/ml and calculated to be 1.61 mM. NMR analysis by the manufacturer revealed NE-biotin to be a mixture of species, with the biotin attached to the primary amine and hydroxyl groups. The ratio of these species was unable to be determined. Due to the nature of the TG reaction, it is reasonable to assume that only NE-biotin moieties in which the biotin was conjugated to the hydroxyl groups could be used as a substrate for the TG reaction, as coupling of the biotin to the amine group in NE would prevent this. In our experiments, the concentration of NE-biotin used was the maximum possible. We feel this justifiable, as NE-biotin was used to track the location of NE in a qualitative, and not quantitative, manner.

9. NE-Biotin uptake in VSMCs

Freshly dissociated RA or RVC cells, or cultured RA VSMCs, were equilibrated in PSS plus the MAO inhibitor pargyline (10 μM) for 30 min prior to incubation with either NE-biotin (12.7 μM) or vehicle (DMF) for 1 h. After 1 h, cells were washed 3x with PBS prior to fixation and immunocytochemical staining (below).

10. NE-Biotin uptake in whole tissues.

Whole tissues were incubated in TG reaction buffer (50 mM Tris-HCl, pH 7.5, 150 mM NaCl, and 5 mM $CaCl_2$) plus protease inhibitors (1 mM PMSF, 2 mg/ml aprotinin and leupeptin, 1 mM sodium orthovanadate) containing NE-biotin in the presence of vehicle or 1 mM cystamine at 37^{o}C for 1 h. Tissues were then homogenized and proteins were separated by SDS-PAGE on 10% SDS gels (Bio Rad, Berkeley, CA, USA), and transferred to nitrocellulose. Blots were blocked overnight at 4^{o}C in 4% CEO (weight/volume in TBST), washed in TBST for 20 min, and incubated for 1 h at 4^{o}C with HRP-conjugated streptavidin. Blots were washed (TBST and TBS)

and then exposed to ECL to visualize bands. Films were scanned and placed within the figure without gamma modifications using Adobe Photoshop.

11. Immunocytochemistry

Freshly dissociated VSMCs were rinsed in PBS and fixed in Zamboni's fixative (Newcomer Supply, Madison, WI, USA) for 20 min, followed by permeabolization by incubating in 0.1% Triton X-100 for 20 min. Cultured VSMCs were rinsed and then fixed with acetone for 1 min. After fixation, cells were washed 3x with PBS, and the appropriate (i.e., from the same species as the host of secondary antibody used) blocking serum (diluted to 1% in PBS) was added. Cells were incubated for 30 min at 37°C, then the appropriate primary antibody was added (see **Table 5**) to the blocking serum. Cells were incubated with primary antibody for 1 h at 37°C, washed briefly 3x with PBS, and then incubated with secondary antibodies (see **Table 6**) for 1 h at 37°C while shielding from light. After incubation in secondary antibodies, cells were washed briefly 3x in PBS. The cover slips that contained the stained cells were then blotted dry and mounted on slides using Prolong Gold medium with 4',6-diamidino-2-phenylindole (DAPI; Invitrogen) and sealed with nail polish. Most slides were viewed and photographed on a Nikon Eclipse Ti-S microscope (Nikon Instruments Inc., Melville, NY, USA) using NIS Elements BR 3.00 software (Nikon Instruments Inc.). The light source was a Nikon intensilight C-HGFI (Nikon Instruments Inc.), and the camera a Nikon Digital Sight DS-Qi1 (Nikon Instruments Inc.). Slides were viewed under either a 60x or a 100x Nikon Plan Apo oil-immersion objective using non-drying immersion oil, type A (Nikon Instruments Inc.). Three Nikon filters were used: UV-2EC 96310 (lot number: C109990), HYQ TRITC 96321 (lot number: C112237) and HYQ FITC 96320 (lot

number: C111294). Excitation ranges were: UV-2EC 340-380 nm, HYQ TRITC 528-552 nm, and HYQ FITC 450-490 nm. Emission ranges were: UV-2EC 435-485, HYQ TRITC 580-632, and HYQ FITC 515-555. OCT3 and NET immunocytochemical staining was visualized on an Olympus FV1000 confocal microscope system. Unless noted, images were unaltered when combined into the overlay image. No gamma modifications were made.

12. TG activity assay

TG activity assays on RA and RVC homogenates from normal rats and on mouse aorta homogenates from Melino TG2 KO and WT mice were performed using the amine donor 5-(biotinamido)pentylamine (BAP; Prod. # 21345, Thermo Scientific) (188). This assay has been used to measure FXIII (157), TG1 (14), TG2 (198), and TG4 (174) activity, supporting the idea that it is an assay for general TG activity. That BAP incorporation is increased in high calcium environments and decreased with low calcium (158) supports the idea that BAP incorporation is dependent on TG-activity, as all TGs require calcium for full activity. In some experiments, NE-biotin was used as a substitute for BAP. Protein homogenate was placed in reaction buffer (50 mM Tris-HCl, pH 7.5, 150 mM NaCl, 1 mM PMSF, 2 mg/ml aprotinin and leupeptin, 1 mM sodium orthovanadate, 5 mM CaCl2) containing 8 mM BAP and either vehicle, 50 μM Z-DON (a TG2-specific inhibitor; Zedira, Darmstadt, Germany), or 1 mM cystamine (a general TG inhibitor; Sigma, St. Louis, MO, USA) for 1 h at 37°C, after which an equal volume of 2X SDS sample buffer was added to stop the reaction. Homogenates were separated by SDS-PAGE, transferred to PVDF, and blocked overnight in CEO [4% w/v in tris-buffered saline (25 mM Tris, 150 mM NaCl, 2mM KCl, pH 7.4) with 0.1 % Tween-20 and 0.025%

NaN_3]. The next day, blots were washed in tris-buffered saline for 20 min, and then incubated with HRP-linked streptavidin (1:2000, 1 h., 4°C, GE Healthcare). BAP incorporation was visualized using ECL® reagents. Quantification of bands in the BAP TG activity assay was done by gel densitometry with UN-SCAN-IT® gel automatic digitizing system software (Silk Scientific, Orem, UT).

13. NE uptake assay

Whole RA and RVC tissues were cleaned and cut into rings (up to six rings for RA, 2 rings for RVC tissues). Samples were equilibrated in PSS with pargyline (10 μM) and RO 41-0960 (1 μM) to inhibit NE metabolism via MAO and COMT enzymes, respectively. Inhibitors of NET uptake (1 to 10 μM nisoxetine), OCT3 uptake (100 μM corticosterone), both (10 μM nisoxetine and 100 μM corticosterone), or vehicles (PSS for nisoxetine, DMSO for OCT3) were added and samples were incubated at 37°C for 30 min prior to the addition of NE (10 μM) or vehicle (PSS). After incubating for 30 min at 37°C, tissues were removed from the solution, washed briefly 3x by dipping tissues in 1 mL of fresh PSS, blotting tissues with Kimwipe® paper (Kimtech Science Brand, Kimberly-Clark Worldwide, Inc., Roswell, GA, USA), and then dipped in a clean 1 mL of PSS. This was then repeated 3x with tissue buffer (0.05 mM sodium phosphate and 0.03 mM citric acid buffer, pH 2.5, containing 15% methanol). After a final blot, tissues were placed into tubes, 75 μl of tissue buffer was added, and samples were frozen overnight at -80°C. The following day, tissues were thawed on ice, briefly sonicated with 3 x 1 s bursts in a cup horn sonicator, and centrifuged at 18,000 g for 10 min at 4°C. Supernatant was removed for analysis of NE content. NE content was measured using HPLC with electrochemical detection. Ten μl of the supernatant was injected into a C-18

reverse-phase analytical column (3 µm particle size, 80 x 4.6 mm H-R80 catecholamine column; Thermo Scientific, Waltham, MA, USA) and coupled to a coulometric electrode-conditioning cell in series with dual-electrode analytical cells (Thermo Scientific). The conditioning electrode potential was set at +0.2 V; the analytical electrodes were set at +0.10 and -0.35 V. Mobile phase (Cat-A-Phase® II) was a proprietary solution from Thermo Scientific (Product # 45-0216). The amount of NE in the samples was determined by comparing peak heights (determined by a Coulochem III detector (Thermo Scientific) with those obtained from standards generating an external standard curve. NE content was expressed relative to protein of the remaining tissue pellet.

In some experiments, cultured RA VSMCs were used in place of whole tissues. VSMCs were grown in P60 dishes until confluent. Cells were starved of serum 24 h prior to experimentation because serum contains NE (determined by HPLC). Cells were incubated for 30 min in PSS with pargyline (10 µM) and RO 41-0960 (1 µM) before incubation with NE. After 30 min in NE, cells were placed on ice, washed 3 times with PSS, then 3 times in tissue buffer, before finally being scraped in tissue buffer. Cells were placed in a 1.5 ml microcentrifuge tube and centrifuged (14,000 rpm, 10 min). The supernatant was removed for HPLC analysis of NE and the protein concentration of the pellet was measured as described above for whole tissues.

To determine the protein concentration in the remaining pellet, 200 µl of 1 M NaOH was added to the remaining tissue, which was subsequently frozen overnight. The following day, the tissue was sonicated, using a microtip attachment, for 15 s at 30 Amps. Samples were then cooled on ice for 1 min, and sonication was repeated until the tissue was completely disrupted (typically 2 to 3 rounds of sonication were

necessary). These samples were centrifuged at 18,000 g for 10 min at 4°C, after which the supernatant was removed and protein concentration was determined with a BCA assay.

14. TG substrate Identification

Two to three RA or 5 to 6 RVC were pooled while making protein homogenates to ensure enough protein was obtained. Tissues were taken fresh from animals, cleaned of perivascular fat and clotted blood, frozen using liquid nitrogen, and pulverized into a powder using a mortar and pestle. Lysis buffer (10 mM Tris, 0.5 mM EDTA, 0.5 mM β-mercaptoethanol, and 0.1% Triton X-100; pH 8.0) plus protease inhibitors (1 mM PMSF, 2 mg/ml aprotinin and leupeptin, 1 mM sodium orthovanadate) was added (250 µl per RA, 50 µl per RVC), tissues were ground for an additional min in buffer, and then lysates were collected in centrifuge tubes. Tubes were briefly sonicated (6 x 1 min), centrifuged at 18,000 g for 10 min, and supernatant was removed and placed in a fresh tube while the remaining pellet was discarded. Protein concentration of the supernatant was immediately determined using a BCA protein assay. Samples were then frozen at -80°C until the TG reaction was performed.

TG reactions were performed in lysis buffer in the presence of 5 mM $CaCl_2$ and 1 mM dithiothreitol (DTT), plus protease inhibitors (same as above). RA and RVC protein was diluted to 1 µg/µL (a total of 400 µg of protein was used per substrate condition), and the appropriate substrate (4 mM BAP or 12.7 µM NE-biotin) or control (lysis buffer) was added. Samples were incubated at 37°C for 1 h, at which point samples were removed, and an aliquot of protein (20 µg) was removed. Fifteen µL of 2x SDS loading buffer was added to the aliquot, samples were boiled for 10 min, and then separated by

SDS-PAGE. Samples were transferred to a PVDF-FL membrane, and visualization of TG substrate incorporation was visualized using IRDye 800CW labeled streptavidin, as described in the Western analysis methods section above.

To the remaining TG reaction solution, 1% SDS was added [to prevent non-specific protein binding to Dynabeads MyOne streptavidin-Coated C1 beads (catalog # 650-02, Invitrogen)] and samples were placed on ice while dialysis units were prepped. Slide-A-Lyzer® Dialysis cassettes (Prod# 66330, Thermo Scientific, Rockford, IL, USA) were used according to the manufacturer's instructions. Cassettes were hydrated by incubating in PBS for at least 2 min prior to use. Samples were diluted to 2 mL with PBS plus protease inhibitors (cOmplete Mini Protease Inhibitor Cocktail Tablets, Roche Applied Science, Indianapolis, IN, USA; 1 tablet/10 mL of PBS) prior to loading sample into dialysis cassette. Samples were allowed to dialyze with 500 mL of PBS for 2 x 2 h, then overnight, at 4°C. Samples were then removed from dialysis unit and added to streptavidin-coated beads (600 µl of beads per sample prepared by washing 3x in PBS, per the manufacturer's instructions, and resuspended in 300 µL of PBS plus Roche Inhibitor cocktail and 0.1% SDS), allowed to tumble for 2 h at 4°C. This volume of beads used was deemed necessary by preliminary experiments (**Figure 7**). Beads were captured using a magnet (Dynal MPC®-M, Prod. No. 120.09, Invitrogen). Supernatant was removed, and beads were washed 3x with PBS plus protease inhibitors. After the final wash, beads were resuspended in 200 µl of PBS plus protease inhibitors, placed on ice, and taken to the proteomics facility at *Michigan State University* to be analyzed by tandem mass-spectrometry to identify proteins captured.

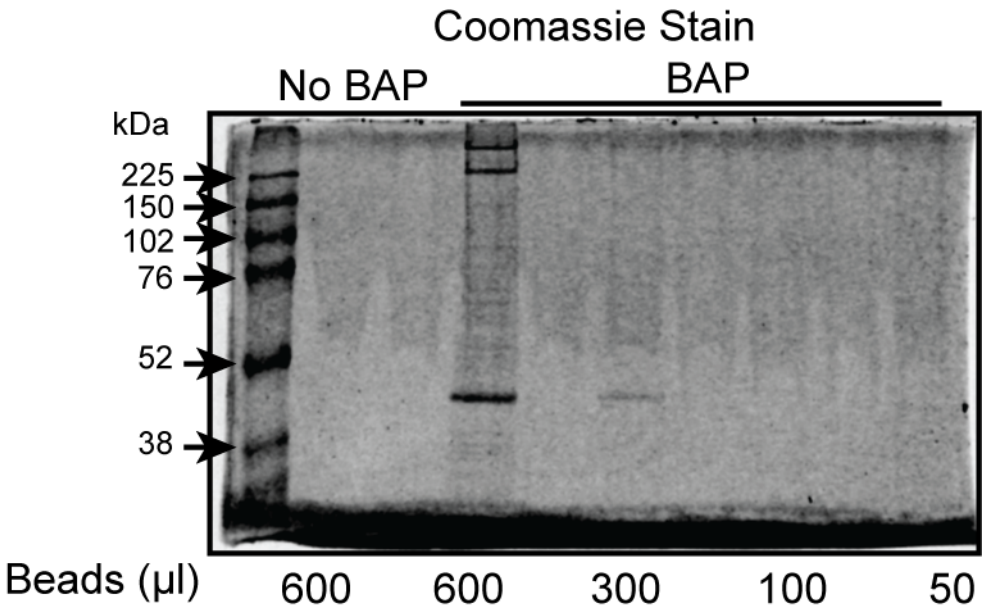

Figure 7. Streptavidin-coated magnetic bead optimization.

Coomassie (stain of RA proteins captured by streptavidin-coated magnetic beads after performing a TG assay in the presence of 4 mM BAP or vehicle, incubating the samples with 1% SDS, and dialyzing the samples. Several concentrations of beads were tested. A control sample of RA that was incubated in vehicle instead of BAP, incubated in 1% SDS, dialyzed, then incubated with 600 µl of beads. The first lane is a molecular weight marker, and the adjacent lane the no BAP control. Every other subsequent lane is loaded with the same sample of RA incubated with BAP, but then captured using the concentration of beads shown. The gel was stained with Coomassie, and imaged using the LiCor Odyssey FC equipment using the 700 nm channel.

15. α-actin immunoprecipitaton

After performing a TG reaction assay (see above) with RA homogenates (200 µg) using 12.7 µM NE-biotin, an anti-α-actin antibody was added and samples were placed on ice. After 2 h, 30 µg of protein A/G beads were added to samples. Samples were diluted with 1 mL of PBS with protease inhibitors (1 mM PMSF, 2 mg/ml aprotinin and leupeptin, 1 mM sodium orthovanadate) and tumbled overnight at 4°C. The next day samples were centrifuged at 900 g, supernatant was removed, and samples were washed with PBS plus protease inhibitors. This was repeated two more times (total of three washes), after which 30 µL of SDS loading buffer was added. Samples were boiled for 10 min, and then centrifuged at 900g for 10 min . Supernatant was collected, separated on a 12% acrylamide SDS gel, transferred to nitrocellulose, and blocked overnight. Bands were subsequently visualized using HRP-linked streptavidin and ECL chemiluminescent reagent. After visualization, blots were reprobed with the anti-α-actin antibody, and α-actin reactive bands were visualized using IRDye 800 anti-mouse LiCor secondary antibody.

16. Isometric contraction

Endothelial cell-intact rings of RA and RVC tissues were hung in tissue baths for isometric tension recordings using Grass transducers and PowerLab data Acquisitions (Colorado Springs, CO, USA). Rings were pulled to optimum resting tension (4000 mg for RA, 1000 mg for RVC), and equilibrated for 1 h, with washing, prior to exposure to compounds. Tissue baths contained 37°C, aerated (95% O_2/CO_2) PSS. To test viability, aortic rings were treated with an initial concentration of 10 µM phenylephrine (PE), an α_1-adrenergic receptor agonist. Since the RVC does not contract to PE, vena cava rings

were treated with an initial concentration of 10 μM NE. All tissues had an intact endothelial layer, evidenced by a robust (>50%) relaxation to acetylcholine (1 μM) in tissues contracted to half-maximum with PE (RA) or contracted to 10 μM $PGF_{2\alpha}$ (RVC). Tissues were incubated with vehicle (water) or the TG inhibitor cystamine (0.01 - 1 mM) for 30 to 60 min prior to cumulative addition of NE (10^{-9} -10^{-5} M). Tissues were then washed, incubated in the same concentration of cystamine or vehicle for 30 to 60 min prior to the cumulative addition of the non-receptor mediated contractant potassium chloride (KCl, 6-100 mM). Data are reported as a percentage of the initial contraction to PE (RA) or NE (RVC).

17. Data Quantification

Band densitometry in the Western analysis was performed using ImageJ. Grayscale images of blots (either from scanned film or captured using the Li-Cor equipment mentioned above) were opened in ImageJ. Using the “Rectangular Selections” tool, bands to be analyzed were selected, ensuring that the rectangles were taller than they were wide and of uniform size for each lane. The first lane was selected by going under “Analyze” drop down menu, going to “Gels” and selecting “Select First Lane.” The rectangular selection was then moved to the second lane, and this process was repeated, substituting “Select First Lane” with “Select Next Lane.” This process was repeated until all lanes had been selected. Lanes were plotted by going to “Analyze” drop down menu, “Gels,” and selecting “Plot Lanes.” The “Straight line selections” tool was used to draw a line across the base of the peak to enclose the peak for each plot created. The area of the blot was assessed by using the “Wand (tracing) tool.” Values

obtained from these data were copied into Microsoft® Excel®. The band intensity of the protein of interest was normalized to a loading control protein, either α- or β-actin, by dividing the densitometric data obtained for the protein of interest with that obtained for the loading control.

Contractility data were recorded in milligrams and normalized to an initial, maximal challenge with adrenergic agonist (NE for the RVC, PE for RA), and reported as a percentage of initial adrenergic response to account for variations in tissue size and viability. Comparisons where $P < 0.05$ are considered significant.

18. Statistical Analysis

Mean, standard error and variance was calculated for all data sets. For comparisons of two samples of equal variance, statistical significance between groups was established using two-tailed, unpaired Student's t-tests ($\alpha=0.05$).

Chapter 3: Results

Overall Hypothesis: The TG-mediated amidation of VSMC proteins by NE stimulates a measureable physiological response.

1. Aim 1: Vascular tissues, and specifically VSMCs within these tissues, express active TGs that can catalyze the amidation of NE to vascular proteins.

Rationale: In many ways, the vasculature is an ideal model to test the hypothesis that the amidation of proteins by NE is a physiologically significant process that stimulates a measureable response. VSMCs express at least one TG enzyme, TG2 (12), and may express more, as the global expression of TGs in the vasculature has, to our knowledge, not been investigated. In addition, vascular tissues not only have access to a plentiful source of NE via the sympathetic nervous system, but also rely on this NE to maintain homeostatic function. NE's function in the vasculature has been entirely attributed to its interaction with adrenergic receptors. However, in this study, we investigate an alternative hypothesis for how NE regulates vascular function; namely, that NE can be utilized as a TG substrate to amidate proteins, thus altering their function and leading to a physiological response. Our hypothesis does not necessarily exclude the possibility that NE is also acting at adrenergic receptors to stimulate vascular function. Rather, it is likely that adrenergic receptor stimulation and protein amidation work cooperatively, as activation of adrenergic receptors may be needed to elevate intracellular calcium levels to a concentration that activates the amidation activity of TGs so that protein NE-amidation can occur. This is supported by studies that have shown that other forms of TG-mediated protein amidation are dependent on concomitantly activated receptors. For example, in A1A1v cells (a rat embryonic cortical

cell line), 5-HT(2A) receptor-coupled phospholipase C activation and subsequent intracellular calcium elevation is required for TG-mediated serotonylation of the small G protein Rac1 to occur (38).

For the amidation of vascular proteins by NE to occur, however, TGs must be expressed and active in vascular tissues, and must be able to use NE as a substrate. Previous studies have demonstrated that at least TG2 is present in VSMCs (10, 11, 14, 62, 68, 97, 128, 148). In this first series of experiments, we aim to test the hypothesis that vascular tissues, and specifically VSMCs within these tissues, express one or more active TG and that the vascular TGs present can use NE as a substrate for protein amidation.

1.1. Vascular TG expression

mRNA expression of vascular TGs

Using RT-PCR, we measured mRNA expression of the known TGs in normal RA and RVC tissues. Notable amounts of TG transcripts were expressed for four of the different TGs measured in both RA and RVC tissues: TG1, TG2, TG4, and FXIII (**Table 8**). In the RA, FXIII had the highest transcript expression when transcript levels were normalized to B2m transcript. TG2 and TG4 were also expressed in modest amounts, while TG1 expression was small but significant. In the RVC, TG2 was the predominant TG isoform expressed, with TG1, TG4, and FXIII all showing similar expression levels. The expression of TG1 and TG2 was significantly greater in the RVC compared to the RA. The relative amount of TG transcript expression was not significantly different between the two tissues for TG4 and FXIII.

	ΔC_t	
	RA	**RVC**
TG1	0.15 ± 0.03	2.0 ± 0.6*
TG2	2 ± 1	12 ± 3*
TG3	ND	ND
TG4	2.0 ± 0.5	2.4 ± 0.7
TG5	ND	ND
TG7	0.02 ± 0.01	0.03 ± 0.02
FXIII	3.7 ± 0.2	4 ± 1

Table 8. TG mRNA transcript expression.

ΔC_t values for TG mRNA transcript expression. Values are mean ± SEM derived from experiments performed on 3 different animals. TG expression is listed relative to B2m. For simplicity, values have been multiplied by 1000. mRNA expression was measured in about 10 mg of RA or RVC tissues. ND = No detection of mRNA by RT-PCR analysis. * = significantly different from RA expression.

Protein expression of vascular TGs

Western analysis was performed using RA and RVC tissues to determine the protein expression of the TGs for which mRNA was detected. Immunoreactive bands were detected using antibodies directed against TG1, TG2, and TG4 (**Figure 8**) in both RA and RVC tissues. Although a band appeared at the appropriate molecular weight in the positive control (HeLa cell lysate), no bands were detected for FXIII protein in RA or RVC samples. Densitometric analysis (**Figure 8B**; immunoreactive bands that were included in the analysis are denoted by arrows to the left of the blots in A) of the bands indicated that RVC tissues expressed slightly, but statistically significant ($P \leq 0.05$), more TG1 and TG2 protein than RA tissues [RA/RVC expression (TG/β-actin densitometry): TG1 = 0.60 ± 0.08; TG2 = 0.57 ± 0.08]. Though this trend continued with TG4 (RA TG4/β-actin = 0.70 ± 0.20 of RVC), it was not significant.

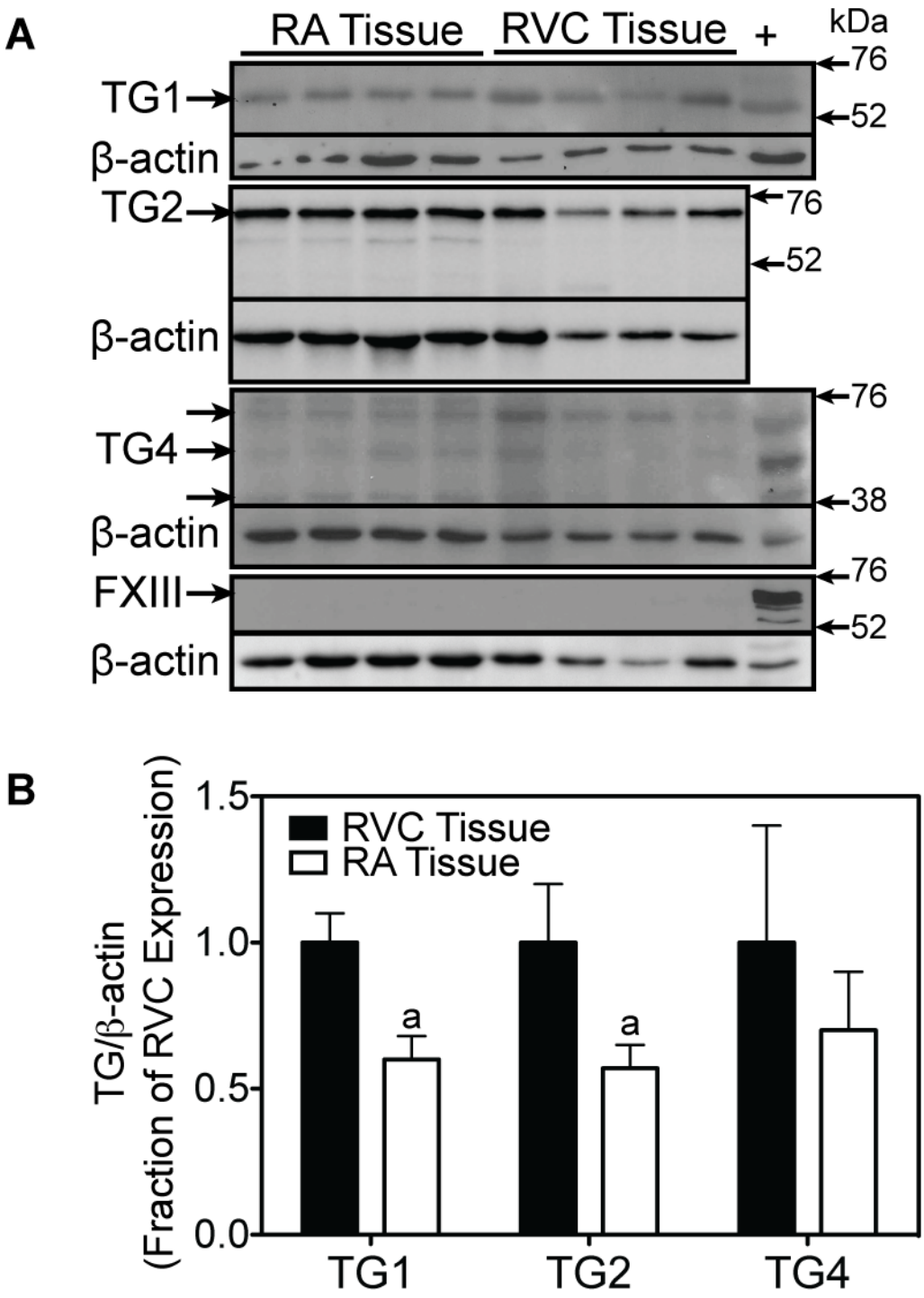

Figure 8. Western analysis for TG1, TG2, TG4, and FXIII protein in whole RA and RVC tissues.

Figure 8 (cont'd)

A) Western blots of RA and RVC proteins probed with anti-TG1, anti-TG2, anti-TG4, or anti-FXIII antibodies. Bands were detected for TG1, TG2, and TG4, but not FXIII, in RA and RVC samples. Blots were reprobed with an anti-β-actin antibody to confirm that similar amounts of protein were loaded in each lane. Each lane is a RA or RVC protein homogenate derived from a different animal; N = 4. + = positive control (TG1 = rat skin lysate; TG2 = not applicable; TG4 = rat prostate lysate; FXIII = HeLa cell lysate). Arrows to the left of the blots point to bands that were quantified for TG expression in B. **B)** Densitometry of the TG1, TG2, and TG4 Western blots from A. TG expression is normalized to β-actin expression, and shown as a fraction of total TG expression found for the TG in RVC tissues. a = significantly less TG protein expression compared to RVC tissues. $P \leq 0.05$.

TG immunohistochemistry

To determine where within vascular tissues TGs reside, immunohistochemistry for the four TGs detected by RT-PCR was performed in sections of RA and RVC tissues. Consistent with the results seen with Western analysis, TG1, TG2, and TG4, but not FXIII, were detected in both RA (**Figure 9**) and RVC (**Figure 10**) tissues. In both the RA and the RVC, TG1 staining (noted by arrows) was observed in all layers of the tissue (**Figure 9A** and **Figure 10A**). In contrast, TG2 staining is primarily localized to VSMCs in these tissues (**Figure 9B** and **Figure 10B**). This is especially evident in the RVC (**Figure 10B**), which is comprised of only a single layer of VSMCs located on the lumen side of the vessel. Here, TG2 staining was almost exclusively found in this innermost layer. TG4 staining, while not as diffuse as TG1 staining, was observed in multiple layers of the vessels, including the VSMC layers of these tissues (see arrows). Positive control tissue sections are shown in **Figure 11**.

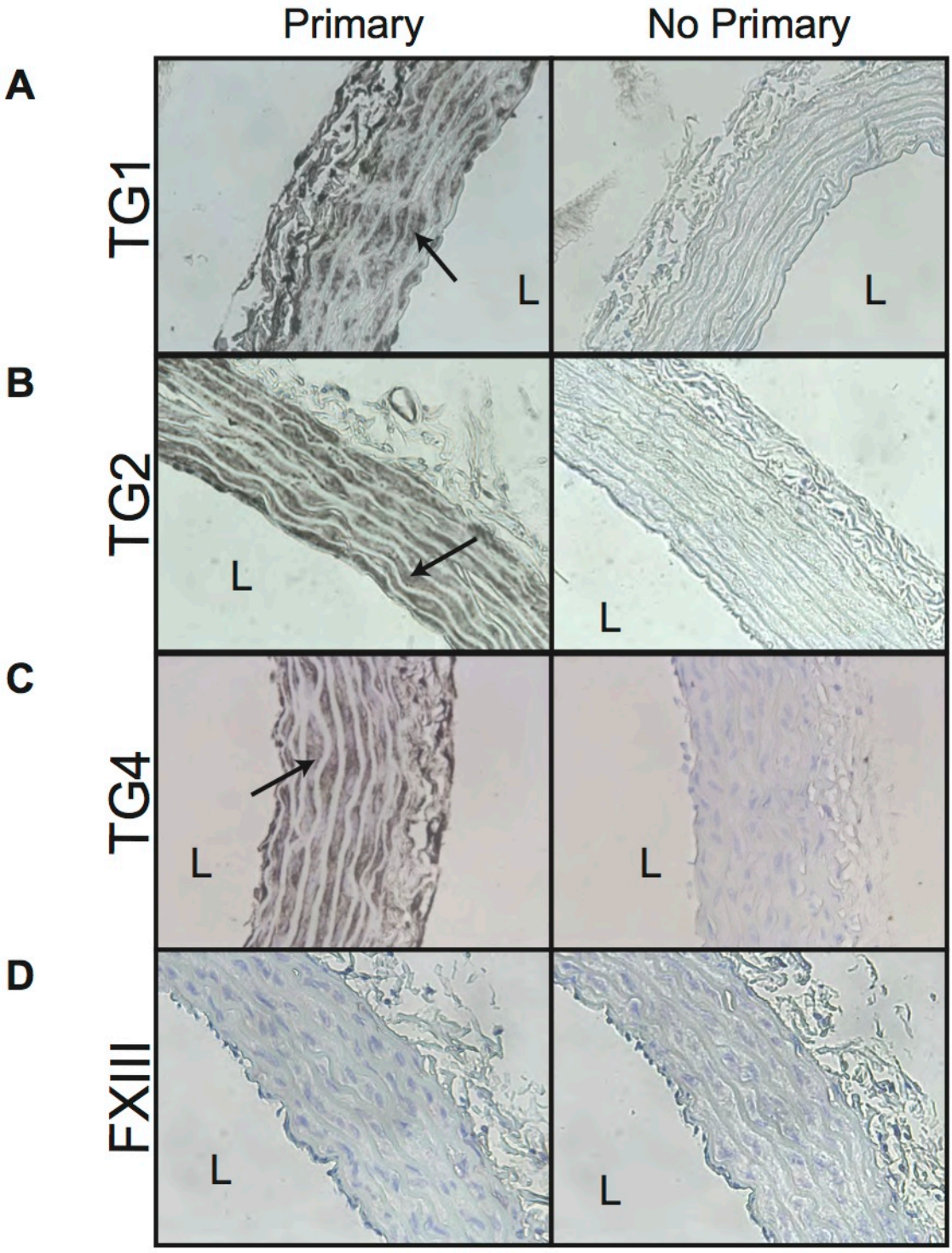

Figure 9. Immunohistochemical staining of vascular TGs in RA tissues.

Immunohistochemical staining in RA tissue sections was performed for **A)** TG1, **B)** TG2, **C)** TG4, and **D)** FXIII. Development of tissue sections resulted in positive staining for all

Figure 9 (cont'd)

TGs except FXIII. Representative of tissues from four different animals. Arrows point to regions of staining. Primary = tissue section incubated with primary antibody; No primary = primary antibody was left out of the reaction. L = lumen of the vessel.

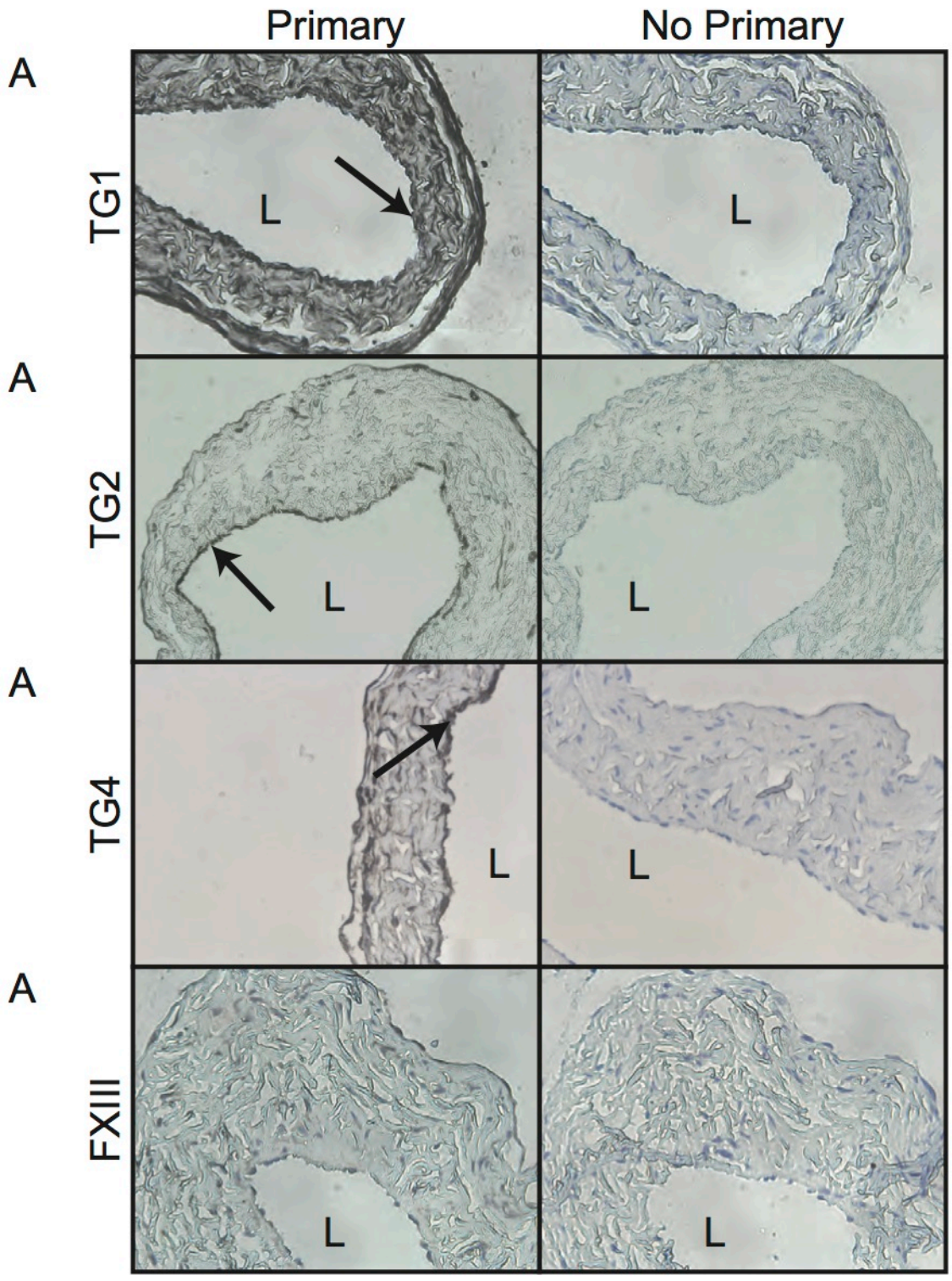

Figure 10. Immunohistochemical staining of vascular TGs in RVC tissues.

Figure 10 (cont'd)

Immunohistochemical staining in RVC tissue sections was performed for **A)** TG1, **B)** TG2, **C)** TG4, and **D)** FXIII. Development of tissue sections resulted in positive staining for all TGs except FXIII. Representative of tissues from four different animals. Arrows point to regions of staining. Primary = tissue section incubated with primary antibody; No primary = primary antibody was left out of the reaction. L = lumen of the vessel.

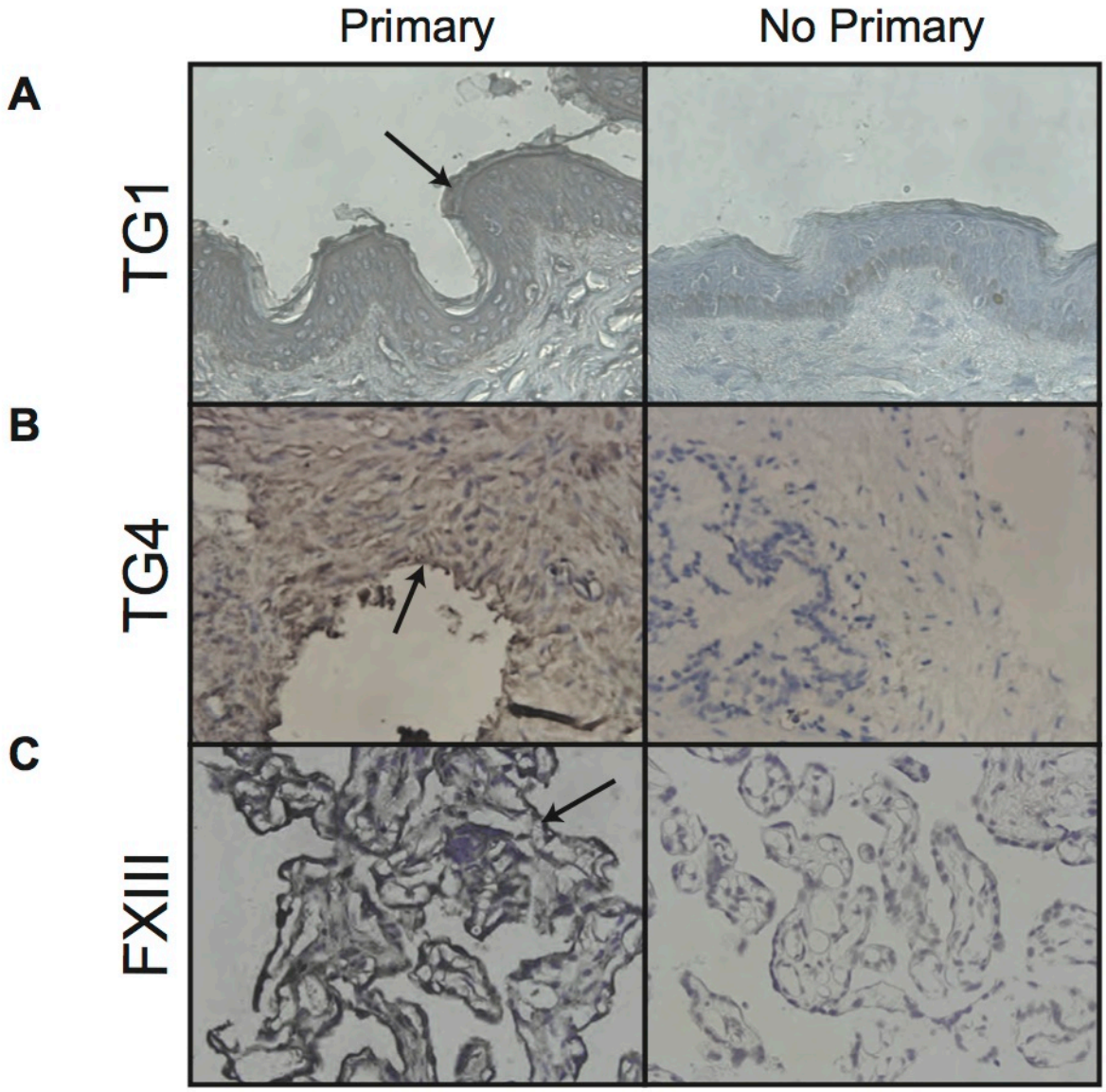

Figure 11. Immunohistochemistry of TG positive controls.

Immunohistochemical staining in positive controls sections was performed for **A)** TG1 (rat skin), **B)** TG4 (rat prostate), and **C)** FXIII (rat placenta). No positive control was included for TG2, as multiple reports have already shown the RA to have high expression (85, 123). Development of tissue sections resulted in positive staining for all

Figure 11 (cont'd)

TGs. Arrows point to regions of staining. Primary = tissue section incubated with primary antibody; No primary = primary antibody was left out of the reaction.

TG immunocytochemistry

Immunocytochemical staining was used to assess cellular vascular TG localization. Freshly dissociated RA (**Figure 12**) and RVC (**Figure 13**), and cultured RA (**Figure 14**) and RVC (**Figure 15**) VSMCs were utilized. Staining was observed in freshly dissociated RA and RVC VSMCs [confirmed as VSMCs by co-immunostaining for α-actin (green)] for TG1 (**Figure 12A** and **Figure 13A**), TG2 (**Figure 12B** and **Figure 13B**), and TG4 (**Figure 12**C and **Figure 13**C, red in the pictures). Paralleling the results observed by immunoblotting and immunohistochemistry, FXIII (**Figure 12D** and **Figure 13D**) was absent in VSMCs from these tissues, although rarely intense immunostaining for FXIII could be observed in non-VSMCs in RVC dissociations (~1 cell/dissociation; red cell in **Figure 13**D). For the expressed TGs, staining was observed throughout the cell. Interestingly, the TGs and α-actin appeared to colocalize (yellow in overlays), suggesting their interaction. In contrast to freshly dissociated VSMCs, staining for TGs (red) in cultured VSMCs from RA (**Figure 14**) and RVC (**Figure 15**), while present, was much less intense compared to freshly dissociated VSMCs, requiring a longer exposure time to observe positive staining. The TG2 detected in cultured RA VSMCs appeared to partially colocalize with α-actin (**Figure 14B**, yellow in the overlays), while in RVC VSMCs, it appeared that both TG1 and TG2 (**Figure 15A** and **B,** respectively) partially colocalized with α-actin (yellow in overlays).

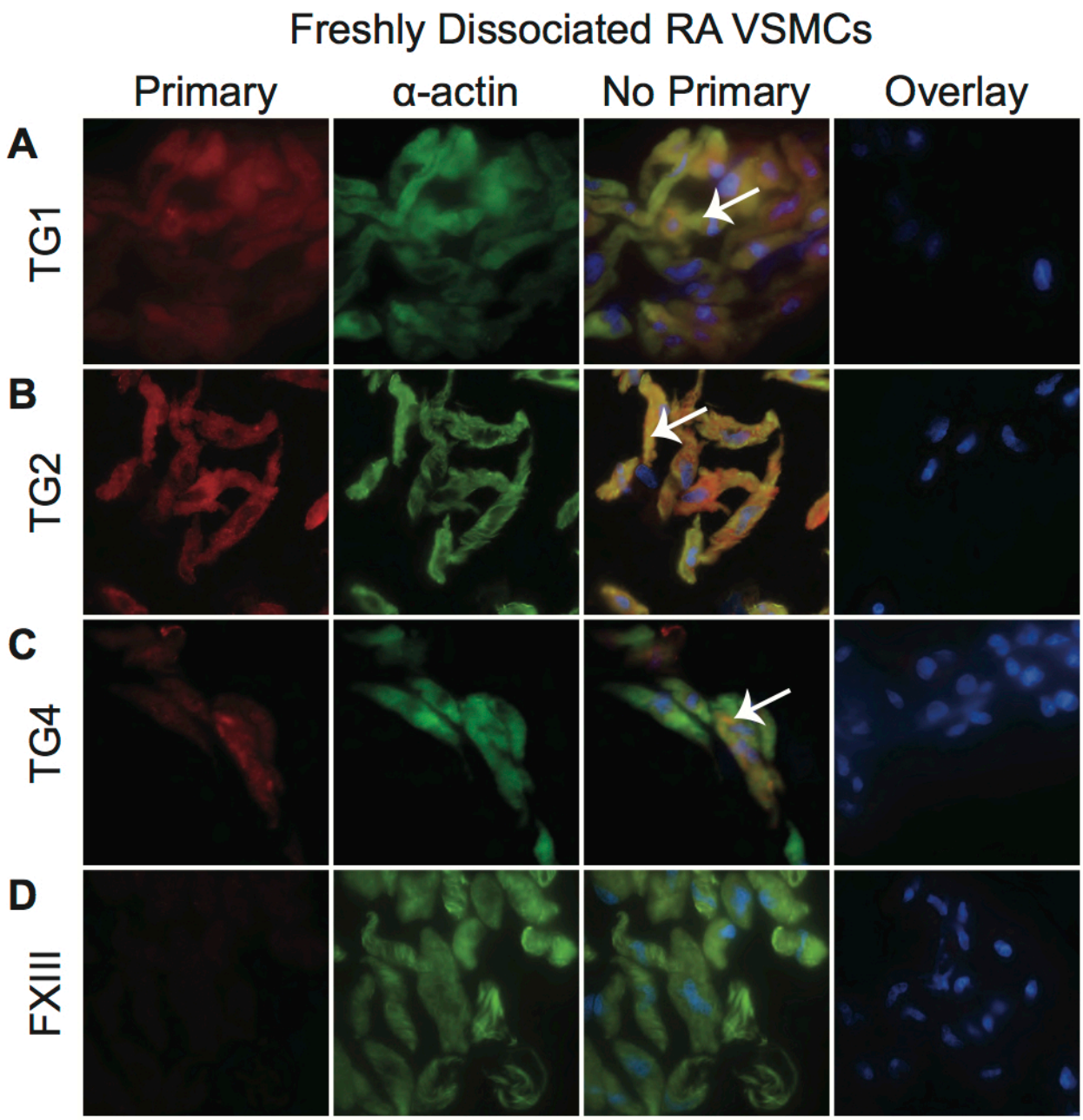

Figure 12. TG immunocytochemistry in freshly dissociated RA VSMCs.

RA tissues were enzymatically dissociated to yield VSMCs. Immunocytochemical detection of the TGs (red) demonstrated the presence of **A)** TG1, **B)** TG2, and **C)** TG4, but not **D)** FXIII. Confirmation that cells were VSMCs was made by costaining the cells with an anti-α-actin antibody (green). Overlaying the red and green channels shows

Figure 12 (cont'd)

colocalization (yellow) of TG1, TG2, and TG4 with α-actin. Arrows point to an area where the TG and α-actin appear to be colocalizing. Nuclei were observed by staining with DAPI (blue). "No Primary" denotes cells from the same tissue dissociation that were incubated with secondary, but not primary, antibody. Pictures are representative of tissue dissociations from 4 different animals.

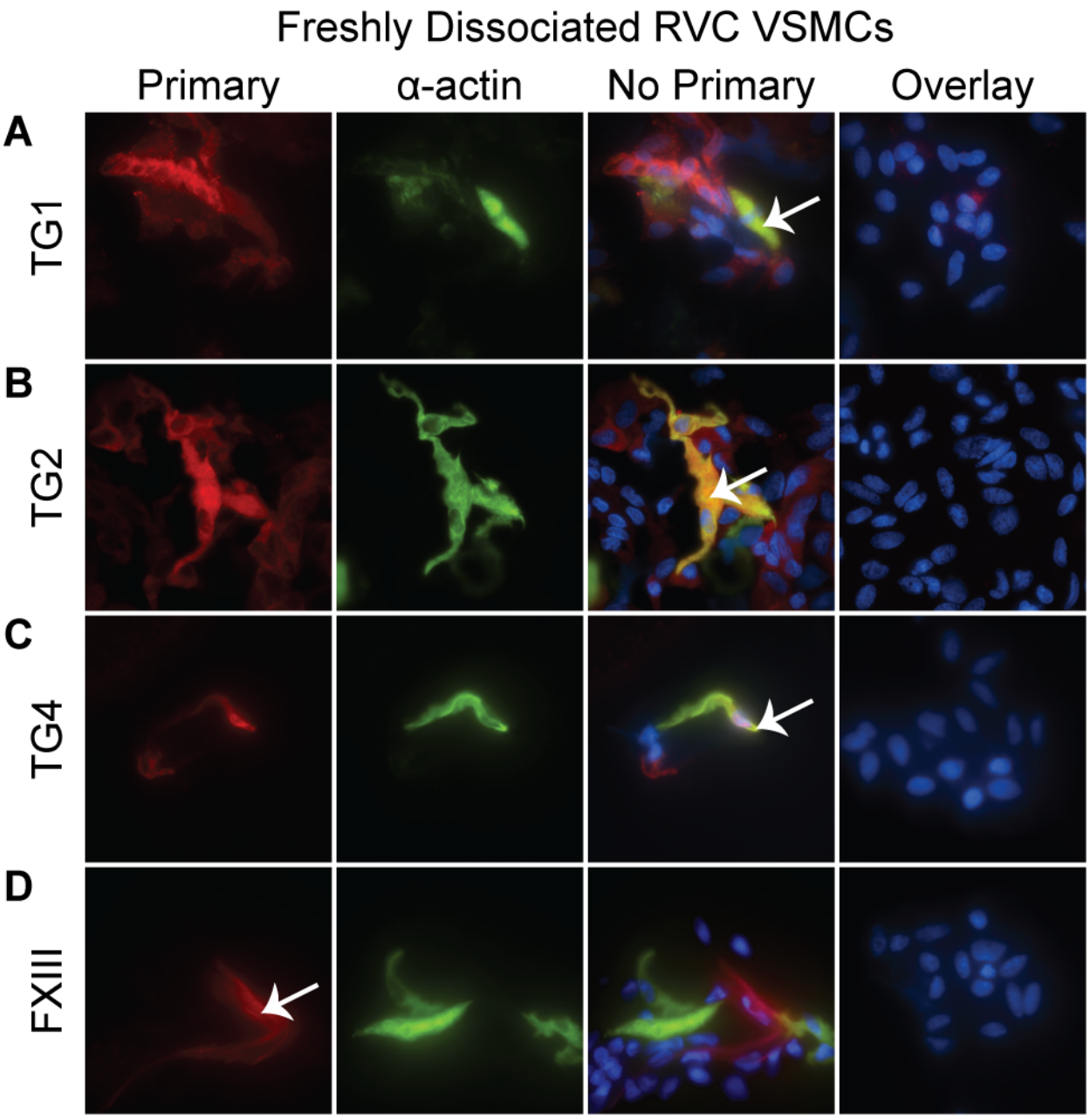

Figure 13. TG immunostaining in freshly dissociated RVC VSMCs.

RVC tissues were enzymatically dissociated to yield VSMCs. Immunocytochemical detection of the TGs (red) demonstrated the presence of **A)** TG1, **B)** TG2, and **C)** TG4, but not **D)** FXIII, in VSMCs. FXIII (red) was occasionally detected in the dissociation, but was absent in VSMCs. Confirmation that cells were VSMCs was made by costaining the

Figure 13 (cont'd)

cells with an anti-α-actin antibody (green). Overlaying the red and green channels shows colocalization (yellow) of TG1, TG2, and TG4 with α-actin. Arrows in A, B, and C point to areas of where the TGs and α-actin appear to be colocalizing. The arrow in D points to a FXIII positive cell in the dissociation that was *not* a VSMC. Nuclei were observed by staining with DAPI (blue). "No Primary" denotes cells from the same tissue dissociation that were incubated with secondary, but not primary, antibody. Pictures are representative of tissue dissociations from 4 different animals.

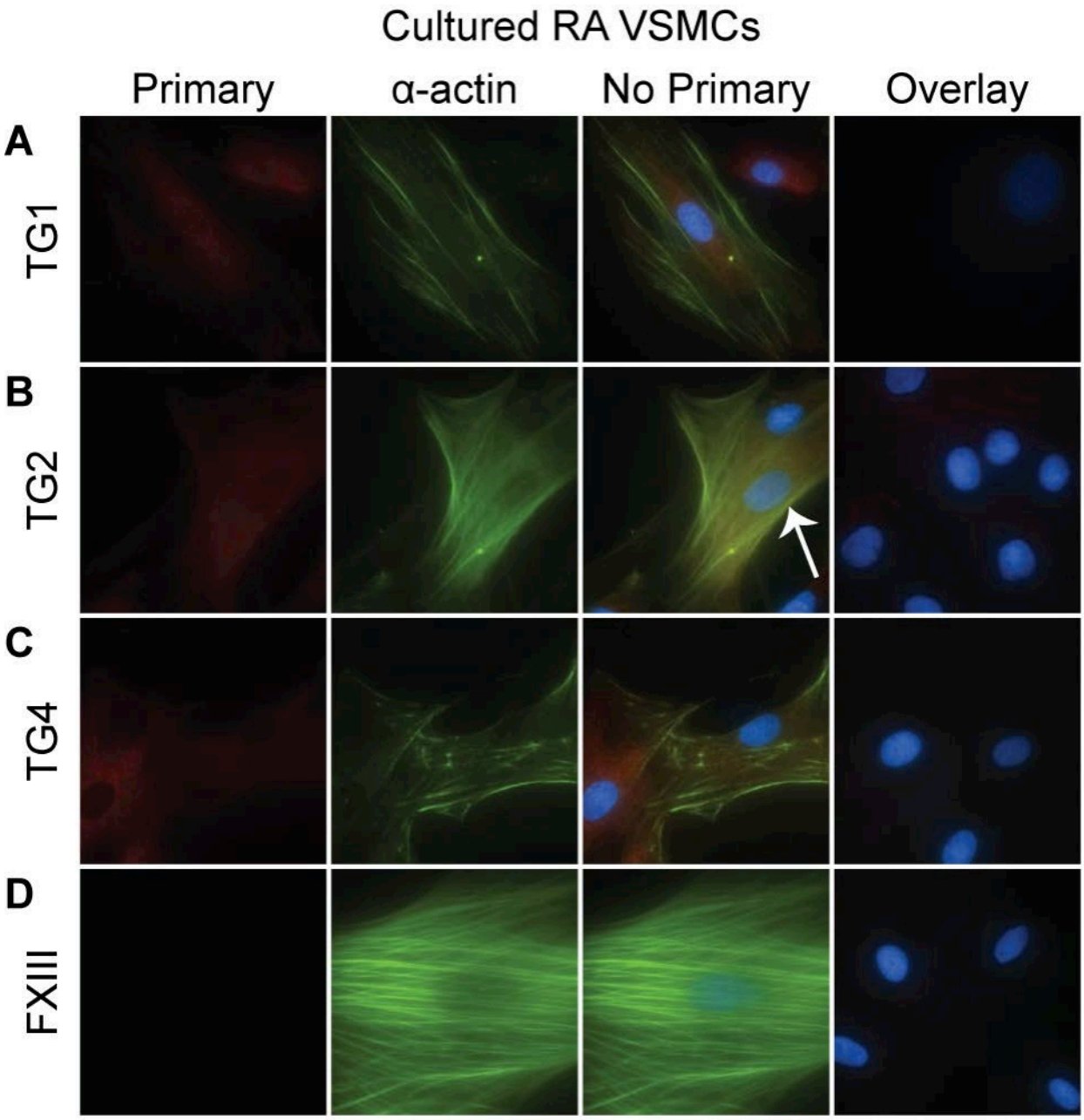

Figure 14. TG immunocytochemistry in cultured RA VSMCs.

Faint staining for TGs in cultured RA VSMCs was observed for **A)** TG1, **B)** TG2, and **C)** TG4. **D)** No staining was observed for FXIII. Confirmation that cells were VSMCs was made by costaining the cells with an anti-α-actin antibody (green). Overlaying the red and green channels shows colocalization (yellow) of TG2 with α-actin. Arrows in the

Figure 14 (cont'd)

overlays point to an area of possible colocalization. Nuclei were observed by staining with DAPI (blue). "No Primary" denotes cells derived from the same animal that were incubated with secondary, but not primary, antibodies. Representative of cultures VSMCs derived from 4 different animals.

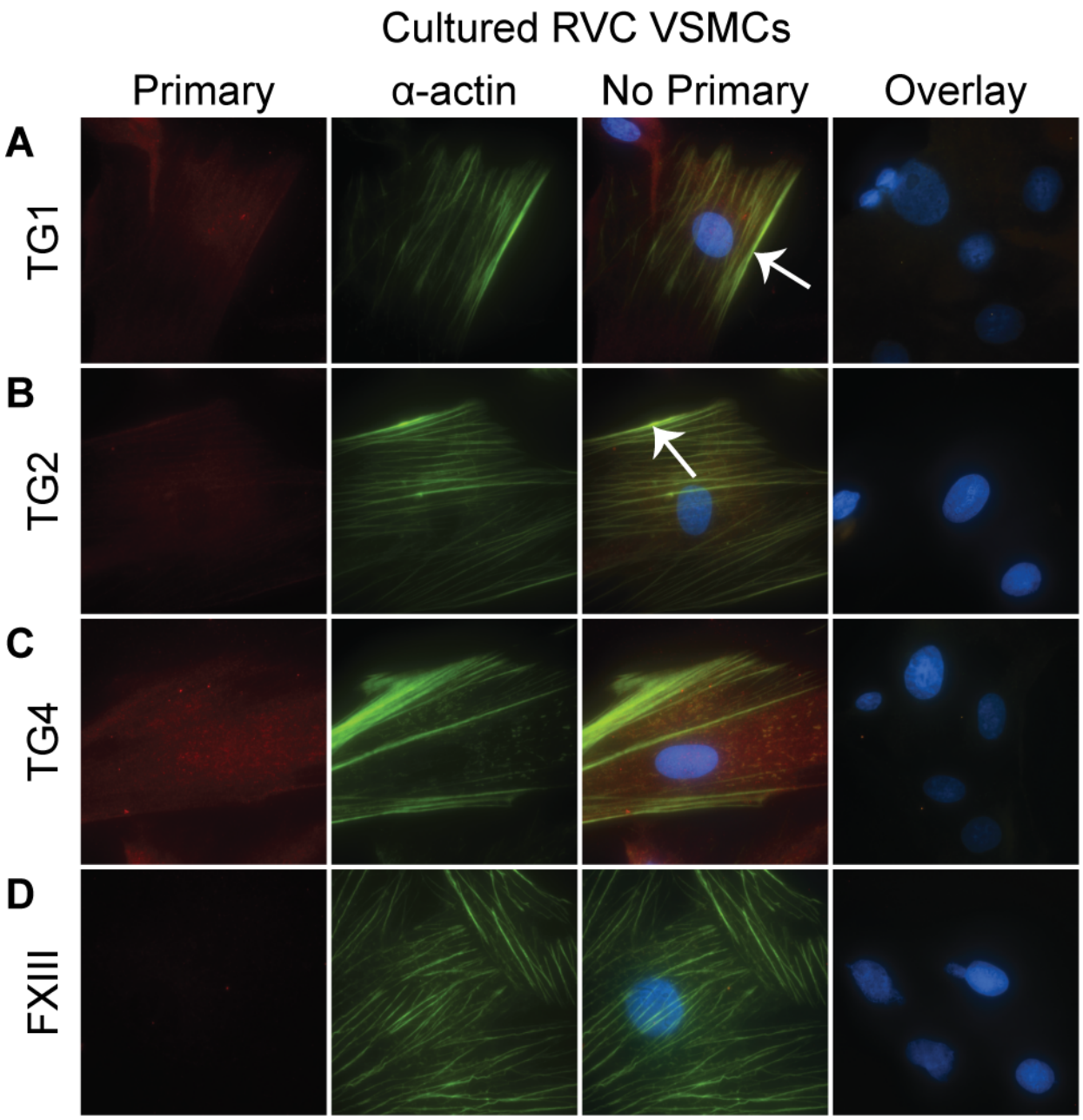

Figure 15. TG immunocytochemistry in cultured RVC VSMCs.

Faint staining for TGs in cultured RVC VSMCs was observed for **A)** TG1, **B)** TG2, and **C)** TG4. **D)** FXIII was not observed even faintly in the cell. Confirmation that cells were smooth muscle cells was achieved by staining the cells with FITC-conjugated smooth muscle cell specific α-actin (green). Nuclei were observed by staining with DAPI (blue).

Figure 15 (cont'd)

Overlaying the red and green channels reveals colocalization (yellow) of TG1 and TG2. Arrows in the overlays point to an area of possible colocalization. "No Primary" denotes cells from the same explant that were incubated with secondary, but not primary, antibodies. Representative of cultures VSMCs derived from 4 different animals.

TG expression in whole tissues compared to cultured VSMCs.

Because in the immunocytochemical staining data it appeared that TG expression was reduced in cultured compared to freshly dissociated VSMCs, Western analysis was performed to compare vascular TG protein expression between whole tissues and cultured VSMCs (**Figure 16**). TG1 expression was not significantly different between whole RA and cultured RA VSMCs (cultured VSMC/whole tissue expression: RA VSMCs = 1.0 ± 0.2 TG1/β-actin protein densitometry). However, for the RVC, cultured VSMC expression of TG1 appeared significantly lower than whole RVC tissues (cultured VSMC/whole tissue: RVC VSMC = 0.21 ± 0.05 TG1/β-actin protein densitometry). TG2 protein was essentially abolished in both RA and RVC VSMCs when compared to whole tissues (as a fraction of whole tissue expression: RA VSMC = 0.039 ± 0.006; RVC VSMC = 0.04 ± 0.02 TG2/β-actin protein densitometry). These data suggest that, upon adaptation to culture, RVC VSMCs have markedly reduced TG1 protein content and both RA and RVC VSMCs essentially lose their expression of TG2.

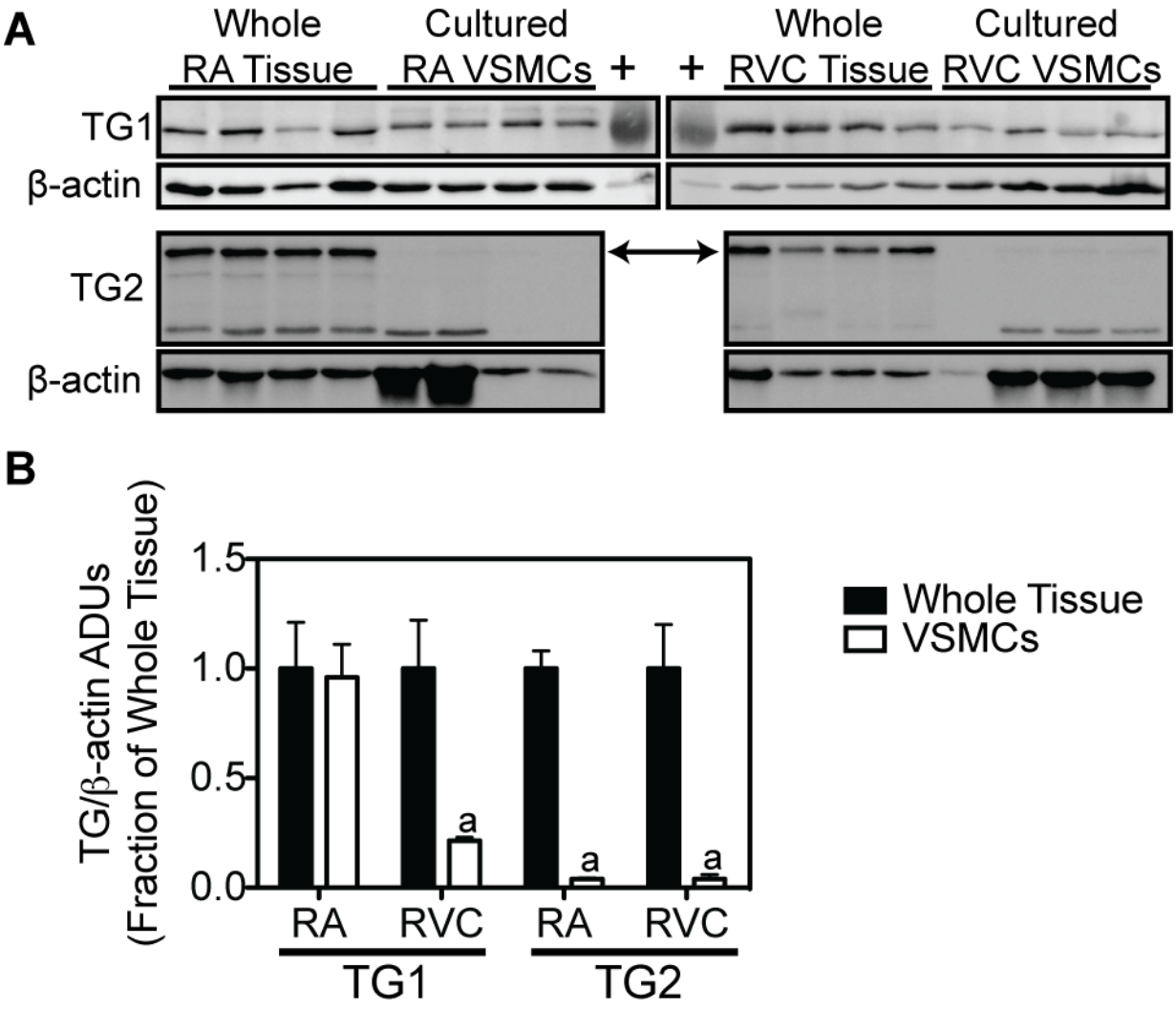

Figure 16. Western analysis of TG1 and TG2 in cultured VSMCs and whole tissues.

A) Western analysis comparing TG1 (top) and TG2 (bottom) protein content of whole tissues and cultured VSMCs from RA (left) and RVC (right). TG1 positive control (+) = rat skin lysate. Blots were redeveloped for β-actin protein expression as a loading control. Arrow points to bands used for densitometric analysis (B). TG band densitometry is expressed relative to β-actin. ADUs = Arbitrary densitometry units. a = significantly lower than whole tissue expression; $P < 0.05$. N = 4. Tissue and cell lysates were derived from different animals.

1.2. TG activity in vascular tissues

In order to visualize where in the tissue TG activity was present, incorporation of the biotinylated TG substrate BAP was visualized in situ using RA and RVC tissue sections (**Figure 17**). BAP acts as a *glutamine-acceptor* substrate, and its incorporation has been used to measure FXIII (157), TG1 (14), TG2 (198), and TG4 (174) activity, supporting the idea that it is an assay for general TG activity. Since all TGs require calcium for full activity, the observation that BAP incorporation is increased in high calcium environments and decreased with low calcium (158) supports the idea that BAP incorporation is TG-dependent. Both RA (top) and RVC (bottom) tissues incubated with BAP showed substantial fluorescence (red) compared to vehicle treated controls when probed with fluorescently labeled streptavidin. Fluorescence was primarily localized to the VSMC layer in these tissues, although fainter staining could be observed in other layers of the tissue as well. This was somewhat surprising, given that we observed TG1 and TG4 immunohistochemically in other layers besides the VSMC layers (**Figures 9A**, **9C**, **10A** and **10C**). This suggests that TGs are primarily active within the VSMC layers of RA and RVC tissues, despite some being present in other layers.

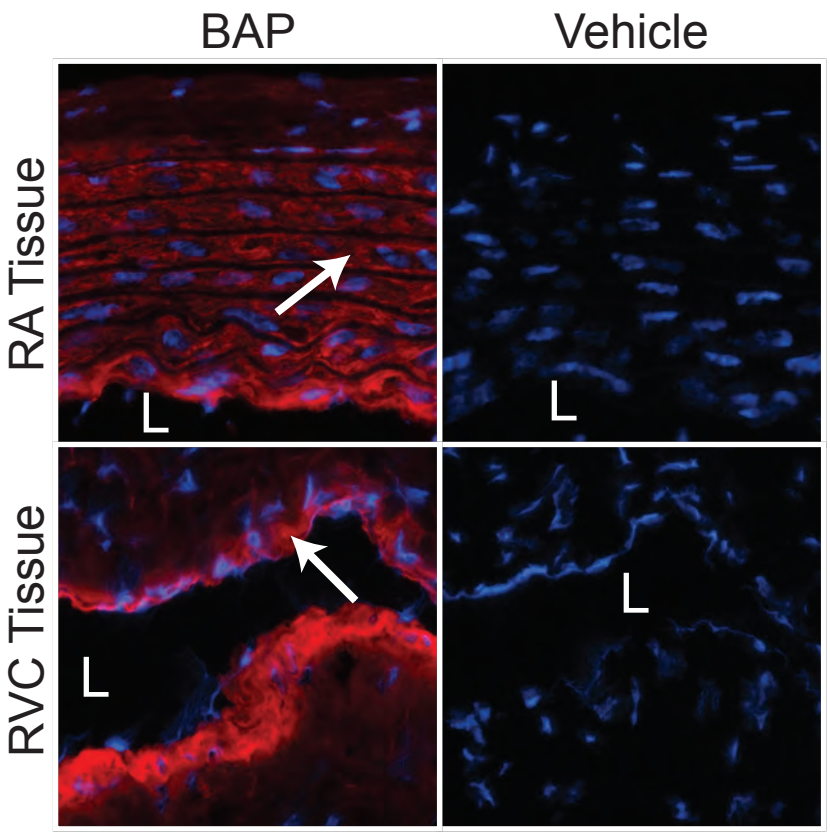

Figure 17. In situ visualization of general TG activity in RA and RVC tissues.

Fresh frozen RA (top) and RVC (bottom) tissues were incubated with the biotinylated TG substrate BAP. Adjacent sections in the same tissue were treated with vehicle. After treatment, tissues were washed, fixed, and immunocytochemical staining was performed to visualize BAP incorporation. BAP was visualized with fluorescently labeled streptavidin (red). Arrows point to areas of straining. DAPI (blue) was used as a nuclear stain. Representative of tissue sections from 4 different animals.

Genetic evidence for non-TG2 derived TG activity in the vasculature.

Previous studies have observed that TG2 KO mice exhibit a vascular phenotype only mildly different from their WT controls, with normal blood pressure and amine-induced vascular contraction (128). To reconcile this observation with data that suggests that TG is important for vascular function, such as previous studies in our laboratory demonstrating that TG activity is necessary for amine-induced vascular contraction (188), we tested the hypothesis that the other vascular TGs observed by Western analysis were also functional. Western analysis confirmed that TG2 protein (normalized to α-actin expression) in the Melino TG2 KO mouse aorta was virtually absent when compared to WT mouse aortae (**Figure 18A**). In contrast, no difference in protein levels were found for the other TGs surveyed (**Figure 18B** and **C**). The ability of TG2 KO mouse aortae to incorporate BAP into proteins in a pattern similar to WT (**Figure 19A**) suggests that these other TGs must be functional. Though the banding pattern of BAP incorporation into proteins was similar between WT and KO mouse aorta, there were some modest alterations in the KO compared to the WT. Overall, the general pattern showed a slight decrease in intensity of the bands in the KO compared to the WT (Representative data in **Figure 19B**, yellow and green lines). Some bands were completely lost (e.g. band 8), while others showed no difference between WT and KO (band 11). Cystamine (1 mM) generally reduced BAP incorporation in both the TG2 KO and WT mouse aorta (**Figure 19A** and **B**, red and blue lines). Interestingly, the presence of cystamine appeared to amplify some of the differences in BAP incorporation between the WT and KO mouse aorta. For example, no difference in intensity was observed between the WT and KO mouse for band 11 in **Figure 19** in the

absence of cystamine. However, when cystamine was added, the WT mouse aorta still had a bands indicating the incorporation of BAP, while these bands were greatly reduced and usually completely absent in the TG2 KO mouse [**Figure 19A** and **B**; in B, observe the difference in peak height for band 11 in the TG2 WT and KO under normal conditions (green and yellow lines) and in the presence of cystamine (red and blue lines)]. Together, these data provide genetic evidence that TGs other than TG2 are active in the vasculature.

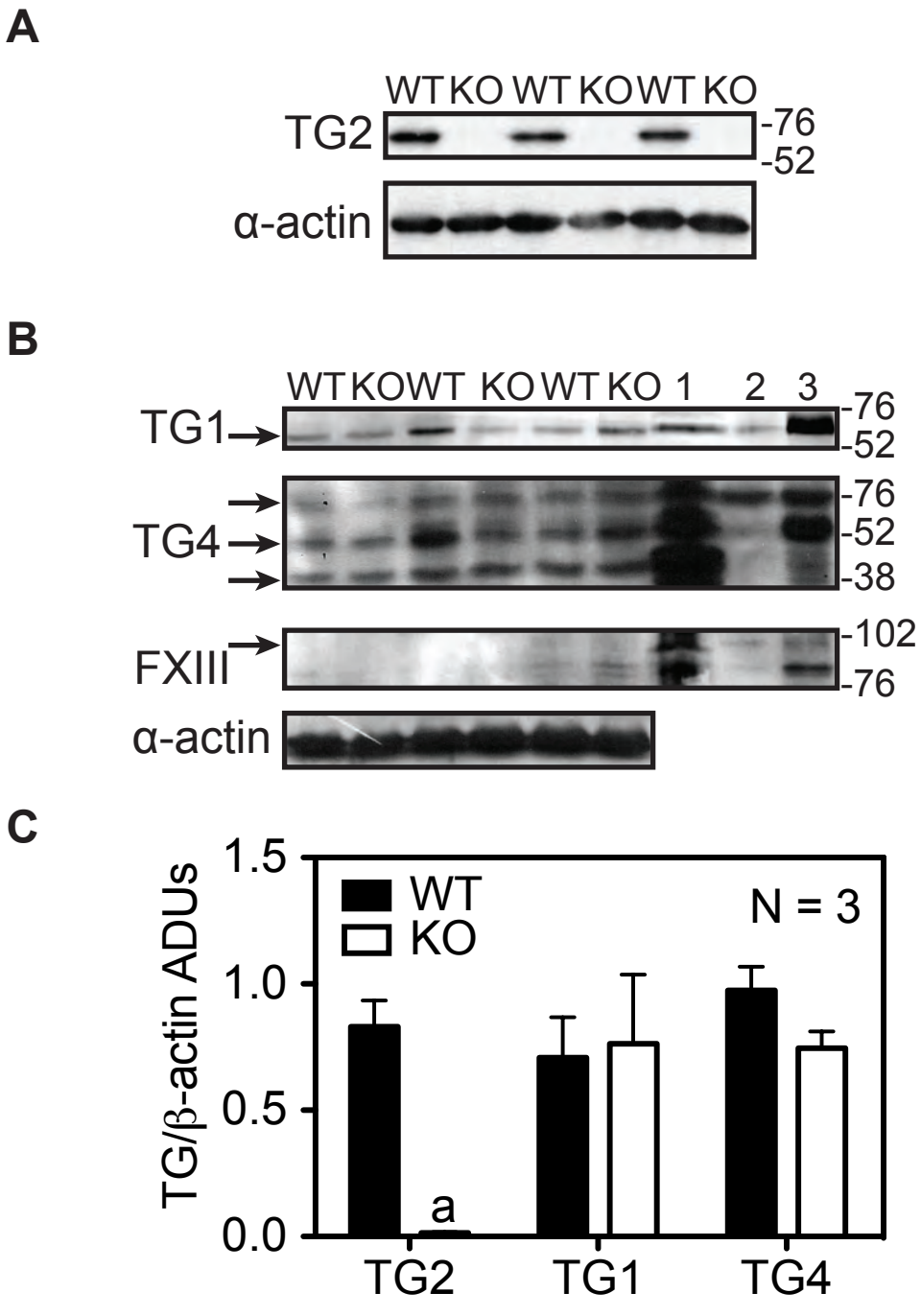

Figure 18. TG expression in TG2 KO and WT mice.

A) Assessment of TG expression in TG2 KO and WT mice confirmed the loss of TG2 protein in the aortae of KO compared to WT mice. **B)** TG1 and TG4 protein was

Figure 18 (cont'd)

expressed in both WT and KO mouse aortae. FXIII protein was not. **C)** Densitometric analysis of TG expression normalized to α-actin revealed that TG2 protein in KO versus WT mouse aortae was essentially abolished. However, the expression of TG1 and TG4 was not significantly different between WT and KO mouse aortae. 1, 2, and 3 are the positive controls lysates. 1 = mouse prostate (TG4 positive control); 2 = mouse placenta (FXIII positive control); 3 = mouse skin (TG1 positive control). ADUs = arbitrary densitometry units. Numbers to the right of the blots represent molecular weight markers, expressed in kDa. Data represents aortae taken from 3 different WT and KO mouse pairs. $P \leq 0.05$.

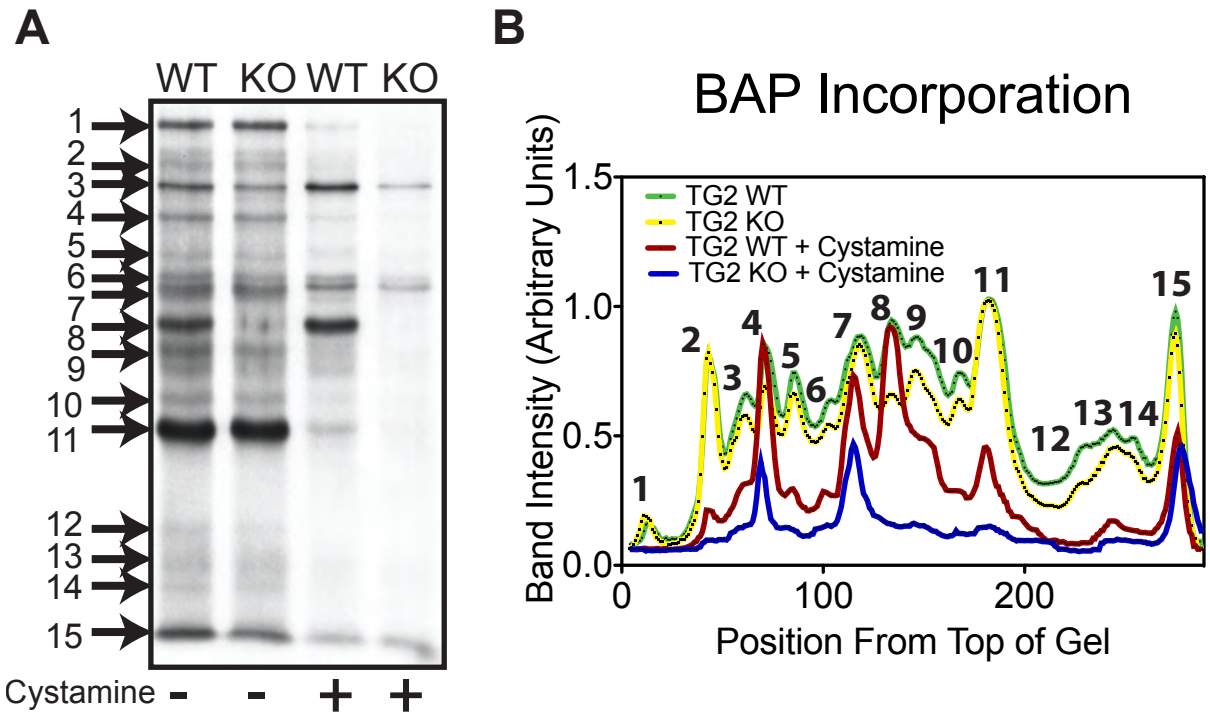

Figure 19. BAP incorporation in TG2 KO mice.

A) Incorporation of the biotinylated TG substrate BAP shows that the TG2 KO mouse still has notable levels of TG activity that is similar to that of WT. Blot is representative of aortae from four different TG2 WT and KO mouse pairs. **B)** Analysis of the blot in A using Un-Scan-It® to determine the relative intensity of each BAP blot. Peaks represent different bands detected in the blot. The numbers next to the bands on the blot corresponds to the peak of the same number in the graph to the left. Green lines represent data from a WT animal; yellow represent data from a KO animal. Red and blue lines represent the same WT or KO animal, respectively, in the presence of 1 mM cystamine. Representative blot and data from experiments done on 4 different TG2 KO/WT pairs.

Pharmacological evidence for TG2-independent TG activity in the vasculature.

BAP incorporation was also assessed for normal RA homogenates in the presence of vehicle, the general TG inhibitor cystamine (1 mM) or the TG2-specific inhibitor Z-DON (50 μM; **Figure 20)**. BAP incorporation into RA proteins in the presence of Z-DON was similar to that observed in the control. In contrast, homogenates incubated in the presence of cystamine had drastically reduced levels of BAP-incorporation compared to vehicle, suggesting that additional TGs besides TG2 are functional in vascular tissues.

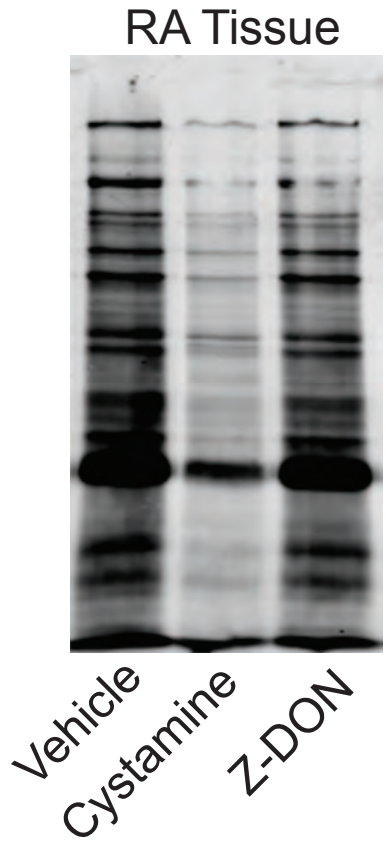

Figure 20. BAP incorporation in the RA in the presence of general and TG2-specific TG inhibitors.

BAP incorporation into RA protein homogenates was assessed in the presence of vehicle, 1 mM cystamine (a general TG inhibitor), or 50 μM Z-DON (a TG2-specific inhibitor). BAP (4 mM). BAP incorporation in the presence of cystamine, but not Z-DON, was notably less than vehicle treated tissues. Data representative of experiments performed on 3 different RA homogenates.

In situ detection of TG1- and TG2- specific TG activity in RA and RVC tissues.

Using fresh frozen RA and RVC tissue sections and FITC-conjugated K5 and T26 substrates, TG-isoform specific activity was assessed. The K5 and T26 peptides are *glutamine-donor* substrates, and are incorporated into lysine-residues of TG substrate proteins. Additionally, K5 and T26 peptides are TG-isoform specific, with K5 only reacting in a TG1-catalyzed reaction, and T26 only reacting in a TG2-catalyzed reaction. Thus, using these peptides, we were able to visualize in RA and RVC tissues the location of *active* TG1 and TG2 enzymes by observing where FITC fluorescence was incorporated. Although we also identified TG4 as another TG that is present in the vasculature, a TG4-specific peptide substrate was not available at the time of this study. Thus, only TG1- and TG2-specific activity was measured. Negative controls (K5QN and T26QN, for K5 and T26, respectively) were identical peptides except the active glutamine residues in the peptide had been substituted with an inactive asparagine residue. In both RA (**Figure 21A**) and RVC tissues (**Figure 21B**), K5 (top) and T26 (bottom) FITC fluorescence was observed, indicating peptide incorporation, and thus TG1-specific and TG2-specific TG activity in these tissues. In contrast, FITC fluorescence was not observable using the same LUT and exposure settings, indicating that this activity was specific for to TG activity. Fluorescence was primarily localized to the VSMC layers in these tissues (arrows). This is exceptionally well illustrated in the RVC (**Figure 21B**), where both the K5 and T26 peptides were most prominently incorporated into the single VSMC layer that exists in this tissue on the lumen side of the vessel. These data suggest that TG1- and TG2-specific TG activity is present in the vasculature, where it is primarily localized to the VSMC layers.

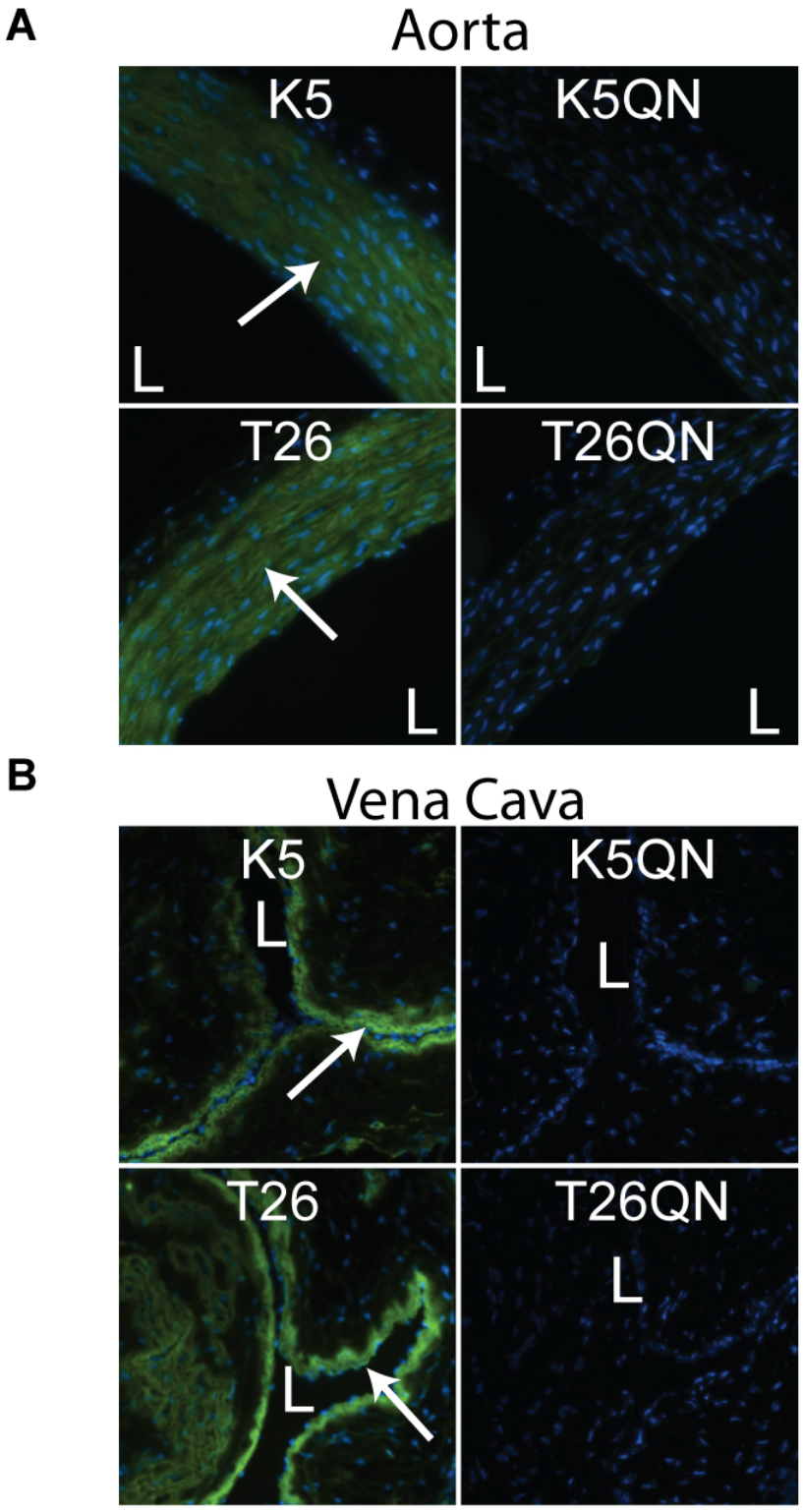

Figure 21. In situ detection of TG1- and TG2-specific TG activity in RA and RVC tissues.

Figure 21 (cont'd)

Sections of fresh frozen RA **(A)** and RVC **(B)** tissues were assessed for their ability to incorporate FITC-labeled peptides that are specific substrates for TG1 (1 μM K5) or TG2 (1 μM T26), demonstrating the presence of active TGs in these tissues. Mutant peptides (1 μM K5QN and 1 μM T26QN) that consisted of the same sequence of amino acids—except that an asparagine residue had been substituted for the reactive glutamine residue, and thus did not incorporate into the active enzymes—were used as negative controls. Images are representative of tissue sections from 3 different animals. Arrows point to areas of TG activity. L = lumen of the vessel. Nuclei are stained with DAPI (blue).

In situ detection of TG1- and TG2- specific TG activity in TG2 KO and WT mouse aortae.

In situ TG1- and TG2-specific activity was also observed in TG2 KO and WT mouse aorta tissues (**Figure 22**). Similar to what was observed in the RA, TG2 WT mouse aorta incorporated K5 and T26 peptides into the VSMC layers in these tissues (**Figure 22A**). As expected, in the TG2 KO mouse aortae, T26 peptide incorporation was not observed (**Figure 22B**, bottom). Somewhat surprisingly, K5 incorporation was also lost in the TG2 KO mouse aortae, suggesting that TG1 was not active in these tissues. To confirm that TG1 was still present in the VSMCs, immunohistochemical staining for TG1 was performed in the TG2 KO and WT mouse aorta (**Figure 23**). TG1 staining was seen in both the WT and TG2 KO mouse aortae, suggesting that the loss of K5 incorporation was not due to a loss of TG1 protein.

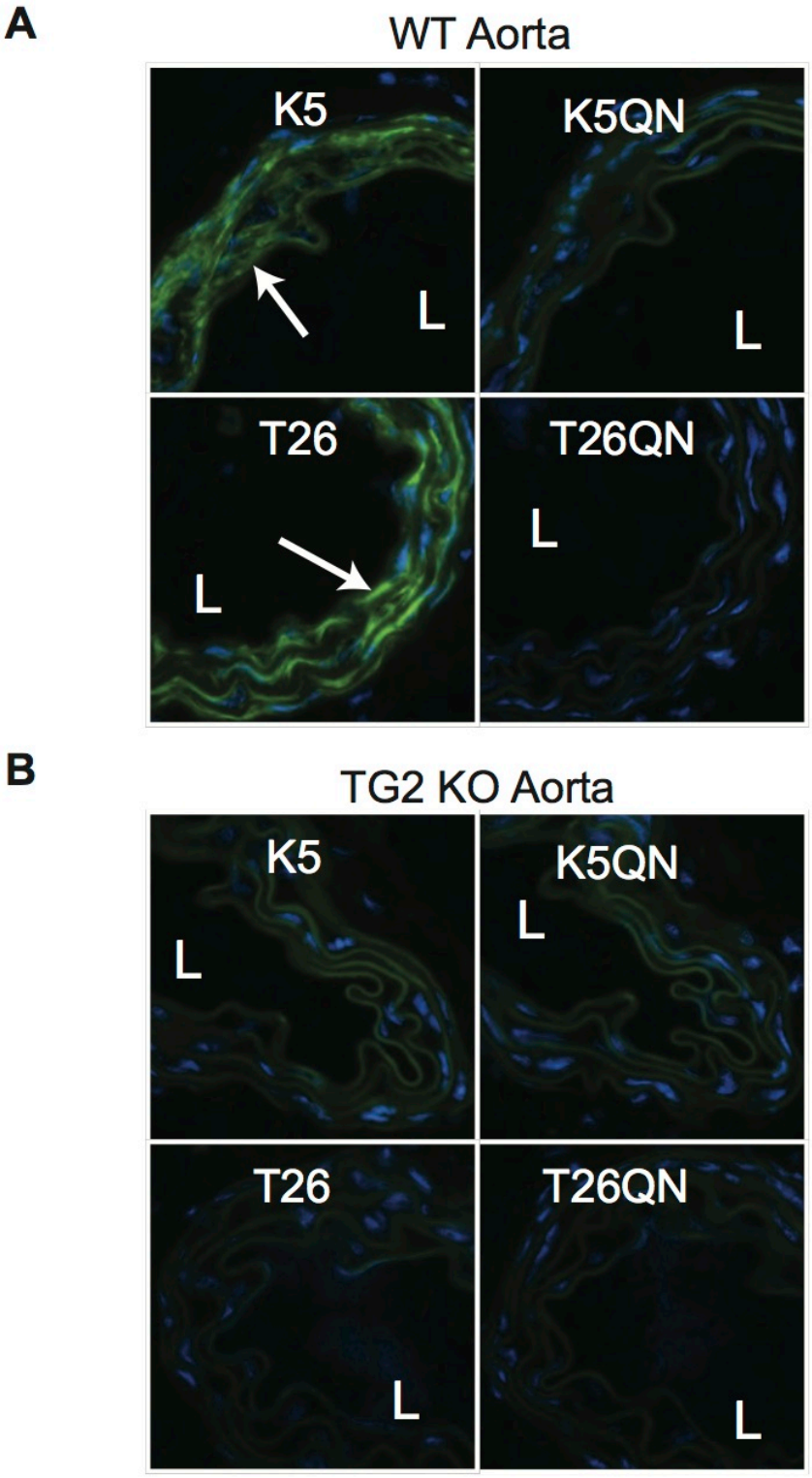

Figure 22. In situ detection of TG1- and TG2-specific TG activity in WT and TG2 KO mouse aortae.

Figure 22 (cont'd)

Sections of fresh WT **(A)** and TG2 KO **(B)** mouse aortae were assessed for their ability to incorporate FITC-labeled peptides that are specific substrates for TG1 (1 μM K5) or TG2 (1 μM T26), demonstrating the presence of active TGs in these tissues. Mutant peptides (1 μM K5QN and 1 μM T26QN) that consisted of the same sequence of amino acids—except that an asparagine residue had been substituted for the reactive glutamine residue, and thus did not incorporate into the active enzymes—were used as negative controls. Images are representative of tissue sections from 3 different WT and TG2 mice pairs. Arrows point to areas of TG activity. L = lumen of the vessel. Nuclei are stained with DAPI (blue).

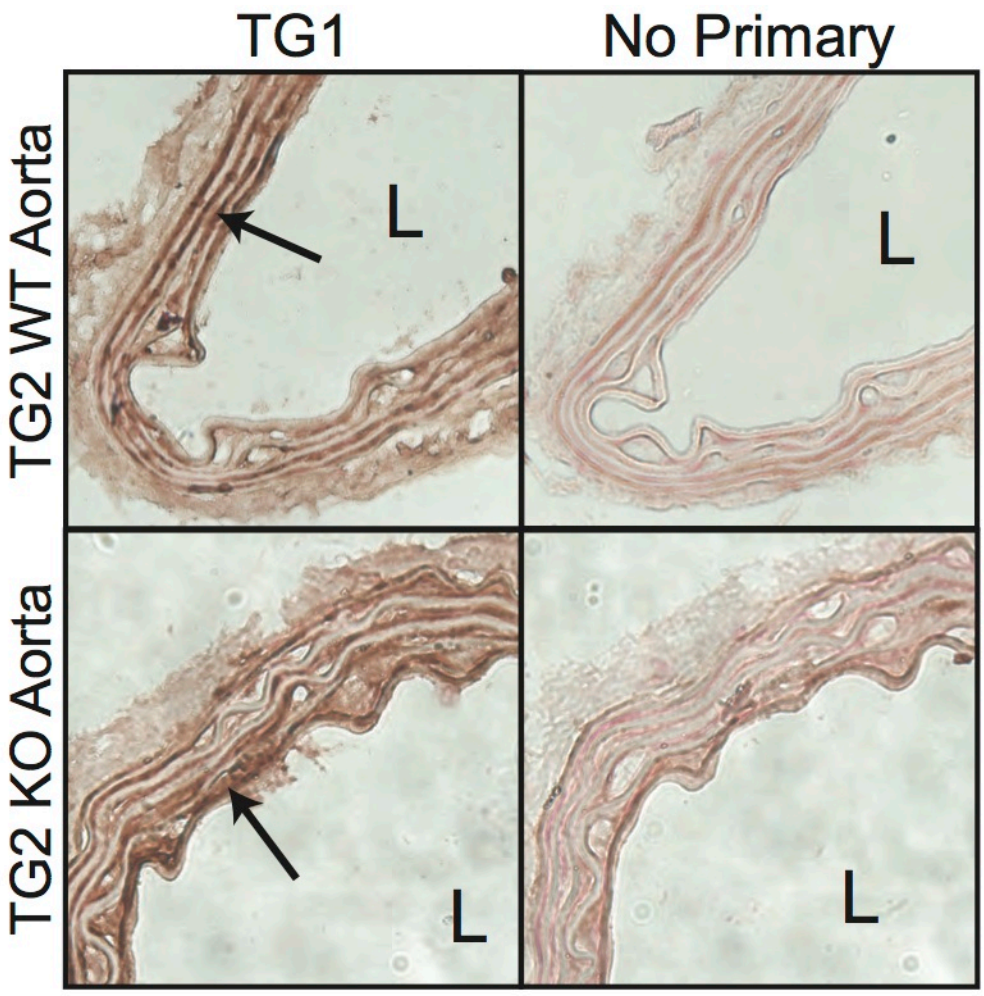

Figure 23. Immunohistochemical staining for TG1 in TG2 KO and WT mouse aortae.

Immunohistochemical staining for TG1 was performed in WT (top) and TG2 KO (bottom) mouse aortae. TG1 staining was observed in the VSMCs layers in both the WT and TG2 KO mouse aorta. Arrows point to areas of positive staining. No Primary = tissue sections adjacent to the sections that were developed for TG1 staining, treated in parallel except that the primary antibody was omitted from the reaction. L = lumen of the vessel. Images are representative of experiments performed on tissues from 3 different WT and TG2 KO mouse pairs.

1.3. Protein amidation by NE

Using an antibody raised against a NE-BSA conjugate, Western analysis was performed to ascertain whether endogenously amidated proteins could be observed in RA and RVC tissues (**Figure 24A**). The anti-NE-BSA antibody detected several bands of higher molecular weight proteins (all >50 kDa). Densitometric analysis of the 5 most prominent bands indicated 3 that were significantly higher in the RVC, 1 that was significantly higher in the RA, and 1 that was not significantly different (**Figure 24B**). These data suggest that amidation of proteins by NE occurs endogenously. However, caution should be used in interpreting these data, as neither 500x NE (weight to weight; **Figure 25A**) nor 5-fold molar excess of NE-BSA (**Figure 25B**) were able to compete off the antibody.

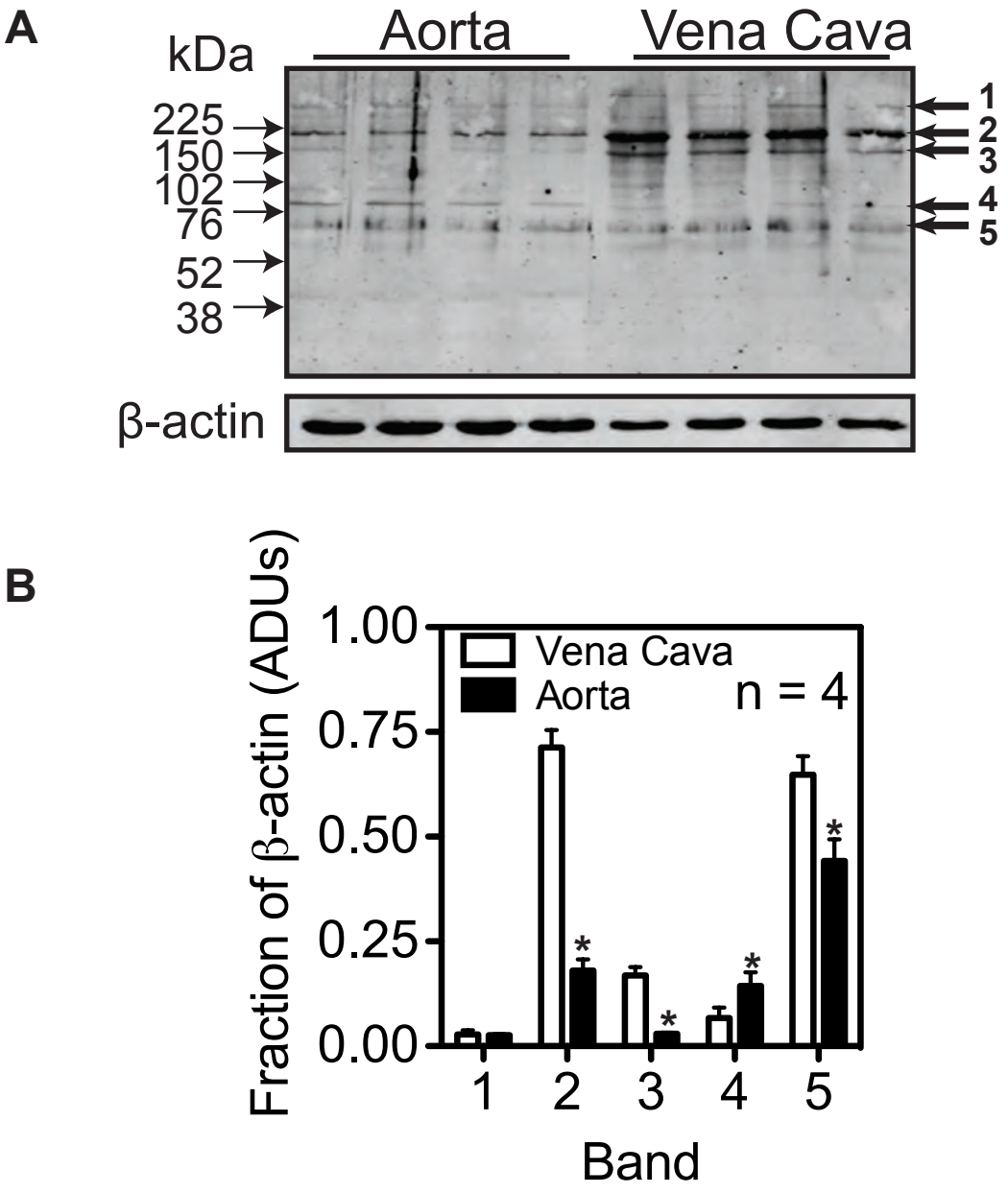

Figure 24. Western for RA and RVC proteins detected with an anti-NE-BSA antibody.

A) RA and RVC homogenates, not exposed to exogenous NE, were immunostained using an antibody directed against a NE-BSA conjugate. **B)** Densitometric analysis of

Figure 24 (cont'd)

the five most prominent bands in A (noted by the arrows to the right of the blot). Densitometry is relative to β-actin protein expression. RA and RVC tissue homogenates were each derived from 4 different animals. ADUs = arbitrary densitometry units. $P \leq 0.05$.

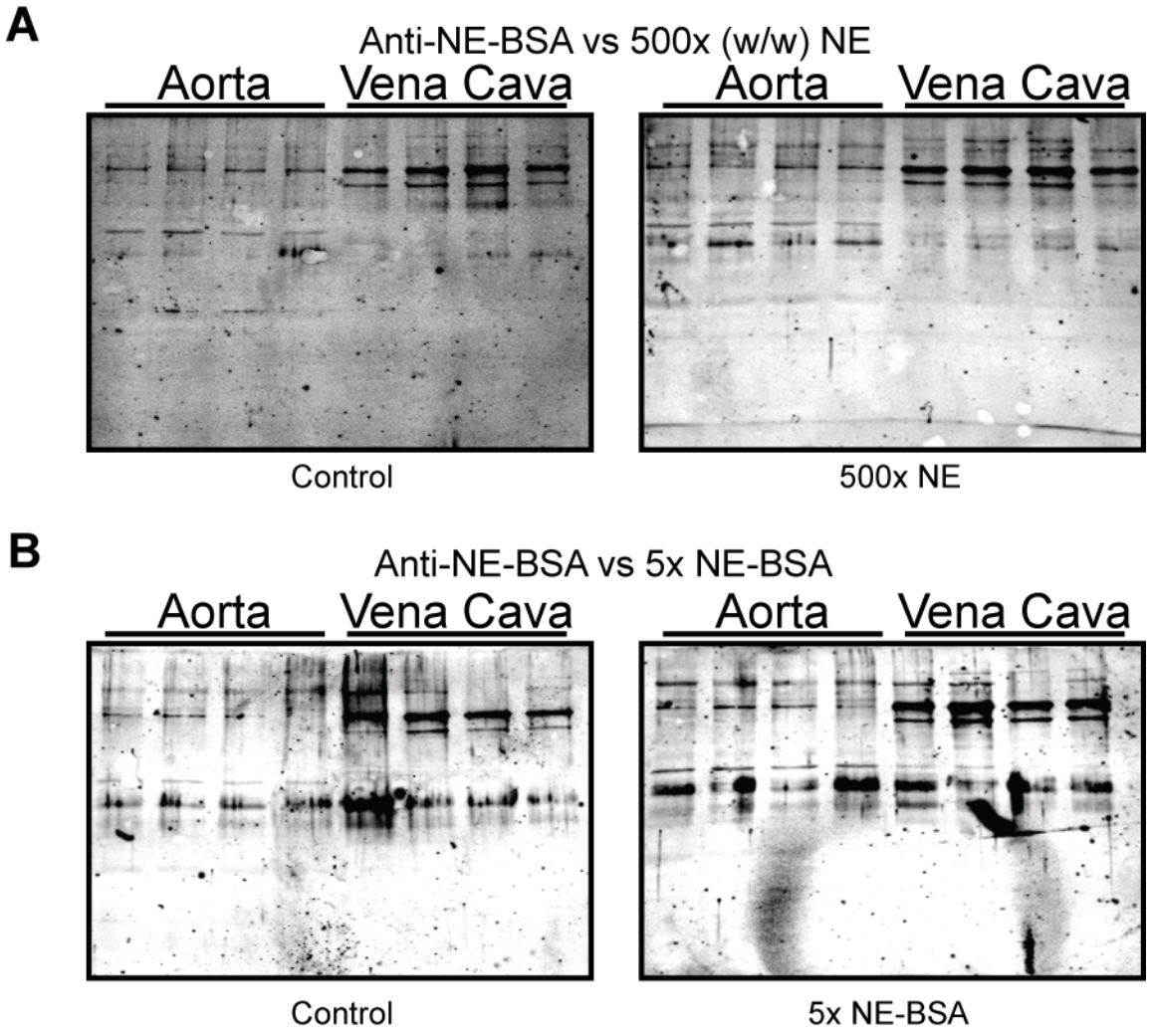

Figure 25. Western analysis of RA and RVC proteins using an anti-NE-BSA antibody in the presence excess NE or NE-BSA.

Western analysis for RA and RVC proteins was performed using an antibody for anti-NE-BSA. Neither excess NE (**A,** right), nor excess NE-BSA (**B,** right), competed off the anti-BSA antibody, as blots incubated in the presence of excess NE or NE-BSA did not differ in banding pattern from control blots (left). RA and RVC tissue homogenates were each derived from 4 different animals. w/w = weight to weight. $P \leq 0.05$.

Immunostaining for RA and RVC proteins amidated by NE.

Using the NE-BSA antibody, immunohistochemical staining was performed in RA and RVC tissues (**Figure 26**), and immunocytochemical staining was performed in freshly dissociated and cultured VSMCs from these tissues (**Figure 27**). Immunohistochemical staining was seen in all layers of the RA and RVC tissues. Similarly, freshly dissociated RA (**Figure 27A**, top) and RVC (**Figure 27A**, bottom) tissues stained for NE (red) in both non-VSMCs and VSMCs (VSMCs were detected by co-immunostaining with an anti-α-actin antibody). Staining in these cells was seen in the cytoplasm of the cell, and colocalized with α-actin (yellow). Cultured VSMCs derived either from RA (**Figure 27B**, top) or RVC (**Figure 27B**, bottom) tissues also produced staining with the anti-NE-BSA antibody (red), which colocalized with α-actin (yellow). These results suggest that proteins are endogenously amidated by NE in vascular tissues, notably in VSMCs, where α-actin may be a target.

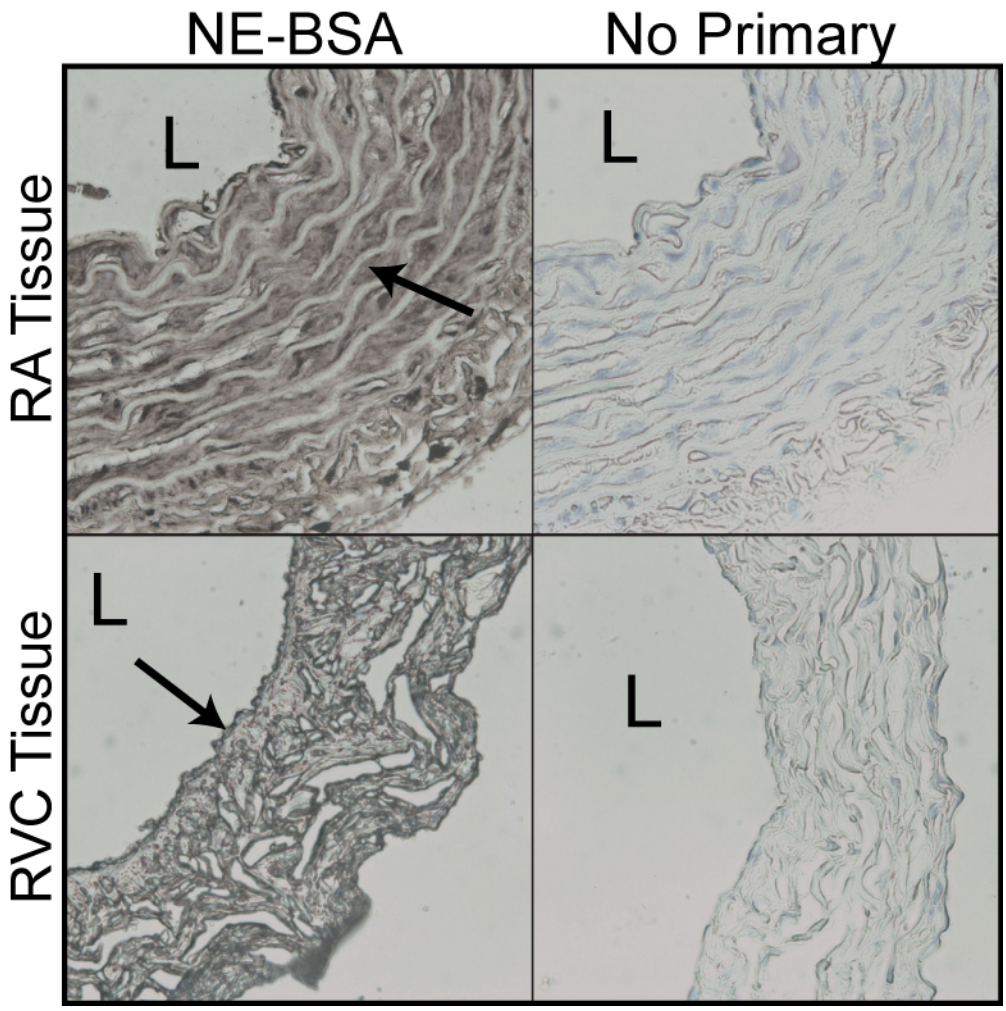

Figure 26. Immunohistochemical staining in RA and RVC tissues for proteins amidated by NE.

Tissue sections of RA (**A**) and RVC (**B**) were immunostained using an antibody directed against NE-BSA. Immunostaining could be seen throughout all the layers of the vessels. No Primary = tissue sections treated in parallel except that the primary antibody was omitted from the reaction. Images are representative experiments performed on tissue sections from 4 different animals. L = lumen of the vessel. Arrows point to areas of staining.

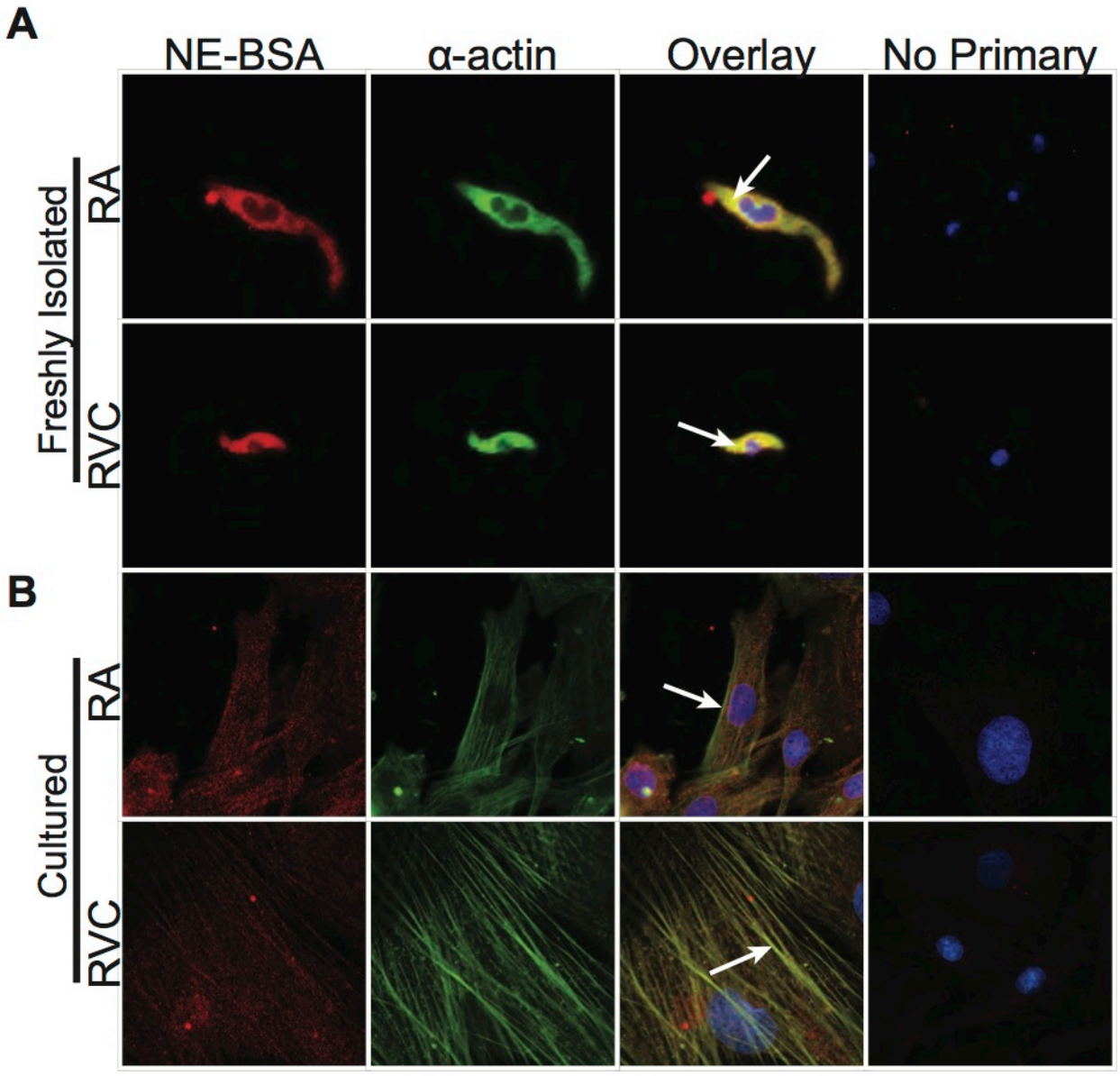

Figure 27. Immunocytochemical staining of RA and RVC VSMCs for proteins amidated by NE.

Freshly dissociated (**A**) and cultured (**B**) RA and RVC VSMCs were immunostained using an antibody directed against NE-BSA. Smooth muscle cells were identified using an anti-α-actin antibody (green). DAPI (blue) was used to visualize nuclei. No primary = cells from the same culture explant or dissociation treated in parallel, excluding the

Figure 27 (cont'd)

primary antibody from the reaction. Arrows point to areas of colocalization between NE and α-actin. Representative images of experiments performed on cells derived from 4 different animals.

TG activity assay for protein amidation by NE using a NE-biotin conjugate.

Incorporation of biotinylated amines (12.7 μM; 5-HT, NE, histamine, and dopamine) into RA homogenates was observed by Western analysis using streptavidin-HRP (**Figure 28**). Biotinylated 5-HT, NE, and dopamine, but not histamine, were incorporated into RA homogenate proteins. This incorporation was blocked by 1 mM cystamine. Incorporation of NE-biotin into RA (**Figure 29A**) and RVC (**Figure 29B**) homogenates could be blocked with non-biotinylated NE in a concentration-dependent (**Figure 29C**) manner, supporting the idea that NE-biotin and NE are treated similarly by TGs. These data suggest that NE can be used as a substrate by TGs to amidate vascular proteins.

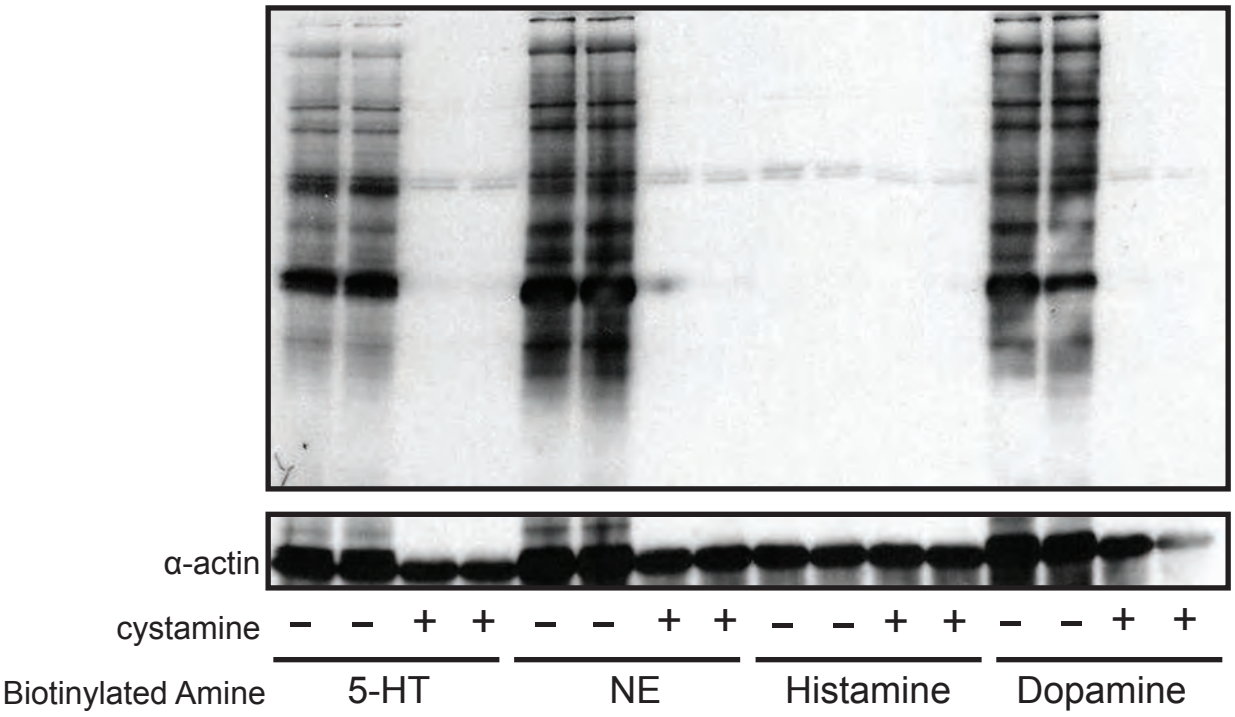

Figure 28. Western analysis for biotinylated amine incorporated proteins.

RA proteins were incubated with biotinylated amine (12.7 μM). Biotinylated 5-HT, NE, and dopamine, but not histamine, were incorporated into RA proteins. This incorporation was blocked by the TG inhibitor cystamine. Representative of experiments performed on 4 RA protein homogenates from 4 different animals.

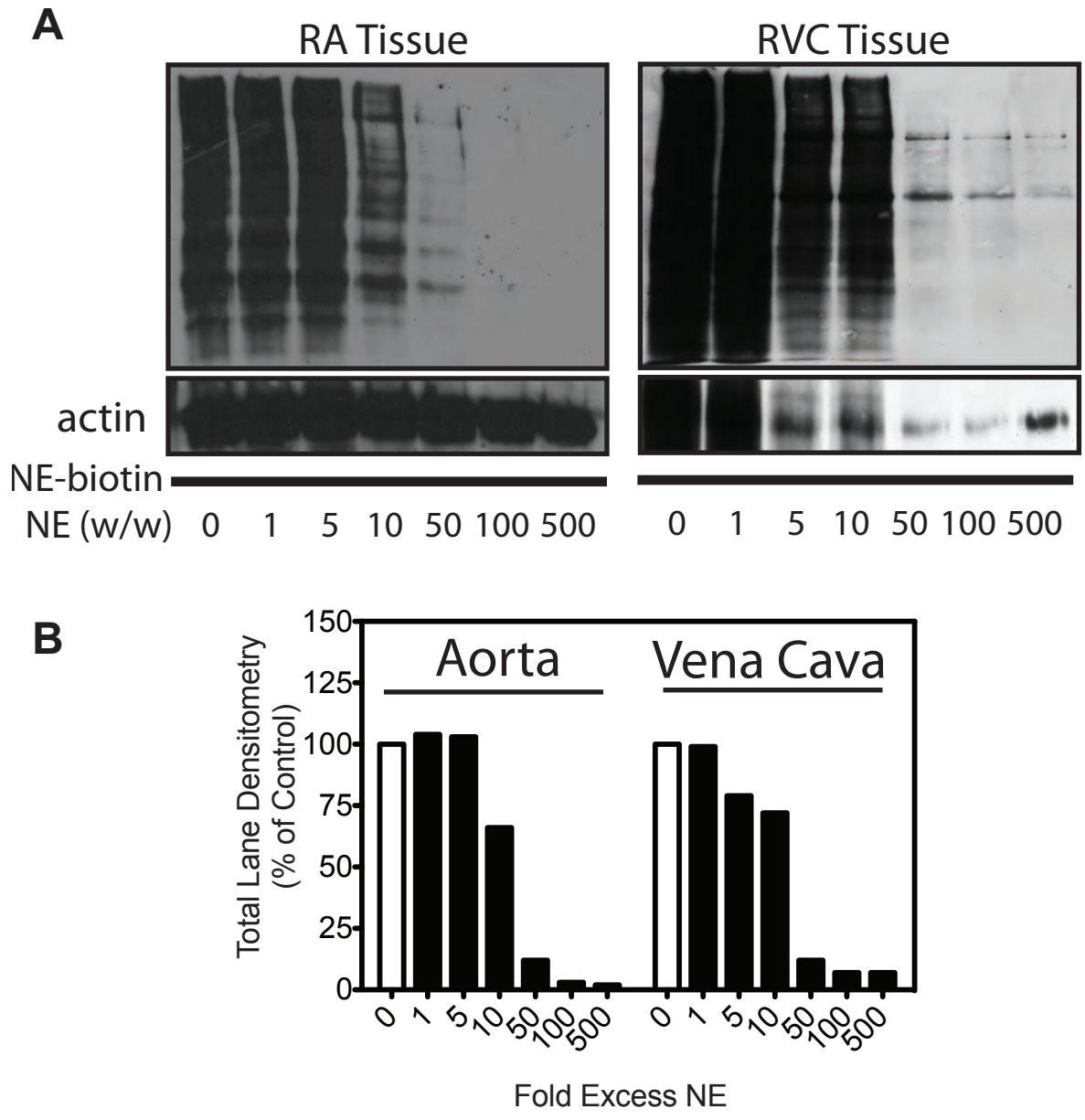

Figure 29. RA and RVC NE-biotin incorporation in the presence of excess NE.

RA (**A**) and RVC (**B**) protein homogenates were incubated with 12.7 μM NE-biotin, and increasing concentrations of unlabeled NE. Incorporation of NE-biotin was blocked by NE in a concentration-dependent manner. **C**) Graphical representation of total lane densitometry of NE-biotin incorporated proteins in the presence of excess NE. w/w =

Figure 29 (cont'd)

weight to weight ratio. Representative experiment of RA and RVC tissues from 3 different animals.

2. Aim 2: Test the hypothesis that NE-is taken up into VSMCs.

Rationale: In addition to their classical role in the removal of extracellular biogenic amines, monoamine transporters can also act as mediators of monoamine function independent of receptor interaction. For example, 5-HT uptake induces a change in the morphology of pulmonary artery VSMCs (100). Subsequent research has shown that this response is dependent on TG-mediated protein amidation (108). The previous series of experiments have shown that NE can act as a substrate for TGs in VSMCs. However, for this modification to occur, an intracellular source of NE is required, either through synthesis or uptake. As the vasculature is highly innervated by the sympathetic nervous system, which provides a plentiful source of exogenous NE, we hypothesized that VSMCs take up NE via OCT3, NET, or both. We test this hypothesis using whole tissues and VSMCs, both freshly dissociated and cultured, Western analysis, immunostaining, and assays for NE uptake.

2.1. NE-biotin uptake.

NE-biotin uptake was assessed in freshly dissociated RA and RVC, and cultured RA, VSMCs. To prevent NE metabolism, 10 μM pargyline was included in these experiments. Cells were incubated with 12.7 μM NE-biotin or vehicle for 30 min. Cells were then washed, fixed, and immunocytochemical staining using fluorescently-labeled streptavidin was performed. Identification of VSMCs was done by costaining with a FITC-labeled anti-α-actin antibody (green). In freshly dissociated VSMCs from either RA (**Figure 30A**) or RVC (**Figure 30B**) tissues, fluorescently-labeled streptavidin (red) produced prominent staining when cells were incubated with NE-biotin, but not vehicle, indicating the NE-biotin was taken up into these cells. NE-biotin staining colocalized

with α-actin in these cells (yellow), suggesting that amidation of α-actin may have occurred. In contrast to freshly dissociated VSMCs, no difference in staining was detected in cultured RA VSMCs incubated with either vehicle or NE-biotin, suggesting that NE-biotin was not taken up by VSMCs in culture (**Figure 30C**). This supports our hypothesis that VSMCs can take up NE to be used as a TG substrate for the amidation of proteins.

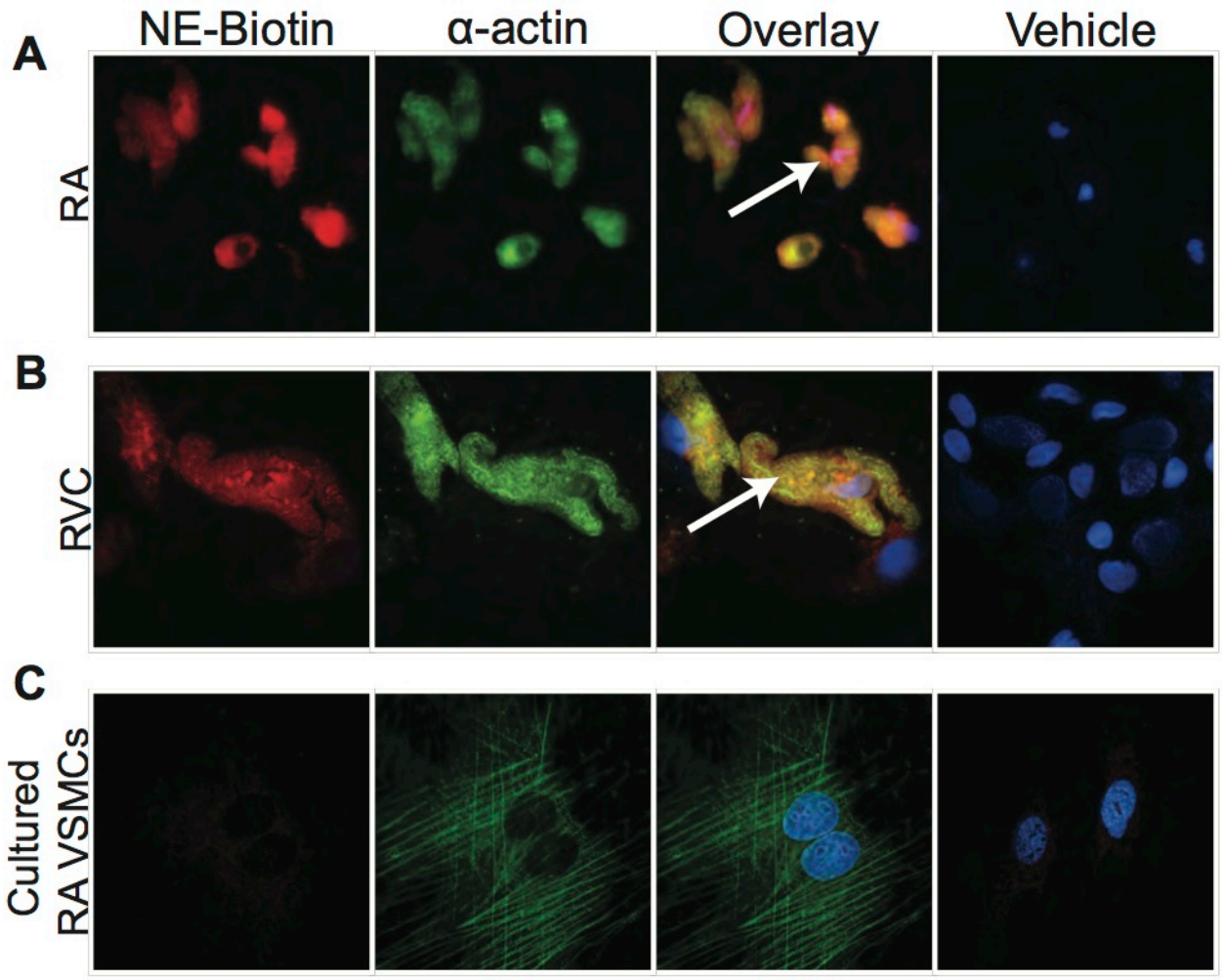

Figure 30. Immunocytochemical detection of NE-biotin uptake in VSMCs.

VSMCs were incubated with 12.7 μM NE-biotin for 30 min, washed, and then fixed for immunocytochemical staining. By probing with fluorescently labeled streptavidin (red), NE-biotin uptake could be indirectly visualized in freshly dissociated RA (**A**) and RVC (**B**), but not cultured RA (**C**), VSMCs. Identification of VSMCs was accomplished by costaining with FITC-labeled anti-α-actin antibody (green). DAPI (blue) was used to visualize cell nuclei. Colocalization of NE-biotin and α-actin (yellow) could be observed in the overlay. Vehicle = cells incubated with DMF vehicle in place of NE-biotin, but otherwise treated identically. Representative of VSMCs derived from 6 (freshly

Figure 30 (cont'd)

dissociated RA), 4 (RVC) or 3 (cultured RA VSMCs) animals.

NE-biotin uptake in whole vascular tissues.

NE-biotin was also used to provide evidence that NE can be taken up and utilized as a TG substrate in whole RVC tissues. In the presence of 10 μM pargyline, RA or RVC tissues were incubated with NE-biotin (with or without 1 mM cystamine) for 1 h, washed, and then homogenized. Western analysis for proteins that incorporated NE-biotin was then performed (**Figure 31)**. NE-biotin incorporation was observed in both RA and RVC proteins. Interestingly, 1 mM cystamine appeared to block this incorporation in the RVC, but not the RA. These data not only support the hypothesis that vascular tissues take up NE, they also suggest that NE taken up into vascular cells may be used as a TG substrate.

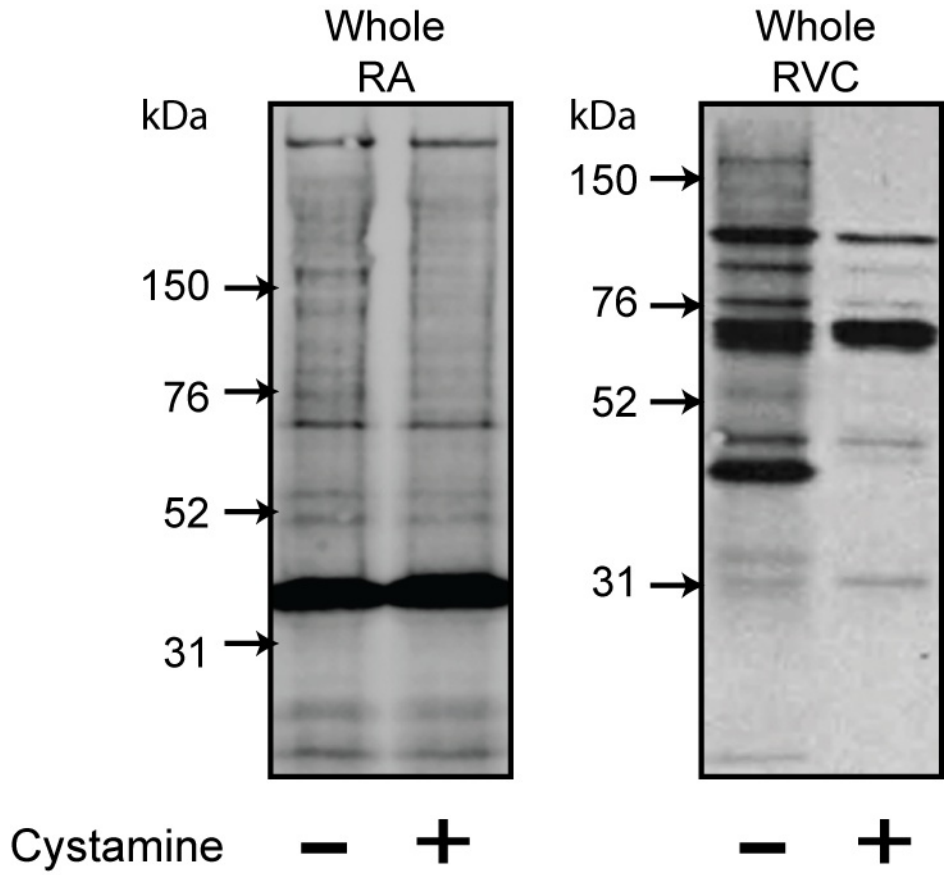

Figure 31. NE-biotin uptake and incorporation into whole vascular tissues.

Whole RA (left) or RVC (right) tissues were incubated with 12.7 μM NE-biotin, plus either cystamine or vehicle for 1 h at 37°C in the presence of 10 μM pargyline. Tissues were then washed and subsequently homogenized. Western analysis using streptavidin-HRP demonstrated that NE-biotin is incorporated into whole RVC tissue proteins. This incorporation was blocked by 1 mM cystamine in the RVC, but not the RA. Representative blot of experiments performed on tissues from 3 - 4 different animals.

2.2. NET and OCT3 protein expression

Western blot protein analysis for OCT3 and NET in whole tissues and cultured VSMCs.

Western analysis for OCT3 (**Figure 32A, B,** and **C**) and NET (**Figure 32D**) was performed using RA and RVC tissues, and cultured RA and RVC VSMCs. Two different OCT3 immunoblots were developed: one using rabbit antibody from Bioworld (**Figure 32A**), and a goat antibody from Santa Cruz Biotechnology (**Figure 32B** and **C**). Both antibodies produced prominent bands between 52 and 76 kDa. However, these bands did not migrate with the positive controls, and, in the case of the Santa Cruz Biotechnology antibody, bands still appeared when the competing peptide was included in the reaction (data not shown). A competing peptide was not available for the Bioworld antibody. Though the immunoblot incubated with anti-OCT3 antibody from Bioworld from produced multiple bands in both whole tissue, as well as cultured VSMC samples, a band (denoted by an arrow to the right of the blot in **Figure 32A**) in RA tissue samples was both consistent with the reported molecular weight of OCT3 (~62 kDa) and migrated with a prominent band in the positive control (rat placenta lysate). Densitometric analysis of OCT3 (**Figure 32E**; the bands at the molecular weight denoted by the arrow to the right of the blot in **Figure 32A** were used for analysis) and NET (**Figure 32F**) normalized to β-actin, demonstrated significantly more OCT3 in whole RA (2.0 ± 0.5 OCT3/β-actin densitometry units) than either cultured VSMCs (RA VSMCs: 0.05 ± 0.03; RVC VSMCs: 0.12 ± 0.03 OCT3/β-actin densitometry units) or the RVC (0.12 ± 0.10 OCT3/β-actin densitometry units). Similarly, expression of NET was significantly higher in RA tissues (2.0 ± 0.3 NET/β-actin densitometry units) than in

cultured VSMCs (aortic: 0.05 ± 0.02; vena cava 0.04 ± 0.02 NET/β-actin densitometry units) or in whole vena cava tissues (0.47 ± 0.09 NET/β-actin densitometry units). Additionally, in contrast to OCT3, NET expression was significantly greater in RVC tissues compared to cultured VSMCs. These data suggest that both RA and RVC tissues express NET, while only the RA expresses OCT3, and that expression of both OCT3 and NET is absent in both RA and RVC VSMCs.

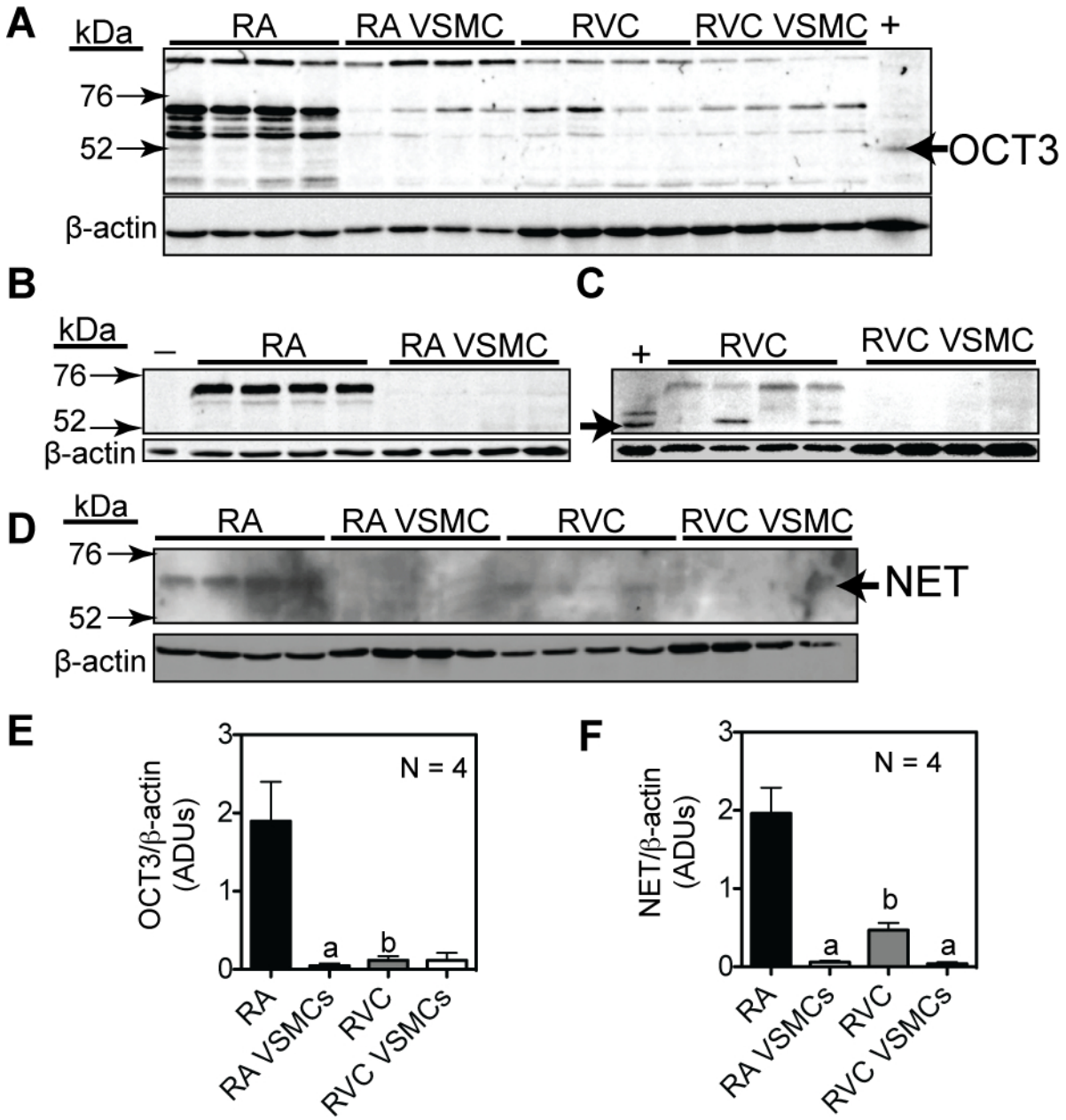

Figure 32. Western analysis for NET and OCT3 in whole vascular tissues and cultured VSMCs.

Western analysis for NET was performed using an antibody from Bioworld (**A**) and one from Santa Cruz biotechnology (**B** and **C**). **D**) Western analysis for NET in whole tissues and cultured VSMCs. Densitometric analysis of OCT3 (**E**) and NET (**F**) proteins from the

Figure 32 (cont'd)

Western blots. The bands quantified were those that migrated to the molecular weight denoted by the arrow to the right of the blots in A and D. For OCT3, this band was chosen, as it appeared in the positive control. The bands analyzed are consistent with the reported molecular weight of OCT3 (~62 kDa) and NET (~54 kDa). OCT3 and NET protein expression is relative to β-actin protein. + = Positive control, rat placenta lysate. Tissues and cultured cells were from four different animals. a = significantly lower than whole tissue; b = significantly lower than aorta. N = 4. $P \leq 0.05$.

OCT3 and NET immunohistochemical staining in RA and RVC tissues.

Immunohistochemical staining of RA and RVC tissues using anti-OCT3 (**Figure 33**) and anti-NET (**Figure 34**) antibodies was performed. Positive staining visually distinct from “No Primary” controls was observed for OCT3 both in RA (**Figure 33A**) and RVC tissues (**Figure 33B**). Sections of rat brain were used as a positive control (**Figure 33C**). OCT3 staining was primarily localized to the VSMC layers in these tissues (large arrows in **Figure 33**), although staining was observed in non-VSMCs as well (small arrows). This is most clearly illustrated in RVC tissues, where the VSMC population is restricted to only a single layer of cells directly adjacent to the lumen of the vessel. OCT3 staining in the RVC tissues is restricted to this VSMC layer and a few isolated cells elsewhere in the tissue. In contrast to OCT3, NET staining for both RA (**Figure 34A)** and RVC (**Figure 34B)** was less intense, localized throughout the tissue, and not as definitive as OCT3 staining. Rat brain was used as a positive control (**Figure 34C**). These data strongly suggest that OCT3 is expressed both in RA and RVC tissues, primarily in the VSMC layers; however, it is unclear from the NET data whether vascular tissues express this transporter.

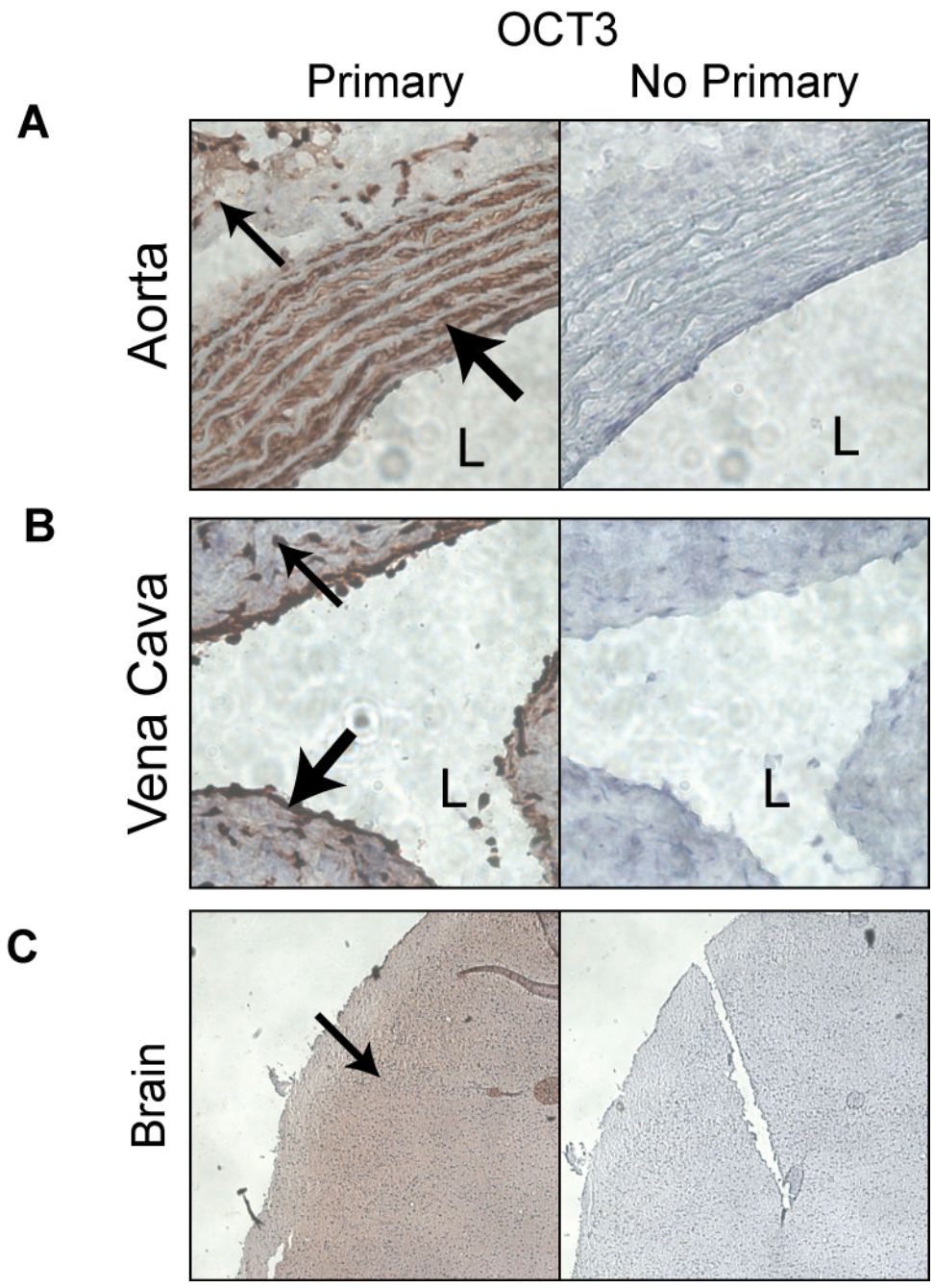

Figure 33. Immunohistochemical staining of OCT3 in RA and RVC tissues.

Immunohistochemical staining for OCT3 in RA (**A**) and RVC tissue sections (**B**). Rat brain (**C**) was used as a positive control. Small arrows point to areas of immunostaining

Figure 33 (cont'd)

in non-VSMC; large arrows point to areas of staining in VSMCs. L = lumen of the tissues. Primary = tissue sections incubated with primary antibody. No primary = tissue sections from the same animal that were treated in parallel except that the primary antibody was excluded from the reaction. Representative of tissues from 4 different animals.

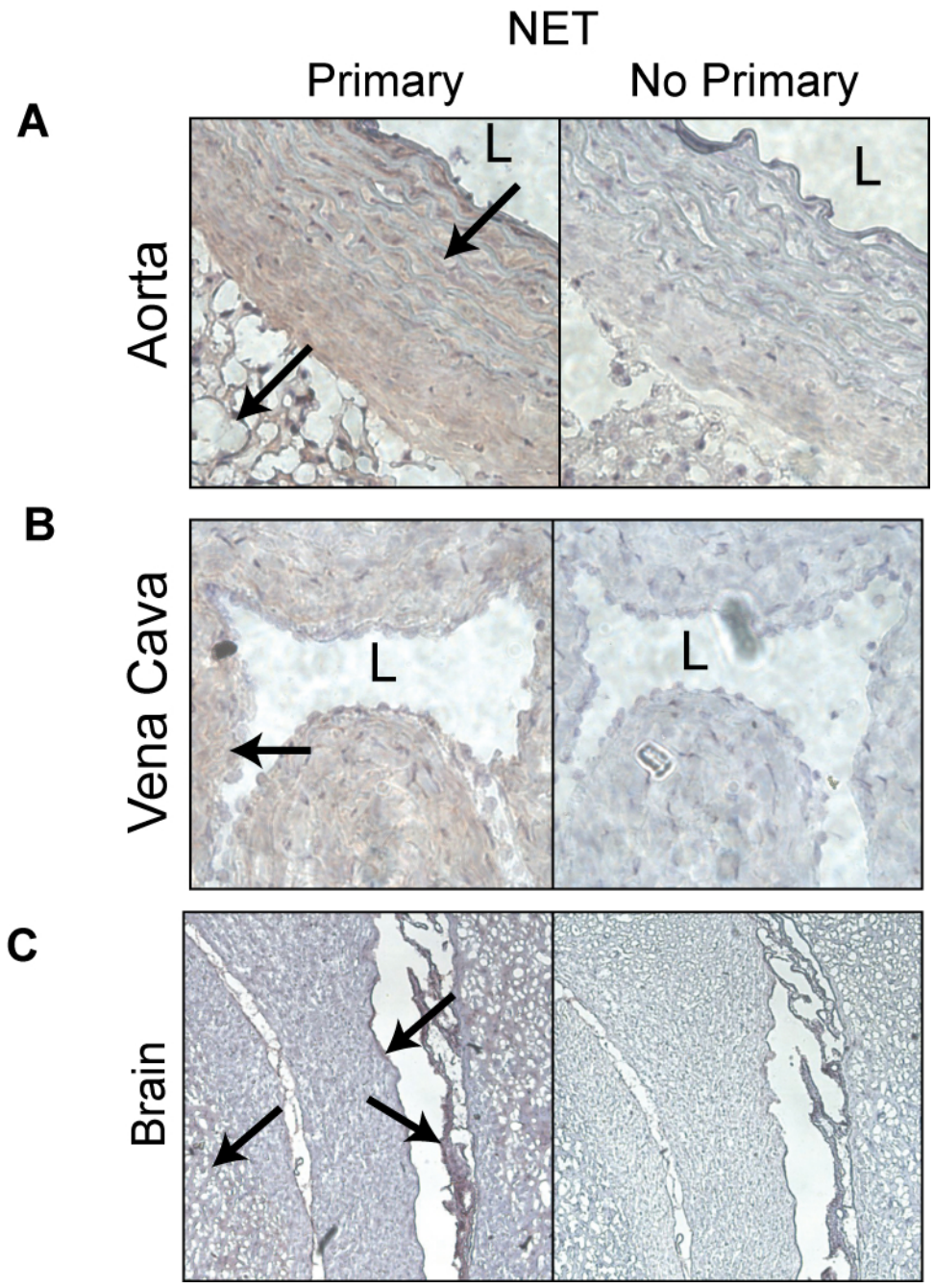

Figure 34. Immunohistochemical staining of NET in RA and RVC tissues.

Immunohistochemical staining for OCT3 in RA (**A**) and RVC tissue sections (**B**). Rat brain (**C**) was used as a positive control. Arrows point to areas of staining. L = lumen of the tissues. Primary = tissue sections incubated with primary antibody. No primary =

Figure 34 (cont'd)

tissue sections from the same animal that were treated in parallel except that the primary antibody was excluded from the reaction. Representative of tissues from 4 different animals.

NET and OCT3 immunocytochemistry

OCT3 (**Figure 35**) and NET (**Figure 36**) were visualized by immunocytochemistry in freshly dissociated (**Figure 35A** and **Figure 36A**) and cultured (**Figure 35B** and **Figure 36B**) RA and RVC VSMCs. VSMCs were identified as such by costaining with an anti-α-actin antibody. Consistent with the immunohistochemical findings, both freshly dissociated RA and RVC VSMCs expressed OCT3. Interestingly, staining was mainly localized to the perimeter of the cell (see arrows), suggesting that this protein was located on the cell membrane. Although some staining was seen in the cells incubated in the absence of primary antibody, this staining was visually distinct, as it was punctate and not localized to the perimeter of the cell. Staining for OCT3 was also seen in cultured RA and RVC VSMCs (**Figure 35B**), although this staining was not restricted to the perimeter of the cell, but rather appeared diffuse throughout, and was not as intense as staining seen in the freshly dissociated VSMCs. In contrast to OCT3 staining, immunostaining for NET was unconvincing; in freshly dissociated RA and RVC VSMCs (**Figure 36A**), NET staining was basically absent. Similar results were obtained for cultured RA and RVC VSMCs (**Figure 36B**). These data suggest that freshly dissociated VSMCs from both RA and RVC tissues express OCT3 and that OCT3 is located on the membrane of these cells. However, it appears that OCT3 is reduced in culture, and may not be localized to the membrane. In contrast, it does not appear that NET is expressed on the surface of VSMCs, regardless of whether the cells were freshly dissociated or cultured.

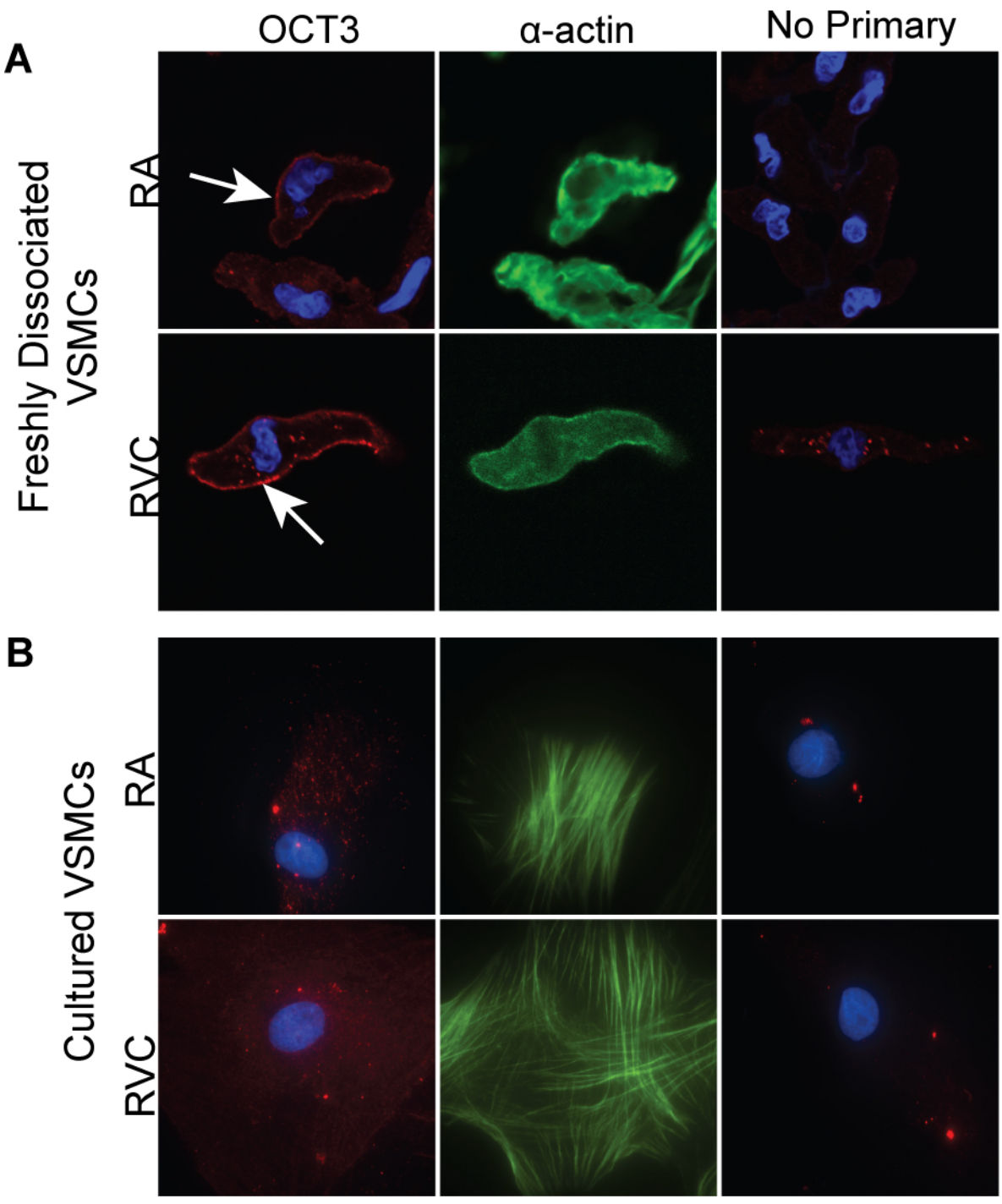

Figure 35. Immunocytochemical staining for OCT3 in freshly dissociated and cultured VSMCs from RA and RVC tissues.

Figure 35 (cont'd)

OCT3 staining (red) in freshly dissociated (**A**) and cultured (**B**) VSMCs derived from RA (top) and RVC (bottom) tissues. Smooth muscle cells were identified using an anti-α-actin antibody (green). DAPI (blue) was used to visualize nuclei. No primary = cells from the same explant or dissociation treated in parallel, excluding the primary antibody from the reaction. Arrows point to areas of OCT3 immunostaining. Representative images of cells derived from 4 different animals.

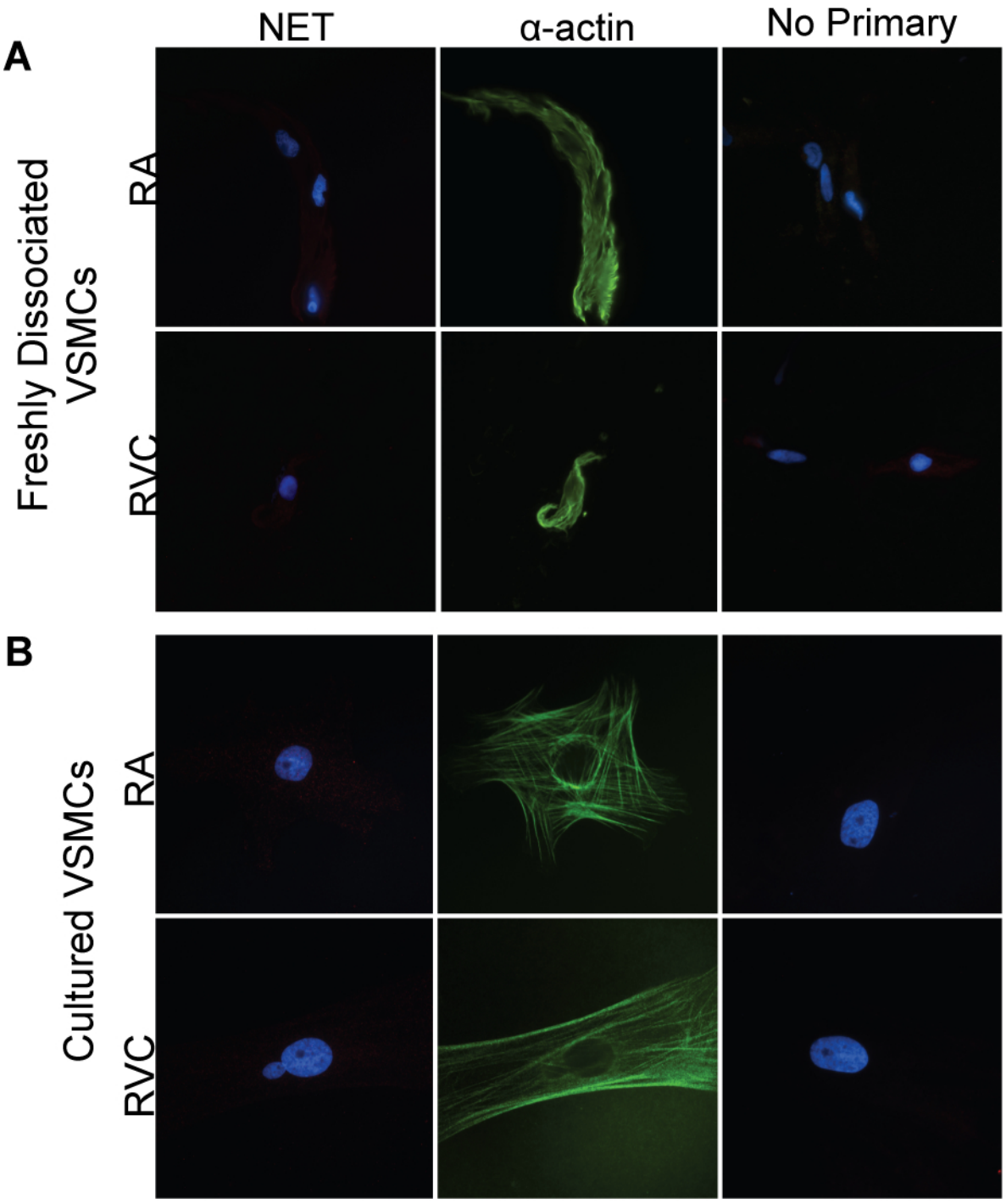

Figure 36. Immunocytochemical staining for NET in freshly dissociated and cultured VSMCs from RA and RVC tissues.

Figure 36 (cont'd)

NET staining (red) in freshly dissociated (**A**) and cultured (**B**) VSMCs derived from RA (top) and RVC (bottom) tissues. Smooth muscle cells were identified using an anti-α-actin antibody (green). DAPI (blue) was used as a nuclear stain. No primary = cells from the same explant or dissociation treated in parallel, excluding the primary antibody from the reaction. Representative images of cells derived from 3 - 4 different animals.

2.3. NE Uptake

NE uptake in cultured VSMCs

A preliminary attempt was made to measure NE uptake in cultured RA VSMCs and whole RA tissues. Cells or tissues were incubated with NE (1 or 10 μM) or vehicle in PSS (with 10 μM pargyline and 1 μM RO 41-0960 to inhibit NE degradation via MAO and COMT, respectively) for 30 min. NE uptake was subsequently assessed. A significant difference in NE content was noticed when tissues and cells were incubated with 10, but not 1, μM NE (**Figure 37A**). However, the NE taken measured with 10 μM NE was indistinguishable from “no cell” controls (plates that were incubated without cells but with 10 μM NE), indicating that the NE measured was residual NE that was not washed out (**Figure 37B**). This issue was avoided with whole tissues, as the tissue was moved to a clean 24 well plates for washing in fresh buffer. These data suggest that cultured RA VSMCs lack the ability to take up NE, while whole RA tissues only take up measureable amounts of NE at concentrations higher than μM concentrations. Thus, 10 μM NE and whole tissues were utilized in subsequent experiments.

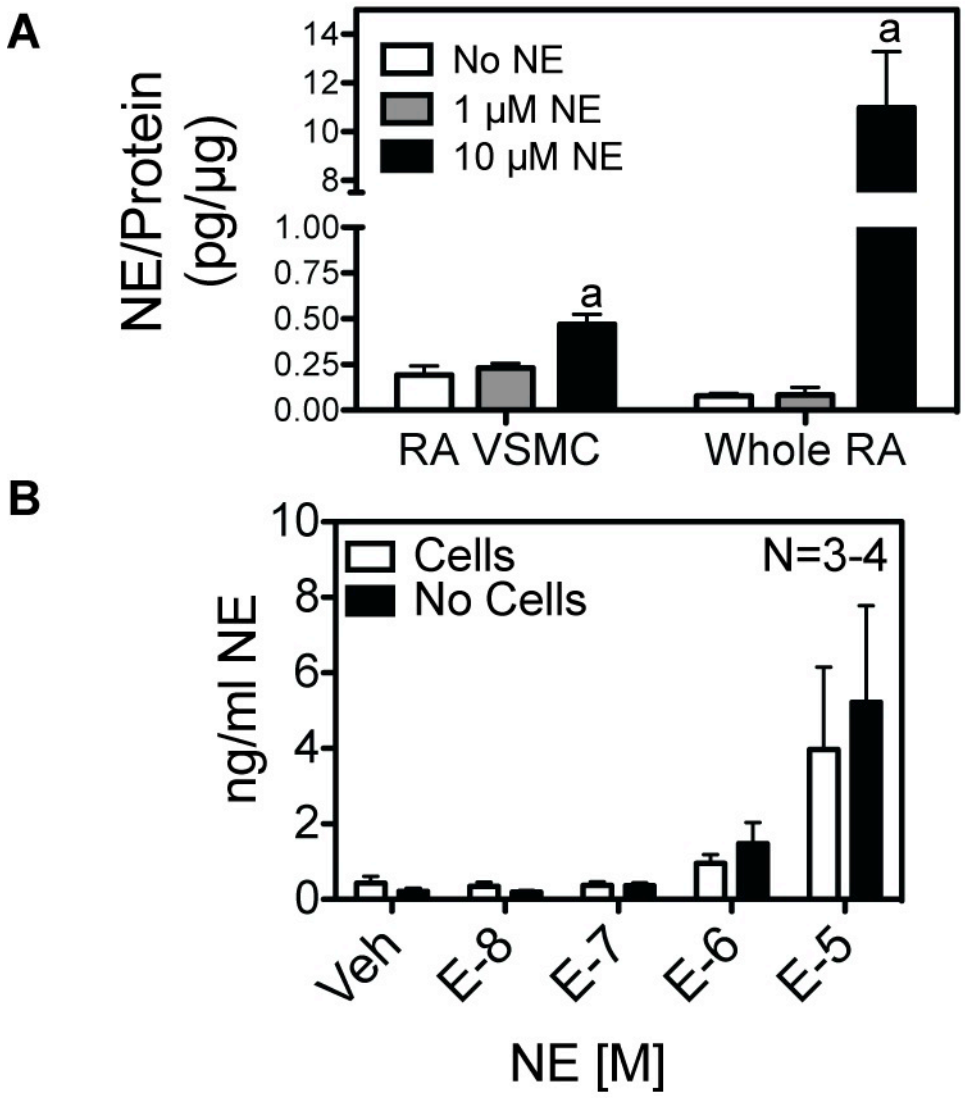

Figure 37. NE uptake in whole RA and RA VSMCs.

The ability of RA VSMCs and whole RA tissues to take up NE was tested. **A**) Significant NE was measured when tissues or cells were incubated with 10, but not 1 µM NE. a = significantly greater NE measured than in tissues/cells incubated without NE. However, **B**) comparison of the NE measured with and without VSMCs, suggested that the NE measured in cultured VSMCs incubated with 10 µM NE was residual NE that had not washed out.

NE uptake in whole RA and RVC tissues.

Whole RA and RVC tissues were incubated in PSS (with 10 μM pargyline and 1 μM RO 41-0960 to inhibit NE degradation via MAO and COMT, respectively) with either uptake inhibitor (nisoxetine for NET, corticosterone for OCT3) or their respective vehicle (corticosterone vehicle was 0.1% DMSO, nisoxetine vehicle was PSS). After 30 min, tissues were incubated with 10 μM NE for 30 min, and NE uptake was determined. For all tissues under all treatment conditions, NE measured was significantly higher in tissues incubated with NE versus vehicle. In the RA (**Figure 38A**), 100 μM corticosterone reduced NE uptake in RA tissues compared to DMSO vehicle. In contrast, NE uptake in the presence of either 1 or 10 μM nisoxetine was not significantly reduced from PSS vehicle. Interestingly, the presence of 10 μM nisoxetine further reduced NE uptake already inhibited by 100 μM corticosterone. In the RVC (**Figure 38B**), neither corticosterone nor nisoxetine at any concentration tested significantly reduced NE uptake, although a trend towards lower uptake was seen in all cases. These results, consistent with what we observed for OCT3 and NET protein, suggest that whole vascular tissues can take up NE and, at least in the RA, this uptake is at least partially attributable to the actions of OCT3.

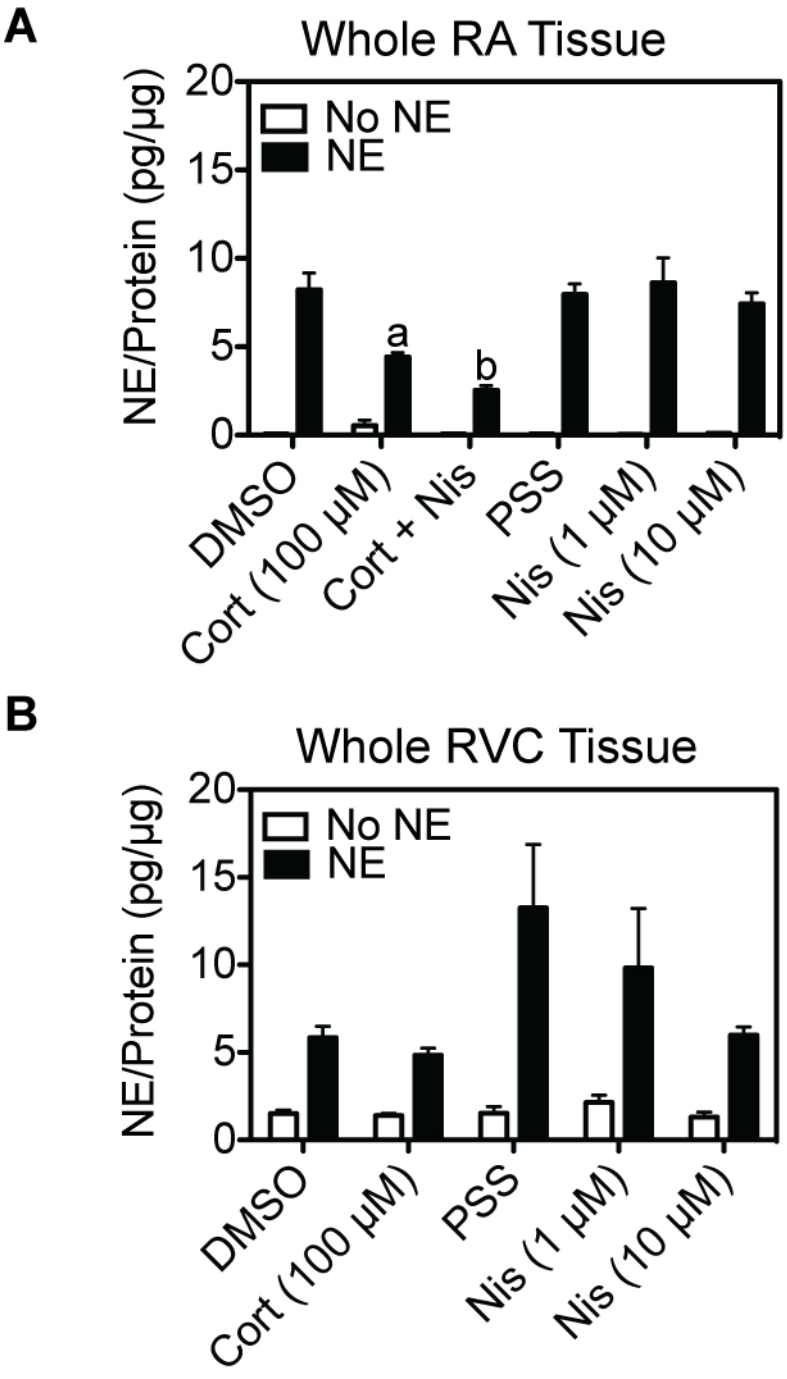

Figure 38. NE Uptake in whole vascular tissues.

NE uptake in whole rat aorta (**A**) and rat vena cava (**B**) tissues. Uptake was assessed in the presence of 0.1% DMSO (corticosterone vehicle), corticosterone (Cort; 100 µM),

Figure 38 (cont'd)

nisoxetine (Nis; 1 and 10 μM), nisoxetine and corticosterone (Nis and Cort; 10 and 100 μM, respectively), or PSS (nisoxetine vehicle). Tissues were incubated in the presence of 10 μM NE (black bars) or PSS (No NE, white bars). N = 4 – 6 animals. a = significantly different from no NE. b = significantly different from corticosterone. c = significantly different from nisoxetine (10 μM) and corticosterone. $P \leq 0.05$.

3. Aim 3: Identify the protein substrates of TGs, with an emphasis on those that are modified by NE.

Rationale: Elucidation of the endogenous TG protein substrates is important, as their identity would give insight into the processes mediated by TG function. Few studies have actually identified the endogenous TG substrates in the vasculature. Several studies have identified potential TG substrates, such as collagen types I and II (122), apolipoprotein (a) (17), and dermatan sulfate proteoglycan (94). However, these studies utilized purified extracellular proteins, and did not investigate endogenous intracellular TG substrates. One of the few studies that used homogenates of vascular tissues to identify endogenous TG substrates identified vimentin, a protein that may play a role in vasodilation (71), as a substrate in human atherosclerotic plaques (64). Even more limited is the identity of the endogenous monoamine-amidation protein substrates. As more thoroughly discussed in the introduction and overviewed in **Table 2**, studies that have investigated monoamine-amidation substrates in the vasculature are limited. Among those that have, small GTPases are the most commonly described (39, 61, 62, 184), although the actins and other contractile and structural proteins have been identified as well (188). Thus, while several candidate proteins have been identified, few endogenous TG substrates have been elucidated.

The identification of the true TG substrates is a challenge, in particularly in relation to those that serve as substrates for monoamine-amidation. This is in part due to the lack of specific tools to identify monoamine substrates. Previously, our lab has identified vascular substrates using a biotinylated 5-HT moiety, and streptavidin conjugated molecular tools (188). In this study, we perform similar functions using a NE-

biotin conjugate. Additionally, no one to our knowledge has investigated global endogenous substrates of TGs in the vasculature. In this study, we aim to identify the global TG substrates in the RA and RVC.

3.1. NE-amidation of α-actin

To confirm that α-actin is a TG substrate for amidation by NE, RA homogenates were subjected to TG reaction conditions in the presence on 12.7 μM NE-biotin or vehicle, and α-actin was subsequently immunoprecipitated from these homogenates. Western analysis was performed on the immunoprecipated proteins (**Figure 39**). NE-biotin was observed in the treated, but not vehicle, samples. Blots were subsequently reprobed with α-actin to confirm that it had indeed by immunoprecipitated in all samples. This experiment strongly supports that α-actin is a substrate for NE-amidation by TGs.

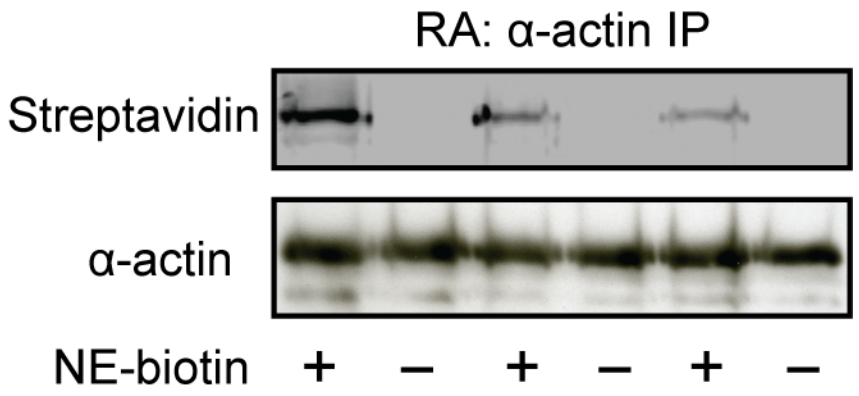

Figure 39. α-actin precipitation and amidation by NE-biotin.

A TG reaction assay was performed using 12.7 μM NE-biotin (or vehicle) as a substrate in RA homogenates. α-actin was subsequently immunoprecipitated from the homogenates, and Western analysis was performed to visualize NE-biotin incorporation. Bands were detected with streptavidin in homogenates incubated with NE-biotin, but not vehicle. Subsequent reprobing with an anti-α-actin antibody confirmed that α-actin was immunoprecipitated in all samples. Experiment was performed with RA homogenates from 3 different animals. Adjacent lanes of NE-biotin and vehicle were reactions performed using the same RA homogenate.

3.2. TG substrate identification by mass-spectrometry

The following experiment was performed to gain a sense of the identities of the different TG substrate proteins that exist in the vasculature: RA and RVC homogenates were incubated in TG reaction buffer in the presence of BAP, NE-biotin, or vehicle (lysis buffer) for 1 h. These substrates were chosen to identify global amine acceptor TG substrate proteins (BAP substrate) and to identify amine acceptor substrate proteins for NE (NE-biotin substrate). TG-substrate incorporation into proteins was confirmed by taking an aliquot of this solution and performing Western analysis and modified proteins by probing with fluorescently-conjugated streptavidin (**Figure 40**). Dialysis was performed on the rest of the reaction cocktail to remove unbound biotinylated substrate. After dialysis, biotin-conjugated substrate-incorporated proteins were captured on streptavidin-coated magnetic beads to be identified by mass-spectrometry.

A number of proteins, mostly keratins, were identified in both in the BAP or NE-biotin samples and in vehicle treated tissues, and were omitted from our subsequent analyses. However, a large number of proteins were found to be specific to the BAP and/or NE-biotin treated samples. In addition, samples that had ≥2x the amount of protein identified in BAP or NE-biotin samples than in the vehicle samples were considered “enriched” and included in our analysis. A total of 157 proteins were found to be present in at least one of the samples tested. A number of protein substrates were identified as specific to NE-biotin or BAP in the RA (**Figure 41A**) and RVC (**Figure 41B**), although most of the proteins identified were common substrates for both BAP and NE-biotin. In addition, commonly shared and unique protein substrates were identified for

NE-biotin (**Figure 41C**) and BAP (**Figure 41D**) in RA and RVC tissues. **Table 9** lists the proteins identified as NE-biotin substrates grouped according to their functions.

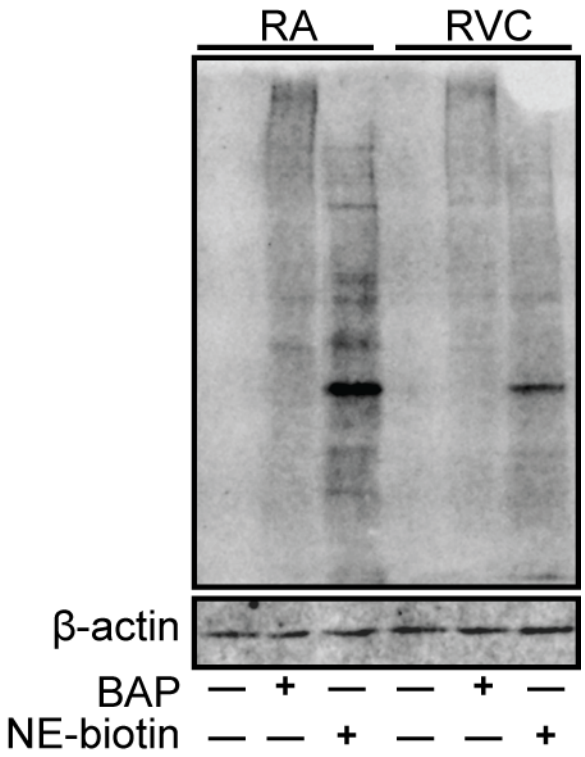

Figure 40. Western analysis for RA and RVC samples used in mass-spectrometry experiments for NE-biotin and BAP substrate identification.

After performing the TG reaction, RA and RVC samples were separated by SDS-PAGE for Western analysis of incorporation of biotinylated TG substrate. Vehicle (no BAP or NE-biotin), 4 mM BAP, or 12.7 μM NE-biotin samples were analyzed. β-actin was used as a loading control. Representative of 3 separate experiments using different pools of RA and RVC tissues from different animals.

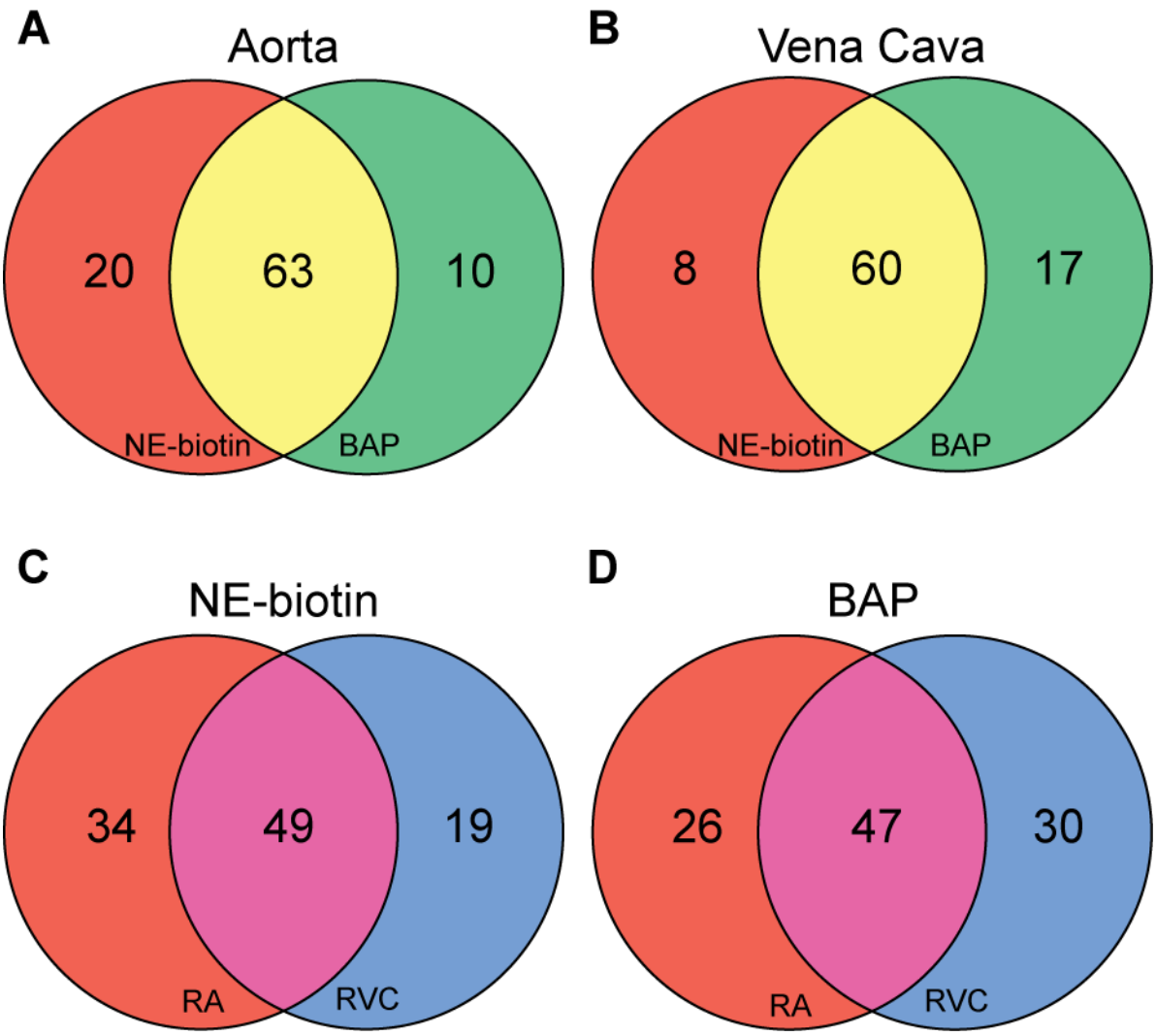

Figure 41. Venn Diagrams of TG substrates in RA and RVC for NE-biotin and BAP.

Venn diagrams comparing the TG protein substrates identified for **A**) NE-biotin and BAP in RA, **B**) NE-biotin and BAP in RVC, **C**) NE-biotin in RA and RVC, and **D**) BAP in RA and RVC. Proteins included in the analysis were identified in at least 2 of the 3 samples assayed, and were either enriched (≥ 2x the number of unique peptides fragments found in NE-biotin or BAP samples compared to vehicle control) or completely absent in vehicle.

Protein	NE-biotin*		BAP*		Notes†
	RA	RVC	RA	RVC	
Cell Metabolism and Redox Regulation					
Glutathione S-transferase Mu 2	3	3	3	3	Redox Regulation
Aldehyde dehydrogenase, mitochondrial	3	3	3	2	
Glyceraldehyde-3-phosphate dehydrogenase	3	3	2	2	Glycolysis
Glutamate dehydrogenase 1, mitochondrial	3	2	3	2	
Pyruvate kinase isozymes M1/M2	3	2	3	2	Glycolysis
ATP synthase subunit alpha, mitochondrial	3	2	2	3	Electron Transport Chain
Aconitate hydratase, mitochondrial	3	2	2	2	TCA Cycle
Isocitrate dehydrogenase [NADP], mitochondrial	2	2	2	2	TCA Cycle
Malate dehydrogenase, mitochondrial	2	2	2	2	TCA Cycle
Aspartate aminotransferase, mitochondrial	2	2	1	2	Amino acid metabolism
Trifunctional enzyme subunit alpha, mitochondrial	2	2	1	2	Lipid metabolism
Glycogen phosphorylase	3	2	3	1	Cell metabolism
Peroxiredoxin-1	2	2	2	1	Redox Regulation
Xaa-Pro aminopeptidase 1	2	1	2	0	Protein catabolism
Glutathione S-transferase Mu 5	3	0	3	1	Redox Regulation
L-lactate dehydrogenase B chain	3	1	3	1	Glycolysis
Glutathione S-transferase P	2	1	3	0	Redox Regulation
Phosphoglycerate kinase 1	2	0	0	1	Glycolysis
3-Mercaptopyruvate sulfurtransferase	2	0	1	0	Cell metabolism
L-lactate dehydrogenase A chain	1	2	3	2	Glycolysis
Glutathione peroxidase 3	1	2	0	2	Redox Regulation
Guanine deaminase	0	3	0	2	Cell metabolism
3-Ketoacyl-CoA thiolase, mitochondrial	1	2	1	1	Lipid metabolism

Table 9. Protein substrates for NE-biotin grouped by function.

Table 9 (cont'd)

Cytoskeletal					
Vinculin	3	2	3	3	F-actin binding
Alpha-actinin-1	3	2	3	2	F-actin cross-linking
Dihydropyrimidinase-related protein 3	3	2	3	2	Cytoskeletal remodeling and cell migration
Transgelin	3	2	3	2	Actin cross-linking
Vimentin	2	3	3	3	Intermediate filament
Actin, alpha cardiac muscle 1	2	3	2	3	α-actin
Actin, cytoplasmic 1	2	3	2	3	β-actin
Myosin-11 (Fragments)	2	3	2	3	Muscle contraction
Tubulin alpha-1B chain	2	3	2	3	Microtubule
Tubulin beta-4B chain	2	3	2	3	Microtubule
Tubulin beta-5 chain	2	3	2	3	Microtubule
Myosin-9	2	3	2	2	Cytokinesis and cell shape
Tubulin alpha-1A chain	2	3	0	3	Microtubule
Calponin-1	2	0	2	0	Muscle contraction
Destrin	3	0	3	0	Actin Depolymerization
Heat shock protein beta-1	3	0	3	0	Actin organization
Profilin-1	3	1	3	0	Polymerization
Myosin-10	3	0	2	0	Cytokinesis and cell shape
Myosin light polypeptide 6	2	1	3	0	Muscle filament sliding
WD repeat-containing protein 1	2	0	3	0	Actin filament disassembly
Unconventional myosin-Ic	2	0	1	2	Intracellular transport
Adenylyl cyclase-associated protein 1	2	0	1	0	Regulates filament dynamics
Septin-7	2	0	1	0	Actin organization
Tubulin beta-2A chain	0	3	2	2	Microtubule
Myosin-6	0	2	0	3	Muscle contraction
Myosin-7	0	3	0	2	Muscle contraction

Table 9 (cont'd)

DNA/RNA/Protein Synthesis and Regulation					
Heat shock cognate 71 kDa protein	3	2	3	2	
Heat shock protein HSP 90-beta	3	2	3	2	Protein folding
Elongation factor 1-alpha 1	2	3	3	3	
Elongation factor 2	2	2	3	2	
T-complex protein 1 subunit gamma	2	2	0	1	Protein folding
Peptidyl-prolyl cis-trans isomerase A	2	0	3	2	Protein folding
Heat shock 70 kDa protein 1A/1B	3	1	3	1	Protein folding
Protein Niban	3	1	2	1	
Endoplasmin	2	1	1	2	Protein folding
Transitional endoplasmic reticulum ATPase	2	1	1	2	
General transcription factor 3C polypeptide 1	3	0	1	0	
Elongation factor 1-gamma	2	1	0	1	
3-hydroxyacyl-CoA dehydrogenase type-2	2	0	0	0	
Mitogen-activated protein kinase 14	2	0	1	0	
Heterogeneous nuclear ribonucleoprotein K	0	2	0	2	
40S ribosomal protein S3	1	2	0	1	
Ubiquitin-60S ribosomal protein L40	1	2	0	1	
Extracellular Matrix					
Decorin	3	3	3	3	
Prolargin	3	3	3	3	
Lumican	3	3	2	3	
Biglycan	2	3	2	3	
Collagen alpha-1(I) chain	2	3	0	2	
Serpin H1	0	2	1	3	Collagen biosynthesis

Table 9 (cont'd)

G-Protein Signaling					
Guanine nucleotide-binding protein G(i) subunit alpha-2	2	2	2	2	α subunit
Ras-related protein Rab-1A	3	2	0	2	Small GTPase
Ras-related protein Rap-1A	2	1	2	2	Small GTPase
Cell division control protein 42 homolog	2	1	2	0	Small GTPase
GTP-binding nuclear protein Ran	3	1	0	0	Small GTPase
Ras-related C3 botulinum toxin substrate 1	1	2	0	0	Small GTPase
Miscellaneous					
Annexin A1	3	3	3	3	Cell membrane
Annexin A2	3	3	3	3	
Clathrin heavy chain 1	3	3	3	3	Endocytosis
Hemoglobin subunit alpha-1/2	3	3	3	3	Blood
Hemoglobin subunit beta-1	3	3	3	3	Blood
Annexin A5	3	2	3	2	Blood
Phosphate carrier protein, mitochondrial	3	2	2	2	Transport
EH domain-containing protein 2	2	3	2	3	Cell membrane
Adenine phosphoribosyltransferase	2	2	3	2	Purine salvage
ADP/ATP translocase 1	3	3	1	3	Transport
Dihydropyrimidinase-related protein 2	2	3	1	2	Development
Membrane primary amine oxidase	2	1	3	2	Cell membrane
E3 ubiquitin-protein ligase NEDD4	2	0	2	0	Ubiquitination
Integrin-linked protein kinase	2	0	2	0	Signal transduction
Cysteine and glycine-rich protein 1	3	0	3	1	Development
Four and a half LIM domains protein 1	3	0	2	0	Differentiation
Lipoma-preferred partner homolog	2	0	3	0	Cell adhesion

Table 9 (cont'd)

Guanine nucleotide-binding protein subunit beta-2-like 1	1	2	2	2	Signal transduction
Alpha-1-inhibitor 3	0	2	1	2	Protease inhibitor
Coatomer subunit gamma-1	1	2	1	2	Transport
Sarcoplasmic/endoplasmic reticulum calcium ATPase 2	0	2	0	2	Transport
Serum albumin	1	3	1	3	Blood
Alpha-1-macroglobulin	0	3	0	3	Protease inhibitor
Fibrinogen gamma chain	0	3	1	1	Blood

Table lists proteins identified by mass spectrometry in at least 2 samples of the RA and RVC tissues incubated with NE-biotin. *Numbers refer to the number of samples that the protein was identified in. †Notes are derived from the UniProt Consortium database (36).

4. Aim 4: The NE-amidation of vascular proteins stimulates VSMC to respond in a way that is physiologically relevant and measureable.

Rationale: The vasculature, in many ways, is an ideal model to test the hypothesis that the amidation of proteins by NE is a physiological significant event that stimulates a measureable response. Vascular tissues have access to a plentiful source of NE via the sympathetic nervous system, and rely on this NE for function and to maintain homeostasis. NE can stimulate VSMCs to respond in a number of ways. Typically, NE signals for VSMC contraction. However, NE can also stimulate their migration and growth. This function of VSMCs is primarily observed when the cells have taken on a "synthetic" phenotype, such as see in cell culture (29). However, VSMCs can exhibit this phenotype *in vivo*, as well (51, 195). Because our experiments demonstrate that cultured VSMCs lose the ability to take up NE, as well as expression of at least some of the vascular TGs, we decided to investigate the role that the amidation of vascular proteins by NE plays in vascular contraction, as this a physiologically significant function of VSMCs *in vivo* that is mediated by NE. We hypothesized that the TG-mediated amidation of proteins by NE was necessary for vascular contraction.

4.1. Contraction

To test the contribution that NE-amidation my play in vascular contraction we tested the ability of RA and RVC tissues to contract to NE in the presence of cystamine, a TG inhibitor. Endothelium intact tissues were exposed to either vehicle or cystamine prior to exposure to increasing concentrations of NE. Cystamine was able to block NE-induced contraction in a concentration-dependent manner in both RA **(Figure 42A**) and RVC (**Figure 42B**) tissues. RVC tissues were more sensitive to the ability of cystamine

to block NE-induced contraction, as concentrations of cystamine (0.1 mM) that modestly decreased NE-induced contraction in the RA (max contraction to NE = 67.5 ± 3.9 % of vehicle) completely abolished NE-induced contraction in the vena cava (**Figure 43**). Contraction to KCl, which causes tissues to contract via a receptor-independent, cell-depolarization mechanism, was only modestly reduced by cystamine at concentrations that completely abolished NE-induced contraction in both RA (**Figure 44A**; KCl-induced contraction with 0.5 mM cystamine = 88 ± 7.5 % of vehicle) and RVC (**Figure 44B**; KCl-induced contraction with 0.1 mM cystamine = 55 ± 21 % of vehicle) tissues. Futhermore, KCl-induced contraction was not significantly reduced at concentrations of cystamine that merely attenuated NE-induced contraction in these tissues. These results suggest that NE-induced vascular contraction is dependent on the amidation of proteins by NE.

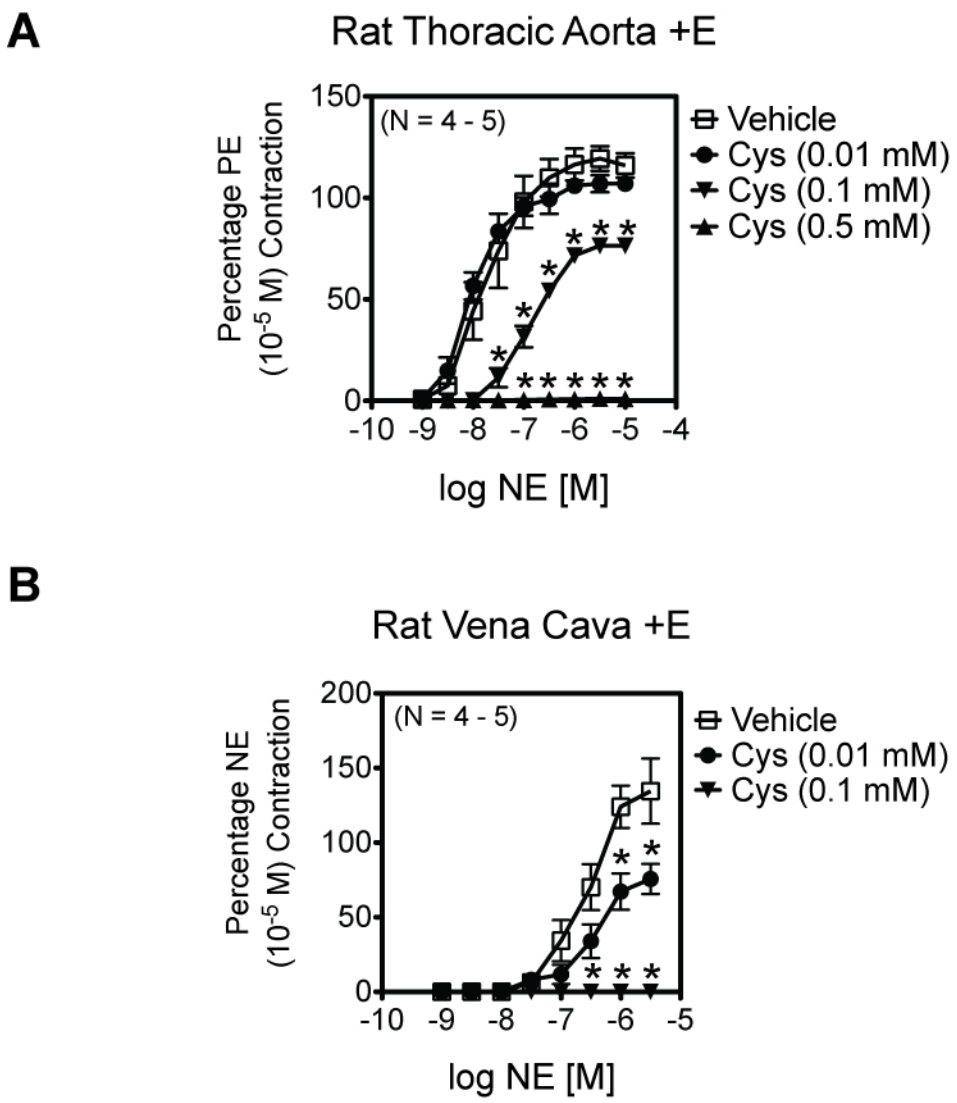

Figure 42. NE-induced RA and RVC contraction in the presence of cystamine.

NE-induced contraction in endothelium intact RA (**A**) and RVC (B) tissues. Cystamine was able to inhibit contraction in both RA and RVC tissues in a concentration-dependent manner. * = significantly reduced contraction compared to vehicle. C) A comparison of the effect of cystamine on maximum contraction to NE in RA and RVC tissues. Cystamine was able to inhibit and abolish NE-induced contraction in the RVC at

Figure 42 (cont'd)

lower concentrations than in the RA. a = significantly reduced contraction compared to vehicle. b = significantly reduced contraction compared to RA. $P \leq 0.05$. Tissues are from 4 - 5 different animals.

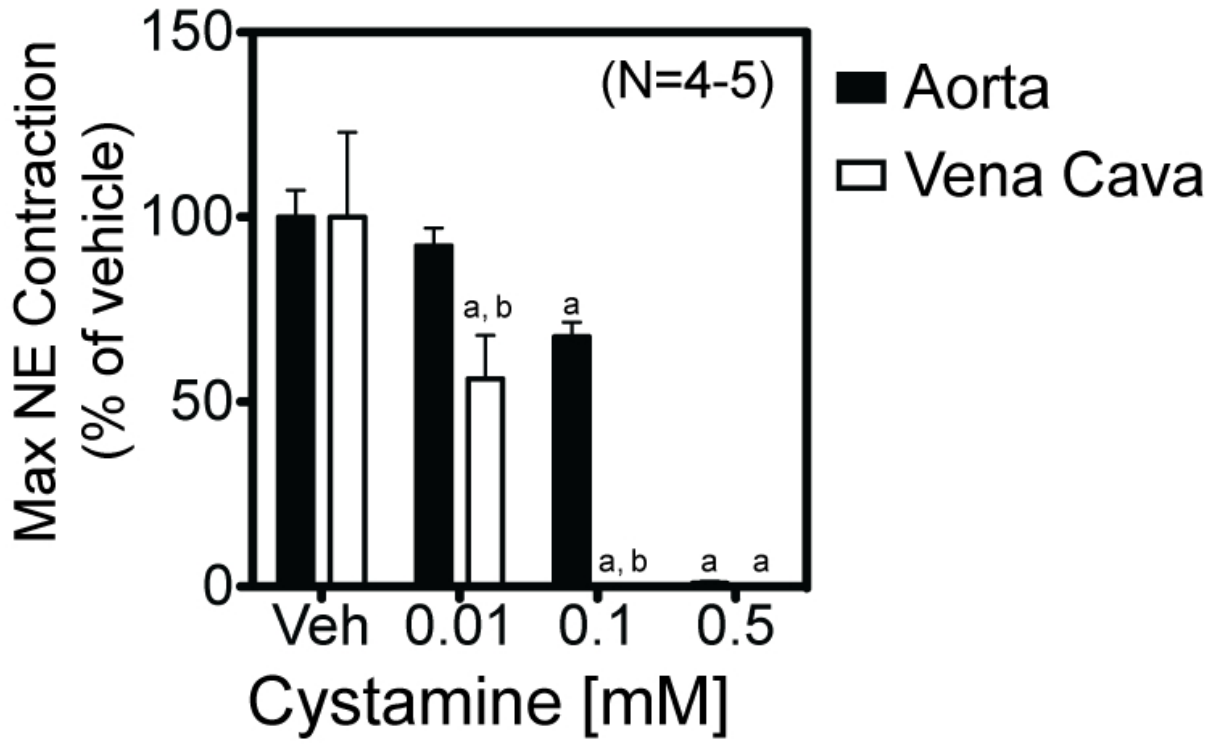

Figure 43. Maximum RA and RVC contraction to NE in the presence of cystamine.

Graphical representation of maximal NE-induced contraction in RA (black bars) and RVC (white bars) in the presence of several concentrations of cystamine. Veh = vehicle (water). a = significantly reduced compared to vehicle. b = significantly lower compared to RA tissue. $P \leq 0.05$. Data was obtained from experiments on different RA and RVC tissues from 4 – 5 different animals.

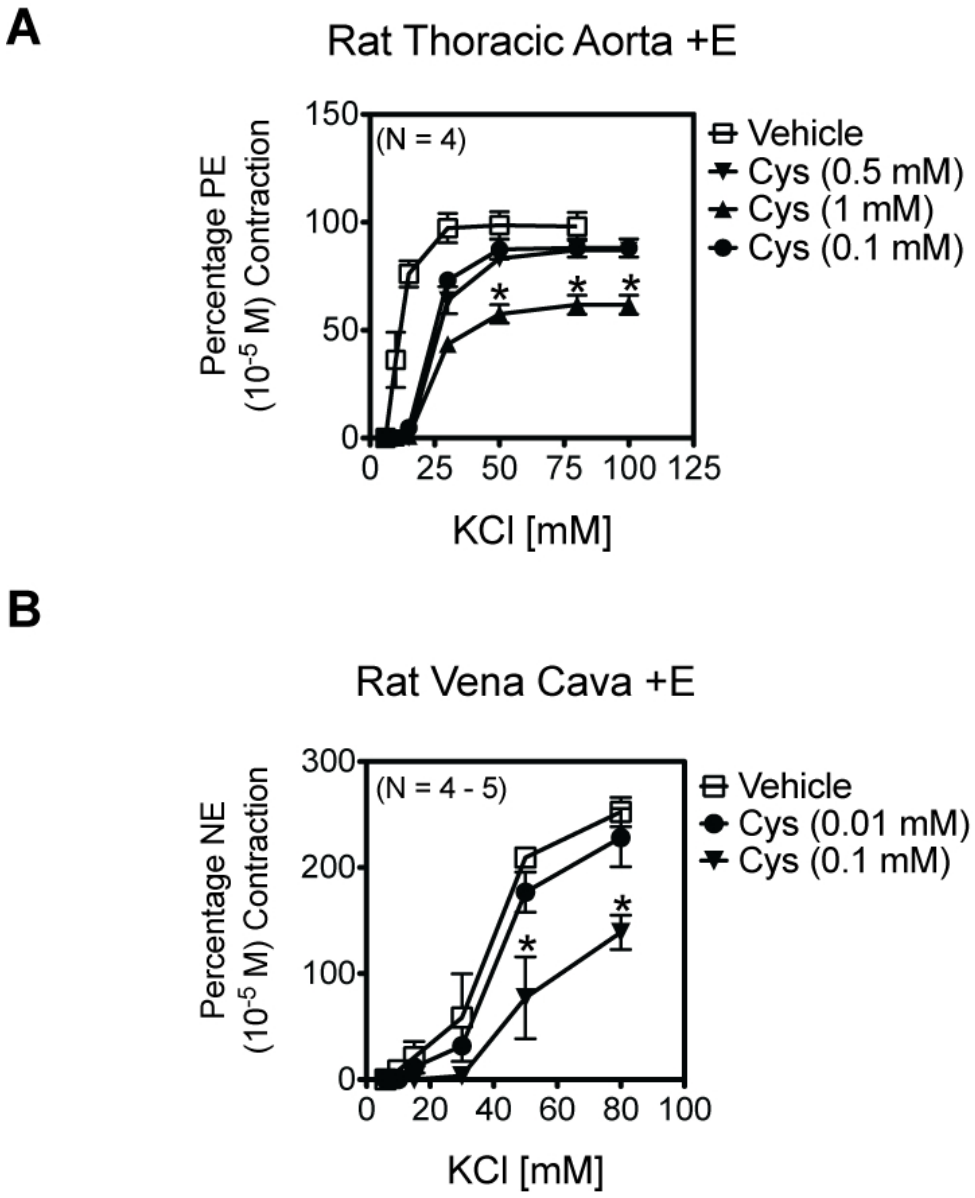

Figure 44. KCl-induced RA and RVC contraction in the presence of cystamine.

KCl-induced contraction in endothelium-intact RA (**A**) and RVC (B) tissues. Cystamine was able to inhibit contraction in both RA and RVC tissues in a concentration-dependent manner. * = significantly reduced contraction compared to vehicle. $P \leq 0.05$. Tissues are from 4 - 5 different animals.

Chapter 4: Discussion

The amidation of proteins by monoamines, and the potential for this modification to lead to a physiological-relevant response, has only recently been described (40). Most studies that have investigated the physiological consequences of protein amidation by monoamines have focused on serotonylation (61, 81, 107, 108, 133, 184, 188, 190). In this study, we demonstrate for the first time that NE may also serve as a substrate for TGs, and that this modification may have physiological implications for vascular contraction. Not only does this study introduce a novel mechanism by which TGs may influence vascular function, it also challenges the paradigm that NE only elicits biological function through interaction with cognate adrenergic receptors. This study also expands our understanding of both venous and arterial physiology, demonstrating a novel way that NE, which vascular tissues rely on for physiological function, may regulate vascular function.

1. Evidence for NE-amidation as a physiologically significant event

The major of the aim of these studies was to demonstrate that NE-amidation was a physiologically significant event. To this end, we demonstrated that NE acts as a substrate for TGs (via the incorporation of NE-biotin; **Figure 28**). NE-biotin incorporation could be inhibited by the TG inhibitor cystamine, suggesting that this was indeed a TG-dependent event. Furthermore, histamine-biotin, which would have the primary amine blocked by biotin, and would therefore could no longer act as a TG substrate, was not incorporated into vascular proteins. This unbiotinylated NE could compete with NE-biotin to be incorporated into vascular proteins, suggesting that NE was handled in a

similar way by vascular TGs (Figure 29). These data suggest that NE acts as a TG substrate.

Though we were able to demonstrate that NE can act as a TG substrate, direct evidence that NE-amidation occurs *in vivo* was limited. Using an anti-NE-BSA antibody, we did observe a number of proteins of higher (>50 kDa) molecular weight that could potentially act as NE-amidation substrates (**Figure 24**), although the specificity of this antibody is called into correction for a number of reasons discussed below.

At the beginning of these studies, we proposed investigating how protein amidation by NE could influence three different physiological processes: vascular contraction, VSMC migration, and VSMC proliferation. Because we observed the loss of TGs and OCT3 in VSMCs that had adapted to cell culture conditions (**Figures 16** and **32**), we decided to abandon our investigation of VSMC migration as growth, as the experiments proposed to study these processes utilized cultured VSMCs. Additionally, we thought it was unlikely that processes that are largely functions of *in vitro* VSMCs, and *in vivo* VSMCs that have a phenotype similar to cultured VSMC and described as “synthetic” (173) would be affected by processes that require cellular machinery that does not exist in culture. This conclusion, however, relies on the assumption that the migration and growth of VSMCs *in vivo* occurs through the same mechanism as the migration and growth of VSMCs *in vitro*. It is possible that VSMC migration and mitogenesis rely on different mechanisms *in vivo* than *in vitro*. Therefore, it may still be too early to completely rule out the possibility that VSMC migration and mitogenesis *in vivo* relies on a mechanism that involves the NE-amidation of proteins. Additionally, while not tested, it is conceivable that the loss of the ability to amidate proteins by

VSMCs may contribute to the phenotypic transition from a contractile phenotype to a synthetic, migratory and proliferative one.

Thus, of the three physiological functions we originally proposed to investigate whether NE-amidation plays a role in, contractility was the only one directly tested. In these experiment, RA and RVC contraction to NE was tested in the presence of the general TG inhibitor cystamine. Cystamine inhibited, and eventually abolished, NE-induced contraction in the RA and RVC in a concentration dependent manner (**Figure 42**). Similarly, we also tested KCl-induced contraction versus cystamine in these two tissues. KCl was used as a non-receptor-dependent contractant. KCl induces VSMC contraction via membrane depolarization, causing an influx of calcium through L-type calcium channels (45), and subsequent Rho kinase activation (147). Although we were able to inhibit KCl-induced contraction with cystamine, this mode of contraction required higher concentrations of cystamine than NE-induced contraction (**Figure 44**). KCl contraction was tested after the tissues had been tested for their contractile response to NE, thus providing an important validation that the lack of contraction observed in tissues incubated with cystamine was not due to a decrease in viability of the tissues. Our observation that the inhibition of NE-induced contraction by cystamine suggests that TG activity is vital for contraction to NE, perhaps via NE-amidation of critical proteins. However, the observation that we were able to also reduce KCl-induced contraction suggests that TGs may also be playing a global role in NE-induced contraction. Thus, at this time, a precise mechanism by which TGs are influencing both global and NE-induced contraction has not been identified.

As mentioned previously, one of the TG substrates that we identified in this study was α-actin. This protein is crucial for VSMC contraction, not just for the vital role it plays in the actomyosin cross-bridge, but also in a range of other cytoskeletal processes (63). In cells, actin can exist in two states: a globular, soluble form known as G actin, and a filamentous, fibrillar form known as F action. G actin serves a reservoir of actin that the cell can call upon, while F actin is the form that associates with myosin and acts in contraction (119). Actin polymerization is crucial for tension development and contraction of VSMCs (63). Thus, it is conceivable that the NE-amidation of proteins may be influencing NE-induced contraction by redelegating actin pools from G- to F-actin forms. One could conceive a situation where modifying the glutamine residues with NE could change how the protein is oriented, thus putting it in a structural configuration that is more conducive to F-actin formation. Alternatively, NE-amidation of glutamine residue could potentially modify how it interacts with other proteins, thus supporting interaction with molecules that stimulate F-actin formation, or conversely, preventing molecules that promote G-actin formation from binding. Finally, it is possible the NE-amidation is supporting NE-induced contraction by a different mechanism completely.

The results of these studies have several implications to vascular physiology. First, NE plays an integral role in vascular function, so understanding how NE mediates vascular responses is important. Because alterations in sympathetic nervous system output are observed in vascular diseases such as hypertension (65, 92, 151), understanding a novel way that NE elicits vascular functions could lead to novel treatment strategies. Given our data, NE-amidation may have physiological significance

in vascular contraction, a function of arteries that mediates blood pressure by modulating vascular tone and a function of veins that contributes to blood pressure regulation through capacitance regulation and subsequent blood volume redistribution (54). Furthermore, NE-amidation—or, more likely, a *loss* of NE-amidation of proteins—could play a role in the migration and proliferation of VSMCs. Evidence that this may be the case is seen in cultured VSMCs, which have decreased expression of the monoamine transporter OCT3 and one or more of the TGs—and therefore, a decreased capacity to NE-amidate proteins—and subsequently take on a proliferative and pro-growth phenotype. However, more data is needed to determine whether the loss of the OCT3 and TGs is causative to this "synthetic" phenotype taken on by VSMCs. In addition to the NE-amidation of proteins, the findings of these studies are physiologically significant in a number of other ways. To our knowledge, this is the first study that demonstrates expression of OCT3 in venous tissues. OCT3 could play an important role in NE and other monoamine signaling pathways by mediating uptake into cells, and thus removing the monoamine from the extracellular space while simultaneously supplying the cell with a source for intracellular monoamines. Furthermore, our findings that vascular tissues express several TGs in addition to TG2 is important, as it broadens the knowledge of the field of vascular TGs, and presents a new degree of complexity to how TGs may be important to vascular function. TG function—independent of its monoamine-amidation abilities—is known to mediate important vascular processes itself, for example, in the remodeling of small arteries (10, 138).

2. TG expression in the vasculature

TG activity is important to a number of physiological processes in the vasculature, including some that depend specifically on VSMC function, and has been implicated as a contributor to a number of vascular disease states (12, 148). Most TG activity in the vasculature has been attributed to TG2 activity. However, the importance of TG2 to the vasculature is called into question by the observation that TG2 KO mice show a mild vascular phenotype similar to their WT counterparts (43, 128). This seeming paradox may be resolved if one or more additional TG is present in VSMCs. To our knowledge, no study has investigated the expression of all the TG isoforms in vascular tissues. Thus, we begin this study by identifying which TGs are expressed by RA and RVC tissues.

2.1. Vascular TG expression

RT-PCR data (**Table 8**) suggest that TG1, TG2, TG4, and FXIII transcripts are all present in vascular tissues. Western analysis confirmed that the TG1, TG2, and TG4, but not FXIII, transcripts lead to measureable amounts of protein (**Figure 8**). Immunohistochemical (**Figures 9** and **10**) and immunocytochemical (**Figures 12**, **13**, **14**, and **15**) data further confirmed that TG1, TG2, and TG4, but not FXIII, were expressed in RA and RVC tissues. Of the observed TGs, the presence of TG4 was perhaps the most surprising. Previous reports have suggested that TG4 expression was restricted to the prostate (7, 32, 46). One of these studies specifically searched for TG4 mRNA in a number of different tissues, including the aorta. Thus, our finding of TG4 expression in the RA and RVC conflicts with the findings of these other studies. There are a number of different explanations that may resolve this, however. For instance, it is possible that there exists a species-specific difference in expression of

this TG, as our studies looked at rat tissues while human tissues were utilized in these other studies cited. This would be important information to have, as though the condition in human tissues is of greater interest than that of rat, knowing that species-specific differences exist is important if one hopes to extrapolate their findings from the rat model to humans. Additionally, it is possible that the primers used are specific for alternatively spliced forms of TG4 (32). Further investigation will be required to elucidate the cause for the discrepancy between our findings and previous studies.

Although mRNA for FXIII was found in RA and RVC tissues (**Table 4**), no protein was detected by Western analysis (**Figure 8**) or immunohistochemistry (**Figures 9** and **10**) in RA and RVC tissues. While possible that the mRNA we detected in RA and RVC tissues is not translated into protein, another potential explanation is that the mRNA detected is derived from macrophages or other FXIII expressing cells that infiltrate the vasculature (124). This could also explain the FXIII-positive, non-VSMCs observed rarely in freshly dissociated RVC tissues (**Figure 13D**).

We observed RVC tissues expressing significantly more TG1 and TG2 protein than RA tissues (**Figure 8**). The higher TG1 and TG2 protein content observed in RA and RVC tissues is consistent with our RT-PCR data, as both TG1 and TG2 mRNA transcripts were greater in the RVC than the RA (**Table 8**). Given that the cDNA and the protein homogenates used in these studies were derived from whole tissues that consisted of *all* layers and not just the VSMC layer, our finding that TG2 protein was actually greater in the RVC is particularly surprising given the observation that TG1 was primarily localized to the VSMC layer in RA and RVC tissues (**Figures 9B** and **10B**). Thus, the TG2 protein expressed in the single VSMC layer found in the RVC was

greater than all the TG2 protein observed in all the VSMC layers in the RA. A number of other observations in these studies that suggest TG activity may be different in the RVC than the RA. For instance, NE-induced contraction in the RVC was more sensitive to TG inhibition by cystamine than RA tissues, as the concentration of cystamine needed to inhibit and eventually abolish NE-induced contraction was less for RVC than RA tissues (**Figures 42** and **43**). Consistent with this was our observation that 1 mM cystamine was able to block NE-biotin incorporation into proteins of whole RVC tissues, but a noticeable reduction in NE-biotin incorporation was not observed in RA tissues in the presence of 1 mM cystamine (**Figure 38**). Thus it appears that RVC tissues are more sensitive to cystamine than RA tissues. One way of interpreting this is that NE-induced contraction relies on TG activity to a greater extent in the RVC than in the RA. However, it is also possible that there was less TG activity in the RVC that cystamine needs to overcome. This second scenario seems unlikely, since most of the TGs expressed in the vasculature appear to be more prevalent in the RVC than in the RA (**Figure 8**). Finally, if immunoreactive bands observed by Western analysis with the anti-NE-BSA antibody are truly endogenously NE-amidated proteins (**Figure 24**), it appears that there are a greater amount of amidated proteins in the RVC than the aorta for most of the bands detected—although not much emphasis is put into the data generated by this antibody, discussed in greater detail below. From these results, we cannot determine whether the greater intensity of immunoreactive bands observed in the RVC reflects a greater amount of these proteins being expressed, or a greater portion of these proteins serving as endogenous TG substrates for amidation by NE.

It should also be noted that our findings do not exclude the possibility that other TGs, or enzymes that carry out a TG-like reaction, are not present in the vasculature, as we did not perform *in silico* or functional searches for novel TGs. Together, these data suggest that, in addition to TG2, TG1 and TG4 are also present in the vasculature, specifically in RA and RVC VSMCs.

3. TG activity in the vasculature

One of the strengths of these studies was the use of TG1- and TG2-specific substrates (K5 and T26 peptides, respectively; generously provided by Dr. Kiyotaka Hitomi from Nagoya University, Japan) that enabled visualization of isoform-specific TG activity within RA and RVC tissues. These peptides are FITC conjugated, so visualization of active TGs could be fluorescently observed. As negative controls, peptides of identical amino acid sequence, except that the active glutamine residue had been replaced with a non-TG-reactive asparagine residue (K5QN and T26QN for K5 and T26, respectively), were used. These peptides were developed and characterized in the laboratory of Dr. Hitomi (75, 166). Although we also identified TG4 as a vascular TG, we were unable to visualize TG activity specific to this TG in the vasculature, as a TG4-specific substrate has not been created as of the time of this study. Thus, only general, and TG1- and TG2-specific TG activity was visualized.

The location of TG1- and TG2-specific activity overlapped to a great degree, as the activities of both seemed to be primarily localized to the VSMC layer in these two tissues (**Figure 21**). Indeed, almost all of the TG activity observed was within the VSMC layers of the tissues, as this was where the general TG substrate, BAP was incorporated (**Figure 17**). This is especially evident in RVC tissues, where fluorescence,

indicating incorporation of the TG substrate, and by extension, location of an active TG, was almost exclusively located in the thin, innermost layer comprised of VSMCs.

It is somewhat surprising that TG1 activity was localized to the VSMC layers of these tissues, as immunohistochemistry suggested that this TG isoform was located throughout all layers of the tissue (**Figures 9** and **10**). This suggests that there is TG1 present in these tissues but that it is not active. Because TG1 acts as a zymogen, requiring cleavage for full activity (161), one explanation is that the TG1 is the full-length, not fully active form of the enzyme. However, in the Western analyses, only a single protein band immunoreactive with the anti-TG1 antibody was observed per sample (**Figures 8** and **18**). This band migrated to a molecular weight (between 52 and 76 kDa) that is consistent with a proteolytically processed, active TG1 protein. Because the same antibody was used in both the immunohistochemical and Western analyses, one would expect that if it was detecting non-proteolytically processed TG1 with immunohistochemistry, it would also detect it by Western analysis. Alternatively, the enzyme may have activity, but the TG1-specific glutamine-acceptor substrates may be absent from these areas of the cell. This second scenario is unlikely for two reasons. First, TGs reportedly have more specificity in the glutamine-donor substrates and are more promiscuous in their glutamine-acceptor specificity (58). Secondly, BAP incorporation, a measure of general TG activity that is incorporated into glutamine *acceptor* protein substrates, was also localized primarily in the VSMC layer of RA and RVC tissues (**Figure 17**). Therefore, if TG1 identified by immunohistochemistry in the non-VSMC layers of the RA and RVC tissues is active, it would mean that both glutamine donor and acceptor TG substrates were absent from this area, which seems

unlikely. Finally, it is possible that the TG1 protein present in non-VSMC components of these vascular tissues is not active due to another mechanism of TG1 regulation not identified. For example, activity of TG1 is increased by its interaction with tazarotene-induced gene 3 (TIG3) protein (165). Thus, another plausible explanation for this the lack of TG1 activity in the non-VSMC layers of RA and RVC tissues that express TG1 is a lack of this, or possibly another, activator protein.

3.1. TG expression and activity in TG2 KO and WT mice

In these studies, we made use of TG2 KO and WT mouse pairs from two different colonies, originally described by Graham (128) and Melino (43). Both pairs of WT and KO mice are in a C57BL/6 background. The Graham mice have been backcrossed onto this background, while the Melino mice were generated in a Svj 129-C57Bl/6 mixed background and have not been backcrossed. We performed Western analysis (**Figure 18**) and BAP TG assays (**Figure 19**) on aortae from the Melino TG2 mice. In contrast, our in situ TG-specific assays were performed on fresh frozen sections of aorta from the Graham TG2 KO and WT mice (**Figure 22**) and TG1 was visualized immunohistochemically in this background (**Figure 23**). Although it is convenient to assume that the findings between these two colonies of mice are interchangeable, because they came from different colonies, it is possible that genetic drift may have occurred and the mice may differ slightly, but perhaps significantly, in their genetics. Caution should therefore be taken when extrapolating our findings in one colony of TG2 KO/WT mice pairs to the other. Although unlikely, it is possible that the expression of one or more of the TGs may vary between the colonies. We did detect TG1 in both TG2 KO/WT mice pairs—by Western analysis in the Melino mice pairs

(**Figure 18**), and by immunohistochemistry in the Graham mice pairs (**Figure 23**). We can therefore say that TG1 is present in both pairs of mice, although we can't relate the relative amounts of this protein between the two pairs, nor did we compare the activity of this protein between the two pairs. The observation that Graham TG2 KO mice appeared to lose TG1 activity (**Figure 22**)—despite the persistence of TG1 protein (**Figure 23**)—is discussed below. In addition, we were able to observe abolition of TG2 in the TG2 KO mice of both colonies. We observed complete loss of TG2 protein the Melino TG2 KO, but not WT, mouse aortae (**Figure 18**); for the Graham TG2 KO/WT mice pairs, abolition of TG2-specific TG activity was observed by in situ T26 substrate incorporation in TG2 KO, but not WT, mouse aorta sections (**Figure 22**). Thus, we can say that both of these mice pairs express TG1, and that TG2 is present in the WT, but not the KO, mice. However, because TG4 and FXIII expression was only tested in the Melino mice pairs (**Figure 18**), we cannot say for certain whether the expression of these TGs is consistent between the two pairs. We also do not know about expression of the other TGs in the vasculature of TG2 KO/WT mice, as we only measured this at the mRNA level in RA and RVC tissues (**Table 8**).

BAP incorporation, a measure of general TG activity, was observed in both TG2 KO and WT mice (**Figure 19**). The banding pattern was similar in the WT and TG2 KO mice, suggesting that either there is natural overlap between the TG2 and other TG substrates, or that the other TGs are able to compensate for the loss of TG2 activity. Although similar, TG2 KO and WT mouse aortae did show a few notable differences in the banding patterns produced by incorporated BAP (**Figure 19B**). The intensity of many of the bands (bands 3, 5, 6, 8, 9, 10, 12, 13, and 14 in **Figure 19**) was slightly

lower in the TG2 KO versus WT mice. Both TG2 KO and WT mouse aortae showed decreased BAP incorporation into proteins in the presence of the TG inhibitor cystamine; however, cystamine was able to block BAP incorporation more fully in the TG2 KO mice versus the WT. This often amplified the differences in the banding pattern produced by the TG2 KO and WT mice [**Figure 19B**; notice how the difference in peak height between TG2 KO (yellow lines) and WT (green lines) mice is often increased in the presence of 1 mM cystamine (red and blue lines for TG2 KO and WT in the presence of cystamine, respectively)]. For example, band 11 in **Figure 19** was virtually identical in intensity in the WT and TG2 KO mice; however, when cystamine was present, it was completely lost in the TG2 KO mouse, but only reduced in the WT. This experiment demonstrates that there is TG2-independent TG activity in the vasculature that is likely able to compensate for the loss of TG2 protein in the TG2 KO mice.

Additionally, we also observed TG2-independent TG activity in the RA using general and TG2-specific TG inhibitors (**Figure 20**). In this experiment, BAP incorporation into RA proteins was measured. This incorporation could be greatly reduced by the inclusion of the general TG inhibitor cystamine (1 mM); however, the reduction by the TG2-specific inhibitor Z-DON (50 μM) was only minor. This suggests that other TGs either play a major role in TG activity in RA tissues themselves, or compensate when TG2 activity is inhibited. This, along with our observations of TG activity in the TG KO mouse, strongly suggests that TG2-independent TG activity is present in vascular tissues.

In addition to observing general TG activity in TG2 KO and WT mice, we also visualized TG1- and TG2-specific TG activity in the aorta of GrahamTG2 KO and WT

mice pairs (**Figure 22A**). When incubated with either FITC-conjugated K5 (the TG1 substrate) or T26 (the TG2 substrate) peptides, FITC fluorescence was observed in the VSMC layers. This fluorescence was distinct from the autofluorescence of the collagen fibers, which was also observed in the K5QN and T26QN negative control sections. TG2 KO mouse aortae did not incorporate either the T26 or the K5 peptides (**Figure 22B**), suggesting that TG2 KO mouse aortae lack TG2- and, surprisingly, *TG1*-specific activity. The lack of TG1 activity did not appear to be due to a lack of the TG1 enzyme, as this protein was shown to be present in both WT and TG2 KO mouse aortae by immunohistochemical staining (**Figure 23**). This raises the possibility that the K5 peptide is actually being used by TG2 in addition to its intended target, TG1. However, a substantial amount of evidence when developing these substrates shows that both K5 and T26 show little cross-reactivity with other TG isoforms (166). Thus, if K5 and T26 are truly TG-isoform specific, these data suggest present an interesting possibility: that TG2 is needed to fully activate TG1 in the vascular tissues surveyed. Furthermore, it would suggest that the residual TG activity observed in TG2 KO (**Figure 19**) is due to the presence of a TG other than TG1. This could very well be TG4, as its presence was observed in vascular tissues (**Figure 8**). Further study will be needed to fully elucidate the full importance of TG1 in the vasculature.

3.2. Endogenous NE-amidation in the vasculature

In this study, we attempted to show that proteins were endogenously NE-amidated in the vasculature. To accomplish this, we used an anti-NE-BSA antibody. Several proteins from RA and RVC tissue homogenates were detected in immunoblots probed with this antibody (**Figure 24**). Densitometric analysis showed that 3 of the 5

most prominent bands were greater in RVC compared to RA tissues. Of the remaining two prominent bands, one was greater in RA tissues, while the other was not significantly greater between the two. There are two possible explanations for these differences: either the tissues expressed different amounts of these proteins, or, if the level of expression is similar, then the degree to which NE is amidated to these proteins could be different. This data would suggest that NE is endogenously amidated to some vascular proteins.

We also tried to visualize endogenous NE-amidated proteins immunohistochemically (**Figure 26**) and immunocytochemically (**Figure 27**) with this antibody. Our immunohistochemical data suggest that the amidation of proteins happened throughout both RA and RVC tissues. Immunocytochemically, this antibody detected NE-amidated proteins in both freshly dissociated VSMCs, where it appeared to colocalize with α-actin.

Previous studies have utilized anti-5-HT antibodies in a similar fashion to identify serotonylated proteins (39, 62, 107, 133, 190). The specificity of using an anti-5-HT-BSA antibody to visualize serotonylated proteins was validated in the observations that they observed an increase in band intensity when the sample is pre-incubated with 5-HT. Additionally, our lab has observed that exogenous 5-HT can compete with serotonylated proteins for the anti-5-HT antibody, suggesting that the antibody is truly specific for 5-HT and is indeed detecting serotonylated antibodies (unpublished data). In contrast, we were unable to compete off the anti-NE-BSA antibody with exogenous NE (**Figure 25A**). More surprisingly, we were unable to prevent immunostaining of RA and RVC protein bands when the blot was developed in the presence of exogenous NE-

BSA (**Figure 25A**). Furthermore, it is difficult to reconcile our observations of anti-NE-BSA staining throughout vena cava tissues (**Figure 26**) with our in situ data that suggests that active TGs are predominantly expressed in the VSMC layer of RVC tissues (**Figures 17** and **21B**). It is possible that TG activity, now absent, was once present in these layers of the RVC, and the NE-amidated proteins are remnants from the time when TGs were active. Alternatively, TG activity may be present at very low levels in these tissues that is not observable using the conditions of our assay. We encounter a similar situation with our immunocytochemical data: though we detected a loss of TGs and NE uptake in cultured VSMCs, we still detect NE-amidated proteins with this antibody. Once again, this would be explained if TG activity and NE uptake was still active, albeit at reduced levels, in these cells, or if the NE-amidated proteins we observed we remnants from when TG activity and NE uptake was present in these cells. However, when these observations (the inability to compete of the anti-NE-BSA antibody with NE and NE-BSA in the Western analysis, and the immunostaining of amidated proteins in locations where TG activity is apparently not present) call into question the specificity of the antibody. This casts doubt into the conclusions we would draw from experiments that utilized this antibody, and we therefore put little credence into those experiments that relied on the anti-NE-BSA antibody. However, even without the support of direct observation of endogenous NE-amidation with the anti-NE-BSA antibody, the rest of our data still strongly supports the idea that the NE-amidation of proteins is a true phenomenon that stimulates physiological processes in the vasculature.

4. NE uptake in the vasculature

In our hypothesis, we suggest that NE can be utilized by VSMCs as a TG substrate for the amidation of proteins. For this to occur, however, an intracellular source of NE must be available; this could occur by either synthesis or uptake of extracellular NE. In this study, we tested the hypothesis that extracellular NE is taken up and utilized by VSMCs for the TG-mediated amidation of vascular proteins. NE uptake, but not NE synthesis was tested, as we felt that if VSMC function depended on TG-mediated protein amidation by NE, it would most likely be coming from an extracellular source. We came to this conclusion for a number of reasons. First, vascular tissues have a nearby source of plentiful NE via the sympathetic nervous system. There is also evidence that NE via the sympathetic nervous system is largely responsible for regulation of vascular function. For instance, celiac ganglionectomy, which disrupts innervation to the splanchnic circulation, alleviates at least some forms of hypertension (87, 93), and reserpine, which depletes peripheral NE by blocking its reuptake via the vesicular monomaine transporter into synaptic storage vesicles (114), lowers blood pressure. Additionally, while some nonneuronal catecholamine-synthesizing cells have been identified, such as small intensely fluorescent cells (16), adrenal chromaffin cells (96, 152), and paraganglia (137), to our knowledge, no one has identified VSMCs as a source for NE synthesis, strongly suggesting that the NE-amidation of VSMC proteins would occur via sympathetically released NE taken up by the VSMC. Furthermore, when glyoxylic acid—which reacts with catecholamines causing them to fluoresce—staining is performed on vascular tissues, sympathetic nerves, but not VSMCs, fluoresce (105). While it is possible that VSMCs could make and utilize NE immediately, this at least demonstrates that VSMCs do not serve as a large reservoir of NE

themselves, and it also demonstrates that they have a large source of it nearby. Additionally, when rat cerebral arteries are stained with an anti-dopamine β-hydroxylase antibody, staining occurs in the nerves surrounding the vessel, but is not observed in the vessel itself (121). Finally, a recent report identified dopamine β-hydroxylase expression in cultured bovine aortic endothelial cells and *in vivo* expression in endothelial cells of the mouse femoral artery; however, they did not observe this enzyme in the VSMC layers of the femoral artery (159). Thus, there is precedence to our assumption that VSMCs do not manufacture NE themselves, and we therefore focused our efforts on NE uptake in VSMCs.

4.1. NE uptake transporter expression

For NE to be taken up into the cell, at least one transporter capable of moving NE across the membrane must be present. One candidate for this function would be the canonical transporter of NE, NET, which has high affinity for both NE and dopamine. Although commonly described as a “neuronal” transporter, NET has been observed in pulmonary endothelial cells (21), so the possibility of its expression in nonneuronal cells such as VSMCs cannot be discounted. In addition to this canonical transporter of NE, there are also several polyspecific (i.e., capable of transporting a variety of substrates with moderate to high efficiency) monoamine transporters capable of NE uptake that have been observed. Of these monoamine transporters—namely, OCT1, OCT2, OCT3, and PMAT—OCT3 appears to be the one most likely for NE transport in VSMCs. NE has relatively lower affinity for the OCT1 transporter (115). Similarly, NE’s affinity for OCT2 is relatively low, and its expression has been described as being limited to the kidney and brain (23, 78). While more widely distributed than either OCT1 or OCT2,

PMAT is expressed primarily in the brain and central nervous system (49). In contrast, among the “nonneuronal” monoamine transporters, NE has the highest affinity for OCT3 (23, 44, 115), which is the most widely distributed (60, 78) of the transporters. Additionally, its expression has been described in bronchial arterial VSMCs (78), indicating that at least some VSMCs may express this transporter. Thus, we chose to focus our efforts on determining whether VSMCs expressed the high affinity NE uptake protein NET, and the low affinity, but high capacity, NE uptake protein OCT3.

Both OCT3 (**Figure 32A, B, and C**) and NET (**Figure 32D**) were detected by Western analysis in whole RA tissues. NET was also present in whole RVC tissues. Though we were able to observe bands consistent with the molecular weight of these proteins in our samples, these immunoblots were not ideal. One of the challenges that plague the NET field is the lack of high quality antibodies that recognize this transporter. The antibody that we used was recently produced in an attempt to circumvent this limitation (117). Thus, it is unlikely that we would be able to find a higher quality antibody for these experiments, and our difficulty in getting high quality data with this antibody may indicate that NET is truly absent from these samples. Our OCT3 antibodies were also less than ideal for Western analysis, as multiple bands appeared in all of our samples. The two most prominent bands observed did not migrate with the positive control, and the bands also persisted even when a competing peptide was included with the Santa Cruz Biotechnology anti-OCT3 antibody (unfortunately, a competing peptide was not available for the Bioworld antibody). Thus, though these bands were consistently observed, even when different antibodies were used, we are hesitant to say that these are due to specific recognition of OCT3 in the samples.

However, in the blot probed with the anti-OCT3 antibody from Bioworld, faint bands migrated at a molecular weight consistent with the reported molecular weight of OCT3. Furthermore, a band at this molecular weight was observed in the rat placenta positive control (**Figure 32A**).

Although the Western blotting results may suggest that OCT3 protein expression in the tissues we examined was specific to the RA, and that both RA and RVC tissues express NET protein, our immunostaining data suggest a different expression profile. OCT3 was detected in both RA and RVC tissues (**Figure 33**) by immunohistochemistry. In these tissues, OCT3 appeared primarily in the VSMC layers (large arrows), although punctate staining was identified elsewhere as well (small arrows). Compare this to the NET staining observed in RA (**Figure 34A**) and RVC (**Figure 34B**) tissues, where, while positive staining was observed, this staining was faint and not defined in a particular cell type throughout the tissue. A similar observation was made with our immunocytochemical staining: OCT3 was present in VSMCs from freshly dissociated RA (**Figure 35A**) and RVC (**Figure 35B**) tissues, where it appeared to localize around the perimeter of the cell (see arrows). While OCT3 staining was also observed in cultured VSMCs (**Figure 35C** and **D**), this staining was faint and was not localized to the perimeter of the cell, as in the freshly dissociated VSMCs, but rather scattered throughout the cell. NET staining, on the other hand, was basically absent, both in cultured and freshly dissociated RA and RVC VSMCs (**Figure 36**). These data suggest that vascular tissues express OCT3—but not NET—and that it is specifically localized to VSMCs. In VSMCs, it localizes to the perimeter of the cell, putting it in position to transport NE into the cell. Because OCT3 is a low affinity, high capacity transporter, this

may indicate that NE is only taken up into the VSMC at high concentrations. While the K_m for NET is ≤ 1 μM, the K_m for OCT3 has been reported to be around 250 μM (77). While this may bring into the question the efficacy of OCT3 for NE transport, it should be noted that the concentration of NE in the neuromuscular junction after its release from synaptic terminals has been estimated to be as high as 300 μM (164). Thus, although OCT3 may have low affinity for NE, its existence on VSMCs may still be physiologically relevant.

4.2. NE uptake in whole tissues

While an attempt to measure NE in VSMCs was made, we did not observe significant NE uptake when VSMCs were incubated with up to 10 μM NE (**Figure 37A**). Though a significant difference in NE was measured when cells were incubated in 10 μM NE, we do not believe that this represents NE uptake, as we measured similar concentrations of NE when empty wells were incubated with 10 μM NE (**Figure 37B**), suggesting that this NE represented residual NE that we had difficulty washing away at high concentrations. This NE persisted even when the number of washes and time of wash was increased (data not shown). This is in contrast to whole RA tissues, in which we were able to demonstrate significant NE uptake at 10—but not 1—μM (**Figure 37A**). In our whole tissue experiments, we were able to circumvent the issue of residual NE confounding our results—as was the issue with RA VSMCs (**Figure 37B**)—as we were able to move the entire vessel into clean tubes for washes and subsequent assessment. Furthermore, when we compare the total NE measured when cultured RA VSMCs were incubated with 10 μM NE compared to that when whole RA tissues were, dramatically more NE was detected in the whole RA samples (**Figure 37C**). Thus, from these

preliminary results, we chose to measure NE uptake in whole tissues, using a concentration of 10 μM, as this was the lowest concentration of NE that we were able to successfully measure uptake in the vessels with.

We observed significant NE uptake (using 10 μM NE) in both RA (**Figure 38A**) and RVC (**Figure 38B**) tissues. In the RA, NE uptake was sensitive to 100 μM corticosterone (significantly decreased compared to corticosterone vehicle, 0.1 % DMSO) suggesting that it was mediated, at least in part, by OCT3. In contrast, the NET inhibitor nisoxetine was unable to attenuate NE uptake compared to PSS vehicle in the RA. This is despite the fact that the highest concentration of nisoxetine used, 10 μM, is ten-fold higher than other studies have used to block NE uptake in NET expressing cells (20, 83, 168). It could be argued that using a high–but still physiologically relevant (164)—concentration of NE, we selected for the low affinity, high capacity uptake of NE by OCT3 (44); however, as we were not able to detect NE in whole RA tissues incubated with 1 μM NE (**Figure 37A**), it is unlikely that VSMCs are taking up NE and concentrating it to a large extent at lower concentrations. Thus, our selection of 10 μM NE to be used in these experiments, and conclusions that transport via OCT3 is the primary mechanism of NE uptake in these tissues, is justified.

Interestingly, 10 μM nisoxetine *was* able to slightly, but significantly, further reduce NE uptake already reduced by 100 μM corticosterone. Whether this indicates that NET contributes slightly to NE uptake in the RA is unclear, as we were unable to completely block NE uptake under any of the conditions tested. In the RVC, we were unable to block NE uptake under any of the conditions tested. This may mean that another mechanism exists by which NE can be taken up into these tissues. Given the

fact that we used high concentrations of the NET inhibitor nisoxetine, it is unlikely that higher concentrations would further reduce NE uptake. We were prohibited from using higher concentrations of corticosterone due to its solubility, so it is possible further OCT3 inhibition would block the residual NE uptake that we observed. **A** final explanation for our inability to completely block NE uptake with the inhibitors we used would be the existence of other NE transporters in these tissues. Although we tested both inhibitors of NET and OCT3, we cannot discount that other transporters may participate in NE uptake. As mentioned above, OCT1, OCT2 (153), and PMAT (44) are additional transporters that can potentially transport NE into a cell, although they show less affinity for NE transport than either NET or OCT3. It is unlikely that this transport is due to the presence of OCT2, as corticosterone shows similar potency in its ability to block NE uptake via OCT2 (IC_{50} = ~4 μM) and OCT3 (IC_{50} = ~5 μM) in the rat, suggesting that we the concentration of corticosterone that we used would also have inhibited OCT2-dependent uptake. Corticosterone can potentially inhibit OCT1 as well, but with much less potency (IC_{50} = 150 μM) (48), which means it is unlikely that OCT1 uptake would have been drastically altered by the concentration of corticosterone we used. It should also be restated that is transported less efficiently with OCT1 and OCT2 (153) compared to OCT3. Similarly, though the NE's affinity for OCT3 and PMAT is comparable, OCT3 is more efficient in transporting NE due to a higher V_{max} (44). Therefore, though these other transporters may be present, they likely would play a more minor role in NE uptake than the OCT3 transporter, which we demonstrated the presence of in both RA and RVC VSMCs (**Figures 33 and 35**).

Although we were unable to significantly reduce NE uptake with corticosterone in the RVC, there are a number of reasons to believe that OCT3-dependent uptake may occur in the RVC. First, although negligible OCT3 protein was detected in the RVC by immunoblotting (**Figure 32A**), immunohistochemical and immunocytochemical staining suggest that this transporter is present in VSMCs in the RVC (**Figures 33 and 35)**. The discrepancy between the Western analysis and the immunostaining data is likely due to the relative abundance of VSMCs in the RVC versus the RA. While the RA is comprised of many layers of VSMCs, the vena cava has only a single layer. Protein derived from VSMCs is therefore highly represented in our RA tissue homogenates, while VSMC derived protein would represent a small fraction of the total protein in RVC homogenates. Thus, it is plausible our inability to observe OCT3 protein in RVC tissues by immunoblotting was due to insufficient expression compared to RA tissues. Finally, we can be fairly certain that NE is taken up by VSMCs in the RVC, as RVC VSMCs concentrated NE-biotin (**Figure 30**). It would be plausible to assume that this is OCT3-dependent uptake, given that OCT3 immunocytochemical staining localized this protein to the perimeter of the cell (**Figure 35B**). The question remains, however, why we were not able to show inhibition of NE uptake in the RVC with corticosterone (**Figure 38B**). The likely explanation for this again relies on the composition of RA and RVC tissues. Because RA tissues are comprised of many VSMCs, it is likely that much of the NE we detected by HPLC in the RA was actually taken up into VSMCs. However, in the RVC, much of the NE we observed may not have been derived from VSMC uptake, as these cells are a minority population in the RVC. Rather, a large portion of the NE we measured in RVC tissues may have been due to non-VSMCs present in these tissues

that also took up the NE (via an OCT3-independent mechanism). Therefore, it is plausible that other forms of NE uptake in other, non-VSMCs of the vena cava overwhelm the NE uptake in VSMCs to a degree that makes this inhibition undetectable.

Finally, as mentioned above, though we made an attempt to measure NE uptake in cultured VSMCs, we were unable to detect significant uptake (**Figure 37**). This observation is consistent with several of our other findings. First, we did not detect OCT3 or NET protein in VSMCs by Western analysis (**Figure 32**), and immunocytochemical staining in regards to these proteins was equivocal (**Figures 35** and **36; C** and **D**). Additionally, despite vivid and intense staining observed in freshly dissociated VSMCs incubated with NE-biotin, cultured RA VSMCs incubated with NE-biotin showed weak to no staining when probed with fluorescently-labeled streptavidin (**Figure 30**). From these results, we concluded that cultured VSMCs did not take up NE. The significance of this observation (i.e., that VSMCs lose expression of NE transport proteins and the ability to take up NE in culture) and its ramifications are discussed in greater detail below.

4.3. NE-biotin validation and uptake

Some experiments in these studies utilized a NE-biotin conjugate as a substitute for NE. This enabled us to track NE using streptavidin-conjugated tools. We demonstrate the ability of NE-biotin—and other biotin-conjugated monoamines—to be incorporated into RA protein homogenates (**Figure 28**). While NE-biotin, 5-HT-biotin, and dopamine-biotin were incorporated into proteins, histamine-biotin incorporation was notably absent. This can be explained by the structure of these amines: while the biotin moiety can be incorporated into multiple locations in NE, 5-HT, and dopamine (i.e., the

hydroxyl groups), in histamine, the only site where it can be incorporated is the primary amine utilized by TGs. Although this means that histamine cannot be utilized in this way like these other amines can, this observation adds strength to the idea that it is the NE, 5-HT, and dopamine moieties—and not the incorporated biotin—in the monoamine-biotin molecules that is reactive towards TGs, and thus supports the idea that we are actually visualizing monoamine incorporation by TGs in these experiments. The idea that TGs are responsible for this incorporation is further supported by the observation that the TG inhibitor cystamine (1 mM) blocks monoamine-biotin incorporation (**Figure 28**). The obvious limitation with using NE-biotin as a substitute for NE is that the biotin conjugation changes the molecule, which in turn could affect how it handled by the cells. This substitution was justifiable, however, as we also demonstrate that “cold”, non-biotinylated NE is able to compete with NE-biotin in the TG reaction in both RA (**Figure 29A**) and RVC (**Figure 29B**) tissues, suggesting that NE and NE-biotin are handled similarly by TGs.

We were able to visualize NE-biotin uptake in freshly dissociated VSMCs from both RA (**Figure 30A**) and RVC (**Figure 30B**) tissues. However, in cultured RA VSMCs, we did not see any significant staining in cells incubated with NE-biotin (**Figure 30C**), suggesting that VSMCs lose the ability to take up and/or amidate proteins with NE in culture (discussed more below). Finally, we also observed NE-biotin uptake in whole RVC and RA tissues and its subsequent incorporation into vascular proteins (**Figure 31**). Peculiarly, we were able to block NE-biotin incorporation into proteins with 1 mM cystamine, the general TG inhibitor, in the RVC *but not* the RA. As discussed above, this was similar to the results we observed in the contractility data, where inhibition of

contraction was seen at a lower concentration of cystamine in the RVC compared to the RA. This may suggest that RA tissues are better at concentrating NE than RVC tissues. Alternatively, TGs in the RA may be less susceptible to inhibition by cystamine, or the TGs in the RA may be more efficient at incorporating NE into proteins that RVC TGs. This particular difference between RA and RVC tissues is interesting, but its full significance is not yet elucidated. Regardless, the observation that whole tissues can take up and incorporate NE-biotin into their tissues is particularly interesting, as it suggests that whole tissues can take up *and* utilize NE in a TG-mediated, protein amidation reaction.

5. The loss of TGs and NE transporters in cultured VSMCs

As mentioned above, cultured RA VSMCs were unable to take up NE-biotin (**Figure 30C**). In addition, an attempt was made to measure NE in cultured VSMCs; however, we were unable to distinguish NE taken up into the cell from background NE (**Figure 37B**), and the NE that we measured in whole tissues was several orders of magnitude greater than that which we observed with cultured cells (**Figure 37C**). Our inability to measure NE uptake into cultured VSMCs is consistent with our observation that neither OCT3 (**Figure 35C** and **D**) nor NET (**Figure 36C** and **D**) protein were observed on the surface of cultured VSMCs. This is despite the observation that OCT3 was observed in the VSMC layers of RA and RVC tissues (**Figure 33**). Furthermore, OCT3 appeared to be present on the surface of freshly dissociated RA (**Figure 35A**) and RVC (**Figure 35B**) VSMCs, and NE—or NE-biotin—was observed to be taken up into freshly dissociated VSMCs (**Figure 30A** and **B**) and whole RA and RVC tissues

(**Figures 31** and **38**). These results suggest that VSMCs normally express OCT3 and take up NE, but lose this ability as they adapt to culture conditions.

In addition to our observations that cultured VSMCs lose expression of OCT3 and the ability to take up NE, it also appears that VSMCs exhibit decreased TG expression in culture as well. This was observed when comparing whole tissue to cultured VSMC protein expression by Western analysis (**Figures 8**). Additionally, less intense immunostaining was observed for TG1 (**Figures 12A**, **13A**, **14A**, and **15A**), TG2 (**Figures 12B**, **13B**, **14B**, and **15B**), and TG4 (**Figures 12C**, **13C**, **14**C, and **15C**) in cultured compared to freshly dissociated VSMCs. This loss was rapid, occurring prior to the first passage of VMSCs. One assumption that we make is that the decrease we observed by Western analysis was, in fact, due to a decrease in expression of these proteins by VSMCs when adapting to culture, and not due to a lack of other cell types that express these proteins in protein homogenates of cultured VSMCs, as our whole tissue protein homogenates undoubtedly contain non-VSMCs in addition to VSMCs. This assumption is just for a number of reasons, particularly in regards to TG2. Immunohistochemical staining placed TG2 (**Figures 9B** and **10B**) proteins almost exclusively in the VSMC layer of RA and RVC tissues, suggesting that most of the TG2 protein observed in the tissue homogenates is indeed derived from VSMCs. In addition, when comparing the intensity of immunocytochemical staining of these proteins in cultured versus in freshly dissociated VSMCs, freshly dissociated VSMCs almost universally had greater staining intensity than cultured VSMCs from the same tissue. However, an argument could be that non-VSMC derived TG1 made up a large percentage of the protein homogenate, especially in regards to the RVC (which is where

we saw a significant difference between whole RVC and cultured RVC VSMC expression; **Figure 8**). While TG1 staining may have arguably appeared less intense in cultured versus freshly disassociated VSMCs (**Figures 12A**, **13A**, **14A**, and **15A**), immunohistochemical TG1 staining was present throughout both RA (**Figure 9A**) and RVC tissues (**Figure 10A**). Given this, and that the reduction of TG1 protein seen by Western analysis was only present in RVC versus RVC VSMCs, it is plausible that this reduction is truly representative of a lack of additional TG1-expressing cells in cultured VSMCs that are present in the RVC.

Though we observed the loss of these proteins in cell culture, we did not investigate the cause for this loss. There are a number of reasons why VSMCs may lose these proteins in cell culture. One possibility is that the loss of all or any combination of these proteins is necessary for the dedifferentiation that occurs as VSMCs adapt to cell culture conditions. For example, the loss of these proteins may drive the VSMC phenotype switching that occurs as they transform from an *in vivo* contractile phenotype to a synthetic, proliferative one *in vitro* that enables the cells to grow and thrive in cell culture (29). Another possibility is that the loss of these proteins in culture is a consequence of the changing environment. Observations in our laboratory suggest that NE is rapidly oxidized and does not persist for long in culture media, even in the absence of cells (unpublished data). With sympathetic nerves—which provided a plentiful and constant supply of NE—no longer in close proximity, VSMCs no longer have need to express proteins for NE uptake, and may reduce their expression of OCT3 as a means of energy conservation. An interesting addendum to this explanation is the possibility that the amidation of proteins by NE may be important to the persistence of

these proteins (or other proteins responsible for the contractile phenotype of VSMCs) under normal conditions, and the loss of NE-amidation of these proteins “switches” the cell from a contractile-supporting to a migratory and proliferative phenotype. However, at this time we do not have the data to fully support or refute this hypothesis, making it mostly speculation.

Perhaps the greatest consequence of the loss of these proteins in culture was the subsequent loss of cell culture as a technique to study this modification. The decision to abandon cell culture in our model was two-fold: the loss of the cellular machinery needed to drive the NE-amidation of proteins not only made it impossible to study this process in cell culture, it also presents the likely scenario that the physiological processes that are primarily ascribed to VSMCs in culture or with a synthetic, culture-like phenotype, such as the migration and proliferation of VSMCs, are not driven by the amidation of proteins by NE. Thus, we chose not to pursue the particular hypothesis that the amidation of proteins by NE leads to the proliferation and/or migration of VSMCs. It should be noted, however, that it is still possible that the migration and proliferation of VSMCs may occur *in vivo* by different mechanisms than those seen in culture; therefore we cannot at this time completely exclude the possibility that VSMC migration and proliferation *in vivo* depend on the amidation of proteins by NE.

6. Identification of TG substrates in the vasculature

6.1. Focus on α-actin

In this study, we aimed to identify the protein substrates that become NE-amidated by TGs. A particular effort was made to identify α-actin as a TG substrate in

these experiments. There are several reasons for this. In assays that used NE-biotin and were visualized by Western analysis, we consistently observed streptavidin-reactive bands at ~42 kDa, consistent with the molecular weight of the actins (**Figures 28**, **29**, and **31**). While many proteins could be present at this molecular weight, evidence that α-actin was at least one of them was suggested by immunocytochemical experiments where NE-biotin and TGs appeared to colocalize with α-actin (**Figures 12, 13, 14, 15, and 30**). In addition to this, immunocytochemical experiments with the anti-NE-BSA antibody colocalized with α-actin (**Figure 27**); however, not a lot of credence was given to experiments performed with our anti-NE-BSA antibody, as both NE (**Figure 25A**) and NE-BSA (**Figure 25B**) we unable to block its binding to protein bands observed by Western analysis. However, given the breadth of our other data that suggested that α-actin was a substrate for NE-amidation by TGs, an effort to determine whether α-actin was truly amidated by NE was made. We performed a TG assay in RA homogenates in the presence of NE-biotin, followed by immunoprecipitation of α-actin and visualization of incorporated NE-biotin using Western analysis techniques (**Figure 39**). When NE-biotin was included in the reaction, its incorporation was observed. The blot was reprobed with an anti-α-actin antibody, we observed that we indeed successfully immunoprecipitated NE-biotin in all the samples. This experiment strongly supports the idea that α-actin is a substrate for NE-amidation.

Though we identified α-actin as a TG substrate, we have not yet elucidated the importance of NE-amidation to this protein. Given that vascular contraction is an α-actin-dependent process (131), it is possible that this protein modification is playing a

role in vascular contraction. Previous reports suggest that Gln-41 is the primary amine acceptor site in α-actin, and that incorporation of monodansylcadaverine to this site can accelerate the rate at which G-actin polymerizes to F-actin (167). However, it is unclear whether this is the site of primary NE incorporation, as actin contains several glutamine residues. Furthermore, we do not know whether NE incorporation into this site would accelerate actin polymerization in a similar manner. Actin polymerization is activated by contractile stimulation (119), and it has been suggested that actin polymerization may play a role in the regulation of smooth muscle contraction (63). The idea that the NE-amidation of α-actin may contribute to contraction is supported in this study by our observation that we could inhibit NE-induced contraction with the TG inhibitor cystamine in a concentration-dependent manner (**Figure 42**).

6.2. Protein identification by mass-spectrometry

In this study, we aimed to identify 1) global expression of TG glutamine-donor substrates using the biotinylated amine donor, BAP, and 2) identify those substrates that were specific for NE-biotin, in both RA and RVC tissues. Excluding the proteins that were found as contaminants in both the amine-donor and vehicle treated samples, a total of 157 proteins were identified. Of these, a total 102 were identified in two or more RA and RVC samples incubated with NE-biotin; 103 were identified in two or more RA and RVC samples incubated with BAP. Most of the proteins were common substrates for both BAP and NE-biotin, although a few unique samples were identified in some of the samples (**Figure 41**).

Table 10 lists the proteins we observed as substrates for NE amidation of proteins divided by function. A number of these proteins, such as α-actin, the small GTPases, collagen, and vimentin, have previously been identified as TG substrates (61, 62, 64, 179, 184, 188). A number of the proteins identified are particularly interesting in regards to their possible implications to NE-amidation mediated VSMC function. Small GTPases can act as monoamine substrates, and, at least in the case of 5-HT (62, 184) and histamine (181), trigger their constitutive activation, and subsequent downregulation by marking them for degradation via the ubiquitin pathway. Thus, our identification of cell division control protein 42 (cdc42) in the RA, Ras-related nuclear protein (Ran; in RA), Rap1A (RA), Rac1 (RVC), Rab1A (RA and RVC) as substrates of NE-biotin is of particular note, as one could imagine the NE-amidation of these proteins regulating their activity in way similar fashion to histamine and 5-HT. Furthermore, small GTPases can have important physiological functions in vascular function. Rac1 overexpression in VSMCs leads to moderate hypertension due to an increase in superoxide production (69). Rap1 has been shown to be a regulator of angiogenic responses (34). In VSMCs, the Ran GTPase has been shown to play an important role in the regulation of the transcriptional factor cAMP-response element-binding protein (CREB) transport into the nucleus (162). CREB attenuates mitogen-stimulated VSMC proliferation, migration, and matrix protein expression (187), and has been shown to be VSMC CREB content has been shown to be a common feature in several models of cardiovascular disease (150). Pulmonary artery VSMCs phenotypic transformation is modulated by Rab1 under hypoxic conditions, with Rab1 activity driving the VSMCs to a proliferative phenotype (193). Finally cdc42 has been shown to play a role in the directional precision of VSMC

migration (194). Thus, small GTPases, and ones that we specifically identified, play important roles in VSMC function and modulation of their phenotypic behavior. Although differences in small GTPases amidation by NE-biotin were observed between RA and RVC tissues, further studies are required to determine if this finding is physiologically relevant. Specifically, studies are needed to determine whether the differences observed are, in fact, true differences between arteries and veins, and also to determine if the discrepancy is due to the differential expression of these proteins, or preferential amidation of them, between these two tissues.

Also of interest, we identified α- and β-actin as proteins that were modified by NE-biotin. We also identified in these samples were a number of proteins that, with the actins, form the cytoskeletal components of the cell, as well as a number of proteins involved in actin polymerization and muscle contraction. It is possible that a number of these proteins were pulled down due to their interaction with actin, and not due to NE-amidation themselves; however, we included SDS in our samples to help reduce molecular interactions. Furthermore, because the actins were present in our vehicle controls—but greatly enriched in our NE-biotin and BAP treated samples—we would expect that proteins that strongly interacted with actin independent of TG NE-amidation action would have shown up in our controls and would be excluded from the analysis. Thus, it is likely that if NE-amidation itself is not occurring on these proteins themselves, NE-amidation of a protein may be triggering a particularly strong interaction of these proteins with one another.

It is interesting to note that a number of proteins observed as substrates for NE-amidation regulate cellular morphology, migration, and proliferation, as these are protein

functions previously shown to be regulated in VSMCs by serotonylation (107). As I discuss in greater detail below, It is unlikely that the migration and proliferation of VSMCs—two functions that are normally ascribed to VSMCs that have taken on a "synthetic" phenotype such as that exhibited by VSMCs in culture—depends on the NE-amidation of proteins, as cultured cells appear to downregulate OCT3 expression and don't appear to have a high propensity for NE uptake. However, given that we identified both contractile- and migration/proliferation-supporting proteins as substrates for NE-biotin, it is conceivable that NE-amidation of proteins may regulate these phenotypes, with high levels of NE-amidation supporting a contractile phenotype in VSMCs, while low levels of NE-amidation supporting the synthetic phenotype. The NE-amidation of proteins may also play a role in the selection of which genes eventually are translated into proteins, as a number of RNA and protein synthesis enzymes were identified as substrates.

In addition to cytoskeletal and small GTPase proteins, a number of other protein groups were identified as substrates. A substantial number of proteins observed function in cell metabolism, such as the glycolytic enzymes pyruvate kinase, glyceraldehyde-3-phosphate dehydrogenase, and phosphoglycerate kinase 1, and the tricarboxylic acid cycle enzymes isocitrate dehydrogenase, aconitate hydratase, and malate dehydrogenase. Additionally, several glutathione S-transferase isozymes were identified. The significance of these proteins as NE-amidation substrates is not immediately clear, and will require further study. While others have described transamidation as a modifier of glyceraldehyde-3-phosphate dehydrogenase activity (146), these studies were of long glutamine peptide chains being incorporated into

reactive *glutamine acceptor* (i.e., lysine residues) of this protein, so it is unclear if NE-amidation of this protein would have an effect on its activity. Aside from protein aggregates of aconitate hydratase being formed in Huntington's disease (91), there is little information on the effect TG activity may have on this protein. Thus, further research will be needed to determine whether these proteins act as true NE-amidation substrates *in vivo*, and, if so, to elucidate how the NE-amidation of these proteins affects their function.

Although several extracellular matrix proteins were identified by mass spectrometry for both BAP and NE-biotin, only collagen has previously been described as a TG substrate. It has been suggested that TG-mediated cross-linking of collagen may play a role in small artery remodeling (10). In addition, cross-linking of collagen may play role in stabilizing atherosclerotic plaques (67). However, to our knowledge, no studies have investigated whether monoamines actually modify collagen *in vivo*, at it is unclear at this time how the NE-amidation of this protein may have physiological significance.

As noted above, more experiments need to be performed to confirm the differences between arterial and venous tissues, and to furthermore characterize whether these differences are due to preferential NE-amidation of these proteins in vascular tissues, or whether these differences are due to differential expression of these proteins. While a number of differences were found between the two tissues, it is hard to determine from these data which may be physiologically relevant, as many of the proteins differentially observed as NE-biotin substrates function in biological processes

shared with those proteins observed as substrates in the other tissue. However, these data do provide a starting point for future studies.

A number of limitations should be mentioned in regards to the mass-spectrometry experiments. First off, these experiments were done *in vitro* in whole RA and RVC tissue homogenates. Further experiments are needed to confirm that these proteins are actual *in vivo* substrates for NE-amidation. Additionally, although an attempt to observe incorporation of the NE-biotin and BAP moieties in the protein itself—by screening for peptide fragments that were increased in size by the molecular weight of these modifications—due to the relatively large size of NE-biotin and BAP, these modifications likely were not stable and fragmented in unpredictable ways while running on the mass spectrometer. Thus, we were neither able to identify the glutamine residues that served as NE-amidation sites on the proteins, nor can we confirm that the proteins we identified in these experiments are actual NE-amidation substrates, as it is possible that some of the proteins we identified are merely interaction partners of proteins that *are* NE-amidation substrates. This possibility was somewhat circumvented by the inclusion of SDS in our sample preparations, but particularly strong interactions likely could have persisted. Furthermore, regardless of whether the proteins we identified are NE-amidation substrates or merely proteins that interact with NE-amidation substrates, this experiment does give us an idea to the processes and pathways in which this modification may be important.

7. Limitations

There are a number of factors that limit the conclusions that may be drawn from these studies. First, these studies used one artery (mouse or RA) and one vein (RVC) as representatives of the arterial and venous vasculature. Though there is physiological relevance to the study of these two vessels, as discussed in the introduction, the fact remains that these are two vessels that primarily function in shuttling blood out of and into the heart. Different results may therefore be obtained in other vascular tissues. Secondly, in some studies, we utilized NE-biotin as a substitute for NE. Experiments that utilized this moiety were mostly qualitative in nature. We also provide evidence that this substitution is valid, as NE-biotin functioned similarly to regular NE. Thirdly, these studies relied heavily on pharmacological inhibitors that may be limited by their efficacy and specificity. For example, as a steroid hormone, corticosterone has the potential to interact with membrane receptors to affect gene expression. The general TG inhibitors cystamine (9) and monodansylcadaverine—although the effect that monodansylcadaverine has on receptor internalization is a subsequent effect to its inhibition of TG activity (42)—have also been shown to have off target effects. Z-DON is a relatively new TG inhibitor and has not been fully characterized; however, it has been shown to inhibit other TGs at higher concentrations, only acts as a intracellular TG2 inhibitor at concentrations above 40 μM, and become cytotoxic in the 100 μM range, limiting its usefulness (149). Although we made attempts to avoid the off target effects that these inhibitors may have (i.e., with corticosterone, the time course that we used is consistent with what others have published as not affecting gene expression but sufficient to inhibit NE uptake (77), and the concentrations of pharmacological inhibitors

were consistent with those described in the literature), it is still possible that off-target effects may skew our results. Although an attempt to use cultured VSMCs in some of these experiments was made, it became clear that cultured VSMCs truly act differently in respect to NE uptake and TG expression then their *in vivo* and *ex vivo* counterparts, preventing us from using pure VSMCs in these experiments. In some ways the move to whole tissue and *ex vivo* freshly dissociated cells is ideal, as it is moving closer to the actual physiological setting; however, it also makes interpretation of some of the data more challenging, as other non-VSMCs in vascular tissues may be skewing the results.

8. Perspectives and future studies

The results of this study suggest that VSMCs can take up and utilize NE for the TG-mediated amidation of proteins, and that this modification may be relevant to NE-induced vascular contraction. Although we were unable to test whether this phenomena plays a role in other NE-mediated vascular functions, we have not excluded the possibility may have roles in other vascular processes, or that this modification may play a role in the maintenance of a contractile phenotype in VSMCs. We have identified several protein substrates for this modification, including α-actin. Although we observed several differences between arteries and veins, these differences are not at first glance, drastic, and the functional importance of these differences was not elucidated. Finally, although we identified NE-amidation of proteins as a novel way for NE to elicit function in the vasculature, the complete mechanism by which this occurs was not elucidated.

Future studies should focus on the characterization of the candidate TG substrate proteins identified by mass-spectrometry (**Table 10**), to determine whether they serve as NE-amidation substrates *in vivo*, and determine how their function may change with this modification. Of particular interest would be proteins that could possibly play a role in the phenotypic modulation of VSMCs, as well as those that could play a role in actin polymerization and contractile dynamics, given our observations. Specifically, I would be interested in determining the possible role the NE-amidation of the small GTPases could play in the regulation of vascular function. Given our observations that 1) cultured VSMCs have a decreased propensity to take up NE, as well as reduced expression of the TGs, 2) that cultured VSMCs take on a synthetic, proliferative and migratory phenotype (29, 173), 3) that a number of the proteins that we

identified in the mass-spectrometry experiments function in cell migration, and 4) that other monoamine-amidation modifications lead to protein degradation via the ubiquitin pathway (62), it would be an interesting study to investigate the hypothesis that the NE-amidation of proteins helps maintain the contractile phenotype of VSMCs, while the loss of NE-amidation of proteins stimulates phenotypical transition to VSMCs that have taken on a migratory and proliferative phenotype. Studying this process may have clinical relevance, as a number of cardiovascular diseases involve VSMC migration and proliferation (88, 187, 190, 197). In addition, further studies to determine the mechanism by which NE-amidation of proteins is important to vascular contraction. Given that α-actin interacts with TGs [**Figures 12** and **13**; as well as (146)], is a substrate for NE-amidation (**Figure 39**), can become disrupted in the presence of TG inhibitor (188), and that contraction is regulated by actin polymerization dynamics (63), it is worthwhile to further investigate the role NE-amidation may play in actin polymerization during contraction.

REFERENCES

REFERENCES

1. **AbdAlla S, Lother H, Langer A, el Faramawy Y, and Quitterer U.** Factor XIIIA transglutaminase crosslinks AT1 receptor dimers of monocytes at the onset of atherosclerosis. *Cell* 119: 343-354, 2004.

2. **Abedin M, Tintut Y, and Demer LL.** Vascular calcification: mechanisms and clinical ramifications. *Arterioscler Thromb Vasc Biol* 24: 1161-1170, 2004.

3. **Adam-Vizi V and Seregi A.** Receptor independent stimulatory effect of noradrenaline on Na,K-ATPase in rat brain homogenate. Role of lipid peroxidation. *Biochem Pharmacol* 31: 2231-2236, 1982.

4. **Ahlquist RP.** A study of the adrenotropic receptors. *Am J Physiol* 153: 586-600, 1948.

5. **Ahvazi B, Boeshans KM, and Rastinejad F.** The emerging structural understanding of transglutaminase 3. *J Struct Biol* 147: 200-207, 2004.

6. **Alberio LJ and Clemetson KJ.** All platelets are not equal: COAT platelets. *Curr Hematol Rep* 3: 338-343, 2004.

7. **An G, Meka CS, Bright SP, and Veltri RW.** Human prostate-specific transglutaminase gene: promoter cloning, tissue-specific expression, and down-regulation in metastatic prostate cancer. *Urology* 54: 1105-1111, 1999.

8. **Bagoly Z, Koncz Z, Harsfalvi J, and Muszbek L.** Factor XIII, clot structure, thrombosis. *Thromb Res* 129: 382-387, 2012.

9. **Bailey CD and Johnson GV.** The protective effects of cystamine in the R6/2 Huntington's disease mouse involve mechanisms other than the inhibition of tissue transglutaminase. *Neurobiol Aging* 27: 871-879, 2006.

10. **Bakker EN, Buus CL, Spaan JA, Perree J, Ganga A, Rolf TM, Sorop O, Bramsen LH, Mulvany MJ, and Vanbavel E.** Small artery remodeling depends on tissue-type transglutaminase. *Circ Res* 96: 119-126, 2005.

11. **Bakker EN, Pistea A, Spaan JA, Rolf T, de Vries CJ, van Rooijen N, Candi E, and VanBavel E.** Flow-dependent remodeling of small arteries in mice deficient for tissue-type transglutaminase: possible compensation by macrophage-derived factor XIII. *Circ Res* 99: 86-92, 2006.

12. **Bakker EN, Pistea A, and VanBavel E.** Transglutaminases in vascular biology: relevance for vascular remodeling and atherosclerosis. *J Vasc Res* 45: 271-278, 2008.

13. **Baumgartner W, Golenhofen N, Weth A, Hiiragi T, Saint R, Griffin M, and Drenckhahn D.** Role of transglutaminase 1 in stabilisation of intercellular junctions of the vascular endothelium. *Histochem Cell Biol* 122: 17-25, 2004.

14. **Baumgartner W and Weth A.** Transglutaminase 1 stabilizes beta-actin in endothelial cells correlating with a stabilization of intercellular junctions. *J Vasc Res* 44: 234-240, 2007.

15. **Bernassola F, Rossi A, and Melino G.** Regulation of transglutaminases by nitric oxide. *Ann N Y Acad Sci* 887: 83-91, 1999.

16. **Borghini N, Dalmaz Y, and Peyrin L.** Effect of guanethidine on dopamine in small intensely fluorescent cells of the superior cervical ganglion of the rat. *Journal of the autonomic nervous system* 32: 13-19, 1991.

17. **Borth W, Chang V, Bishop P, and Harpel PC.** Lipoprotein (a) is a substrate for factor XIIIa and tissue transglutaminase. *The Journal of biological chemistry* 266: 18149-18153, 1991.

18. **Bottaro D, Shepro D, Peterson S, and Hechtman HB.** Serotonin, histamine, and norepinephrine mediation of endothelial and vascular smooth muscle cell movement. *Am J Physiol* 248: C252-257, 1985.

19. **Brengelmann GL.** A critical analysis of the view that right atrial pressure determines venous return. *J Appl Physiol* 94: 849-859, 2003.

20. **Bruss M, Porzgen P, Bryan-Lluka LJ, and Bonisch H.** The rat norepinephrine transporter: molecular cloning from PC12 cells and functional expression. *Brain Res Mol Brain Res* 52: 257-262, 1997.

21. **Bryan-Lluka LJ, Westwood NN, and O'Donnell SR.** Vascular uptake of catecholamines in perfused lungs of the rat occurs by the same process as Uptake1 in noradrenergic neurones. *Naunyn Schmiedebergs Arch Pharmacol* 345: 319-326, 1992.

22. **Bund SJ and Lee RM.** Arterial structural changes in hypertension: a consideration of methodology, terminology and functional consequence. *J Vasc Res* 40: 547-557, 2003.

23. **Busch AE, Karbach U, Miska D, Gorboulev V, Akhoundova A, Volk C, Arndt P, Ulzheimer JC, Sonders MS, Baumann C, Waldegger S, Lang F, and Koepsell H.** Human neurons express the polyspecific cation transporter hOCT2, which translocates monoamine neurotransmitters, amantadine, and memantine. *Molecular pharmacology* 54: 342-352, 1998.

24. **Busch AE, Quester S, Ulzheimer JC, Gorboulev V, Akhoundova A, Waldegger S, Lang F, and Koepsell H.** Monoamine neurotransmitter transport mediated by the polyspecific cation transporter rOCT1. *FEBS Lett* 395: 153-156, 1996.

25. **Caja S, Myrsky E, Korponay-Szabo IR, Nadalutti C, Sulic AM, Lavric M, Sblattero D, Marzari R, Collighan R, Mongeot A, Griffin M, Maki M, Kaukinen K, and Lindfors K.** Inhibition of transglutaminase 2 enzymatic activity ameliorates the anti-angiogenic effects of coeliac disease autoantibodies. *Scandinavian journal of gastroenterology* 45: 421-427, 2010.

26. **Candi E, Paradisi A, Terrinoni A, Pietroni V, Oddi S, Cadot B, Jogini V, Meiyappan M, Clardy J, Finazzi-Agro A, and Melino G.** Transglutaminase 5 is regulated by guanine-adenine nucleotides. *Biochem J* 381: 313-319, 2004.

27. **Cascella NG, Santora D, Gregory P, Kelly DL, Fasano A, and Eaton WW.** Increased Prevalence of Transglutaminase 6 Antibodies in Sera From Schizophrenia Patients. *Schizophrenia bulletin*, 2012.

28. **Cassidy AJ, van Steensel MA, Steijlen PM, van Geel M, van der Velden J, Morley SM, Terrinoni A, Melino G, Candi E, and McLean WH.** A homozygous missense mutation in TGM5 abolishes epidermal transglutaminase 5 activity and causes acral peeling skin syndrome. *American journal of human genetics* 77: 909-917, 2005.

29. **Chamley-Campbell JH, Campbell GR, and Ross R.** Phenotype-dependent response of cultured aortic smooth muscle to serum mitogens. *J Cell Biol* 89: 379-383, 1981.

30. **Chen BS, Wang MR, Xu X, Cai Y, Xu ZX, Han YL, and Wu M.** Transglutaminase-3, an esophageal cancer-related gene. *International journal of cancer Journal international du cancer* 88: 862-865, 2000.

31. **Cho S-Y, Choi K, Jeon J-H, Kim C-W, Shin D-M, Lee JB, Lee SE, Kim C-S, Park J-S, Jeong EM, Jang G-Y, Song K-Y, and Kim I-G.** Differential alternative splicing of human transglutaminase 4 in benign prostate hyperplasia and prostate cancer. *Experimental and Molecular Medicine* 42: 310, 2010.

32. **Cho SY, Choi K, Jeon JH, Kim CW, Shin DM, Lee JB, Lee SE, Kim CS, Park JS, Jeong EM, Jang GY, Song KY, and Kim IG.** Differential alternative splicing of human transglutaminase 4 in benign prostate hyperplasia and prostate cancer. *Exp Mol Med* 42: 310-318, 2010.

33. **Chowdhury ZA, Barsigian C, Chalupowicz GD, Bach TL, Garcia-Manero G, and Martinez J.** Colocalization of tissue transglutaminase and stress fibers in human vascular smooth muscle cells and human umbilical vein endothelial cells. *Exp Cell Res* 231: 38-49, 1997.

34. **Chrzanowska-Wodnicka M.** Regulation of angiogenesis by a small GTPase Rap1. *Vascular pharmacology* 53: 1-10, 2010.

35. **Cicco G, Carbonara MC, Stingi GD, and Pirrelli A.** Cytosolic calcium and hemorheological patterns during arterial hypertension. *Clin Hemorheol Microcirc* 24: 25-31, 2001.

36. **Consortium TU.** Reorganizing the protein space at the Universal Protein Resource (UniProt). *Nucleic Acids Research* 40: D71-D75, 2012.

37. **Cordella-Miele E, Miele L, Beninati S, and Mukherjee AB.** Transglutaminase-catalyzed incorporation of polyamines into phospholipase A2. *J Biochem* 113: 164-173, 1993.

38. **Dai Y, Dudek NL, Li Q, and Muma NA.** Phospholipase C, Ca2+, and calmodulin signaling are required for 5-HT2A receptor-mediated transamidation of Rac1 by transglutaminase. *Psychopharmacology* 213: 403-412, 2011.

39. **Dai Y, Dudek NL, Patel TB, and Muma NA.** Transglutaminase-catalyzed transamidation: a novel mechanism for Rac1 activation by 5-hydroxytryptamine2A receptor stimulation. *J Pharmacol Exp Ther* 326: 153-162, 2008.

40. **Dale GL, Friese P, Batar P, Hamilton SF, Reed GL, Jackson KW, Clemetson KJ, and Alberio L.** Stimulated platelets use serotonin to enhance their retention of procoagulant proteins on the cell surface. *Nature* 415: 175-179, 2002.

41. **Dardik R, Loscalzo J, and Inbal A.** Factor XIII (FXIII) and angiogenesis. *J Thromb Haemost* 4: 19-25, 2006.

42. **Davies PJ, Cornwell MM, Johnson JD, Reggianni A, Myers M, and Murtaugh MP.** Studies on the effects of dansylcadaverine and related compounds on receptor-mediated endocytosis in cultured cells. *Diabetes care* 7 Suppl 1: 35-41, 1984.

43. **De Laurenzi V and Melino G.** Gene disruption of tissue transglutaminase. *Molecular and cellular biology* 21: 148-155, 2001.

44. **Duan H and Wang J.** Selective transport of monoamine neurotransmitters by human plasma membrane monoamine transporter and organic cation transporter 3. *J Pharmacol Exp Ther* 335: 743-753, 2010.

45. **Duarte J, Perez-Vizcaino F, Torres AI, Zarzuelo A, Jimenez J, and Tamargo J.** Vasodilator effects of visnagin in isolated rat vascular smooth muscle. *Eur J Pharmacol* 286: 115-122, 1995.

46. **Dubbink HJ, Verkaik NS, Faber PW, Trapman J, Schroder FH, and Romijn JC.** Tissue specific and androgen-regulated expression of human prostate-specific transglutaminase. *The Biochemical journal* 315 (Pt 3): 901-908, 1996.

47. **Eddahibi S.** Serotonin transporter overexpression is responsible for pulmonary artery smooth muscle hyperplasia in primary pulmonary hypertension. *Journal of Clinical Investigation* 108: 1141-1150, 2001.

48. **Eisenhofer G.** The role of neuronal and extraneuronal plasma membrane transporters in the inactivation of peripheral catecholamines. *Pharmacol Ther* 91: 35-62, 2001.

49. **Engel K, Zhou M, and Wang J.** Identification and characterization of a novel monoamine transporter in the human brain. *J Biol Chem* 279: 50042-50049, 2004.

50. **Erami C, Zhang H, Ho JG, French DM, and Faber JE.** Alpha(1)-adrenoceptor stimulation directly induces growth of vascular wall in vivo. *Am J Physiol Heart Circ Physiol* 283: H1577-1587, 2002.

51. **Erami C, Zhang H, Tanoue A, Tsujimoto G, Thomas SA, and Faber JE.** Adrenergic catecholamine trophic activity contributes to flow-mediated arterial remodeling. *Am J Physiol Heart Circ Physiol* 289: H744-753, 2005.

52. **Fesus L, Szucs EF, Barrett KE, Metcalfe DD, and Folk JE.** Activation of transglutaminase and production of protein-bound gamma-glutamylhistamine in stimulated mouse mast cells. *The Journal of biological chemistry* 260: 13771-13778, 1985.

53. **Fesus L and Tarcsa E.** Formation of N epsilon-(gamma-glutamyl)-lysine isodipeptide in Chinese-hamster ovary cells. *The Biochemical journal* 263: 843-848, 1989.

54. **Fink GD.** Arthur C. Corcoran Memorial Lecture. Sympathetic activity, vascular capacitance, and long-term regulation of arterial pressure. *Hypertension* 53: 307-312, 2009.

55. **Fink ML and Folk JE.** gamma-Glutamylamine cyclotransferase. An enzyme involved in the catabolism of epsilon-(gamma-glutamyl)lysine and other gamma-glutamylamines. *Molecular and cellular biochemistry* 38 Spec No: 59-67, 1981.

56. **Greenberg CS, Achyuthan KE, Borowitz MJ, and Shuman MA.** The transglutaminase in vascular cells and tissues could provide an alternate pathway for fibrin stabilization. *Blood* 70: 702-709, 1987.

57. **Grenard P, Bates MK, and Aeschlimann D.** Evolution of transglutaminase genes: identification of a transglutaminase gene cluster on human chromosome 15q15. Structure of the gene encoding transglutaminase X and a novel gene family member, transglutaminase Z. *The Journal of biological chemistry* 276: 33066-33078, 2001.

58. **Griffin M, Casadio R, and Bergamini CM.** Transglutaminases: nature's biological glues. *Biochem J* 368: 377-396, 2002.

59. **Grundemann D, Koster S, Kiefer N, Breidert T, Engelhardt M, Spitzenberger F, Obermuller N, and Schomig E.** Transport of monoamine transmitters by the organic

cation transporter type 2, OCT2. *The Journal of biological chemistry* 273: 30915-30920, 1998.

60. **Grundemann D, Schechinger B, Rappold GA, and Schomig E.** Molecular identification of the corticosterone-sensitive extraneuronal catecholamine transporter. *Nat Neurosci* 1: 349-351, 1998.

61. **Guilluy C, Eddahibi S, Agard C, Guignabert C, Izikki M, Tu L, Savale L, Humbert M, Fadel E, Adnot S, Loirand G, and Pacaud P.** RhoA and Rho kinase activation in human pulmonary hypertension: role of 5-HT signaling. *American journal of respiratory and critical care medicine* 179: 1151-1158, 2009.

62. **Guilluy C, Rolli-Derkinderen M, Tharaux PL, Melino G, Pacaud P, and Loirand G.** Transglutaminase-dependent RhoA activation and depletion by serotonin in vascular smooth muscle cells. *J Biol Chem* 282: 2918-2928, 2007.

63. **Gunst SJ and Zhang W.** Actin cytoskeletal dynamics in smooth muscle: a new paradigm for the regulation of smooth muscle contraction. *Am J Physiol Cell Physiol* 295: C576-587, 2008.

64. **Gupta M, Greenberg CS, Eckman DM, and Sane DC.** Arterial vimentin is a transglutaminase substrate: a link between vasomotor activity and remodeling? *J Vasc Res* 44: 339-344, 2007.

65. **Guyenet PG.** The sympathetic control of blood pressure. *Nature reviews Neuroscience* 7: 335-346, 2006.

66. **Hadjivassiliou M, Aeschlimann P, Strigun A, Sanders DS, Woodroofe N, and Aeschlimann D.** Autoantibodies in gluten ataxia recognize a novel neuronal transglutaminase. *Annals of neurology* 64: 332-343, 2008.

67. **Haroon ZA, Hettasch JM, Lai TS, Dewhirst MW, and Greenberg CS.** Tissue transglutaminase is expressed, active, and directly involved in rat dermal wound healing and angiogenesis. *FASEB journal : official publication of the Federation of American Societies for Experimental Biology* 13: 1787-1795, 1999.

68. **Haroon ZA, Wannenburg T, Gupta M, Greenberg CS, Wallin R, and Sane DC.** Localization of tissue transglutaminase in human carotid and coronary artery atherosclerosis: implications for plaque stability and progression. *Lab Invest* 81: 83-93, 2001.

69. **Hassanain HH, Gregg D, Marcelo ML, Zweier JL, Souza HP, Selvakumar B, Ma Q, Moustafa-Bayoumi M, Binkley PF, Flavahan NA, Morris M, Dong C, and Goldschmidt-Clermont PJ.** Hypertension caused by transgenic overexpression of Rac1. *Antioxidants & redox signaling* 9: 91-100, 2007.

70. **Henriksson P, Becker S, Lynch G, and McDonagh J.** Identification of intracellular factor XIII in human monocytes and macrophages. *J Clin Invest* 76: 528-534, 1985.

71. **Henrion D, Terzi F, Matrougui K, Duriez M, Boulanger CM, Colucci-Guyon E, Babinet C, Briand P, Friedlander G, Poitevin P, and Levy BI.** Impaired flow-induced dilation in mesenteric resistance arteries from mice lacking vimentin. *J Clin Invest* 100: 2909-2914, 1997.

72. **Hitomi K, Ikeda N, and Maki M.** Immunological detection of proteolytically activated epidermal-type transglutaminase (TGase 3) using cleavage-site-specific antibody. *Bioscience, biotechnology, and biochemistry* 67: 2492-2494, 2003.

73. **Hitomi K, Ikura K, and Maki M.** GTP, an inhibitor of transglutaminases, is hydrolyzed by tissue-type transglutaminase (TGase 2) but not by epidermal-type transglutaminase (TGase 3). *Bioscience, biotechnology, and biochemistry* 64: 657-659, 2000.

74. **Hitomi K, Kanehiro S, Ikura K, and Maki M.** Characterization of recombinant mouse epidermal-type transglutaminase (TGase 3): regulation of its activity by proteolysis and guanine nucleotides. *J Biochem* 125: 1048-1054, 1999.

75. **Hitomi K, Kitamura M, and Sugimura Y.** Preferred substrate sequences for transglutaminase 2: screening using a phage-displayed peptide library. *Amino acids* 36: 619-624, 2009.

76. **Hitomi K, Yamagiwa Y, Ikura K, Yamanishi K, and Maki M.** Characterization of human recombinant transglutaminase 1 purified from baculovirus-infected insect cells. *Bioscience, biotechnology, and biochemistry* 64: 2128-2137, 2000.

77. **Horvath G, Lieb T, Conner GE, Salathe M, and Wanner A.** Steroid sensitivity of norepinephrine uptake by human bronchial arterial and rabbit aortic smooth muscle cells. *Am J Respir Cell Mol Biol* 25: 500-506, 2001.

78. **Horvath G, Sutto Z, Torbati A, Conner GE, Salathe M, and Wanner A.** Norepinephrine transport by the extraneuronal monoamine transporter in human bronchial arterial smooth muscle cells. *American journal of physiology Lung cellular and molecular physiology* 285: L829-837, 2003.

79. **Huang Y.** Inhibition of contractions by tricyclic antidepressants and xylamine in rat vas deferens. *European journal of pharmacology* 327: 41-47, 1997.

80. **Hummerich R Fau - Thumfart J-O, Thumfart Jo Fau - Findeisen P, Findeisen P Fau - Bartsch D, Bartsch D Fau - Schloss P, and Schloss P.** Transglutaminase-mediated transamidation of serotonin, dopamine and noradrenaline to fibronectin: evidence for a general mechanism of monoaminylation.

81. **Hummerich R and Schloss P.** Serotonin--more than a neurotransmitter: transglutaminase-mediated serotonylation of C6 glioma cells and fibronectin. *Neurochemistry international* 57: 67-75, 2010.

82. **Hummerich R, Thumfart JO, Findeisen P, Bartsch D, and Schloss P.** Transglutaminase-mediated transamidation of serotonin, dopamine and noradrenaline to fibronectin: Evidence for a general mechanism of monoaminylation. *FEBS Lett* 586: 3421-3428, 2012.

83. **Inazu M, Takeda H, and Matsumiya T.** Functional expression of the norepinephrine transporter in cultured rat astrocytes. *J Neurochem* 84: 136-144, 2003.

84. **Iversen LL.** The uptake of catechol amines at high perfusion concentrations in the rat isolated heart: A novel catechol amine uptake process. *Br J Pharmacol Chemother* 25: 18-33, 1965.

85. **Johnson KA, Polewski M, and Terkeltaub RA.** Transglutaminase 2 is central to induction of the arterial calcification program by smooth muscle cells. *Circ Res* 102: 529-537, 2008.

86. **Johnson KB, Thompson JM, and Watts SW.** Modification of proteins by norepinephrine is important for vascular contraction. *Frontiers in physiology* 1: 12, 2010.

87. **Kandlikar SS and Fink GD.** Splanchnic sympathetic nerves in the development of mild DOCA-salt hypertension. *Am J Physiol Heart Circ Physiol* 301: H1965-1973, 2011.

88. **Kang SK, Yi KS, Kwon NS, Park KH, Kim UH, Baek KJ, and Im MJ.** Alpha1B-adrenoceptor signaling and cell motility: GTPase function of Gh/transglutaminase 2 inhibits cell migration through interaction with cytoplasmic tail of integrin alpha subunits. *J Biol Chem* 279: 36593-36600, 2004.

89. **Kang Yh Fau - Kang JS, Kang Js Fau - Shin HM, and Shin HM.** Vasodilatory Effects of Cinnamic Acid via the Nitric Oxide-cGMP-PKG Pathway in Rat Thoracic Aorta. LID - 10.1002/ptr.4708 [doi].

90. **Kim HC, Lewis MS, Gorman JJ, Park SC, Girard JE, Folk JE, and Chung SI.** Protransglutaminase E from guinea pig skin. Isolation and partial characterization. *The Journal of biological chemistry* 265: 21971-21978, 1990.

91. **Kim SY, Marekov L, Bubber P, Browne SE, Stavrovskaya I, Lee J, Steinert PM, Blass JP, Beal MF, Gibson GE, and Cooper AJ.** Mitochondrial aconitase is a transglutaminase 2 substrate: transglutamination is a probable mechanism contributing to high-molecular-weight aggregates of aconitase and loss of aconitase activity in Huntington disease brain. *Neurochemical research* 30: 1245-1255, 2005.

92. **King AJ, Novotny M, Swain GM, and Fink GD.** Whole body norepinephrine kinetics in ANG II-salt hypertension in the rat. *Am J Physiol Regul Integr Comp Physiol* 294: R1262-1267, 2008.

93. **King AJ, Osborn JW, and Fink GD.** Splanchnic circulation is a critical neural target in angiotensin II salt hypertension in rats. *Hypertension* 50: 547-556, 2007.

94. **Kinsella MG and Wight TN.** Formation of high molecular weight dermatan sulfate proteoglycan in bovine aortic endothelial cell cultures. Evidence for transglutaminase-catalyzed cross-linking to fibronectin. *The Journal of biological chemistry* 265: 17891-17898, 1990.

95. **Kiraly R, Demeny M, and Fesus L.** Protein transamidation by transglutaminase 2 in cells: a disputed Ca2+-dependent action of a multifunctional protein. *The FEBS journal* 278: 4717-4739, 2011.

96. **Krukoff TL, Fernandez MC, and Vincent DH.** Effects of neonatal sympathectomy with 6-hydroxydopamine or guanethidine on survival of neurons in the intermediolateral cell column of rat spinal cord. *J Auton Nerv Syst* 31: 119-126, 1990.

97. **Lai TS, Liu Y, Li W, and Greenberg CS.** Identification of two GTP-independent alternatively spliced forms of tissue transglutaminase in human leukocytes, vascular smooth muscle, and endothelial cells. *FASEB journal : official publication of the Federation of American Societies for Experimental Biology* 21: 4131-4143, 2007.

98. **Lampasona V, Bonfanti R, Bazzigaluppi E, Venerando A, Chiumello G, Bosi E, and Bonifacio E.** Antibodies to tissue transglutaminase C in type I diabetes. *Diabetologia* 42: 1195-1198, 1999.

99. **Langer SZ.** Presynaptic regulation of catecholamine release. *Biochemical pharmacology* 23: 1793-1800, 1974.

100. **Lee SL, Dunn J, Yu FS, and Fanburg BL.** Serotonin uptake and configurational change of bovine pulmonary artery smooth muscle cells in culture. *J Cell Physiol* 138: 145-153, 1989.

101. **Lee SL and Fanburg BL.** Serotonin produces a configurational change of cultured smooth muscle cells that is associated with elevation of intracellular cAMP. *J Cell Physiol* 150: 396-405, 1992.

102. **Lee SL, Wang WW, Lanzillo JJ, and Fanburg BL.** Regulation of serotonin-induced DNA synthesis of bovine pulmonary artery smooth muscle cells. *Am J Physiol* 266: L53-60, 1994.

103. **Lee SL, Wang WW, Lanzillo JJ, and Fanburg BL.** Serotonin produces both hyperplasia and hypertrophy of bovine pulmonary artery smooth muscle cells in culture. *Am J Physiol* 266: L46-52, 1994.

104. **Levin JA and Wilson SE.** The effect of monoamine oxidase and catechol O-methyltransferase inhibitors on the accumulation and metabolism of [l-3H] norepinephrine by the adventitia and media of rabbit aorta. *J Pharmacol Exp Ther* 203: 598-609, 1977.

105. **Li M, Galligan J, Wang D, and Fink G.** The effects of celiac ganglionectomy on sympathetic innervation to the splanchnic organs in the rat. *Autonomic neuroscience : basic & clinical* 154: 66-73, 2010.

106. **Linnoila M, Karoum F, and Potter WZ.** High correlation of norepinephrine and its major metabolite excretion rates. *Archives of general psychiatry* 39: 521-523, 1982.

107. **Liu Y, Wei L, Laskin DL, and Fanburg BL.** Role of protein transamidation in serotonin-induced proliferation and migration of pulmonary artery smooth muscle cells. *American journal of respiratory cell and molecular biology* 44: 548-555, 2011.

108. **Liu Y, Wei L, Laskin DL, and Fanburg BL.** Role of Protein Transamidation in Serotonin-induced Proliferation and Migration of Pulmonary Artery Smooth Muscle Cells. *American journal of respiratory cell and molecular biology*, 2010.

109. **Lorand L.** Factor XIII and the clotting of fibrinogen: from basic research to medicine. *J Thromb Haemost* 3: 1337-1348, 2005.

110. **Lorand L and Conrad SM.** Transglutaminases. *Molecular and cellular biochemistry* 58: 9-35, 1984.

111. **Lorand L and Graham RM.** Transglutaminases: crosslinking enzymes with pleiotropic functions. *Nat Rev Mol Cell Biol* 4: 140-156, 2003.

112. **Luo M, Hess MC, Fink GD, Olson LK, Rogers J, Kreulen DL, Dai X, and Galligan JJ.** Differential alterations in sympathetic neurotransmission in mesenteric arteries and veins in DOCA-salt hypertensive rats. *Autonomic Neuroscience* 104: 47-57, 2003.

113. **Luo M, Hess MC, Fink GD, Olson LK, Rogers J, Kreulen DL, Dai X, and Galligan JJ.** Differential alterations in sympathetic neurotransmission in mesenteric arteries and veins in DOCA-salt hypertensive rats. *Auton Neurosci* 104: 47-57, 2003.

114. **Mahata M, Mahata SK, Parmer RJ, and O'Connor DT.** Vesicular monoamine transport inhibitors. Novel action at calcium channels to prevent catecholamine secretion. *Hypertension* 28: 414-420, 1996.

115. **Martel F, Ribeiro L, Calhau C, and Azevedo I.** Comparison between uptake2 and rOCT1: effects of catecholamines, metanephrines and corticosterone. *Naunyn Schmiedebergs Arch Pharmacol* 359: 303-309, 1999.

116. **Matlung HL, VanBavel E, van den Akker J, de Vries CJ, and Bakker EN.** Role of transglutaminases in cuff-induced atherosclerotic lesion formation in femoral arteries of ApoE3 Leiden mice. *Atherosclerosis* 213: 77-84, 2010.

117. **Matthies HJ, Han Q, Shields A, Wright J, Moore JL, Winder DG, Galli A, and Blakely RD.** Subcellular localization of the antidepressant-sensitive norepinephrine transporter. *BMC neuroscience* 10: 65, 2009.

118. **McConoughey SJ, Basso M, Niatsetskaya ZV, Sleiman SF, Smirnova NA, Langley BC, Mahishi L, Cooper AJ, Antonyak MA, Cerione RA, Li B, Starkov A, Chaturvedi RK, Beal MF, Coppola G, Geschwind DH, Ryu H, Xia L, Iismaa SE, Pallos J, Pasternack R, Hils M, Fan J, Raymond LA, Marsh JL, Thompson LM, and Ratan RR.** Inhibition of transglutaminase 2 mitigates transcriptional dysregulation in models of Huntington disease. *EMBO molecular medicine* 2: 349-370, 2010.

119. **Mehta D and Gunst SJ.** Actin polymerization stimulated by contractile activation regulates force development in canine tracheal smooth muscle. *The Journal of physiology* 519 Pt 3: 829-840, 1999.

120. **Melino G, Bernassola F, Knight RA, Corasaniti MT, Nistico G, and Finazzi-Agro A.** S-nitrosylation regulates apoptosis. *Nature* 388: 432-433, 1997.

121. **Mione MC, Sancesario G, D'Angelo V, and Bernardi G.** Increase of dopamine beta-hydroxylase immunoreactivity in non-noradrenergic nerves of rat cerebral arteries following long-term sympathectomy. *Neurosci Lett* 123: 167-171, 1991.

122. **Mosher DF.** Cross-linking of fibronectin to collagenous proteins. *Molecular and cellular biochemistry* 58: 63-68, 1984.

123. **Munezane T, Hasegawa T, Suritala, Tanaka A, Okada K, and Okita Y.** Activation of transglutaminase type 2 for aortic wall protection in a rat abdominal aortic aneurysm formation. *Journal of vascular surgery* 52: 967-974, 2010.

124. **Muszbek L, Adany R, and Mikkola H.** Novel aspects of blood coagulation factor XIII. I. Structure, distribution, activation, and function. *Critical reviews in clinical laboratory sciences* 33: 357-421, 1996.

125. **Nahrendorf M, Hu K, Frantz S, Jaffer FA, Tung CH, Hiller KH, Voll S, Nordbeck P, Sosnovik D, Gattenlohner S, Novikov M, Dickneite G, Reed GL, Jakob P, Rosenzweig A, Bauer WR, Weissleder R, and Ertl G.** Factor XIII deficiency causes cardiac rupture, impairs wound healing, and aggravates cardiac remodeling in mice with myocardial infarction. *Circulation* 113: 1196-1202, 2006.

126. **Nakajima K.** Recent advances in dermatitis herpetiformis. *Clinical & developmental immunology* 2012: 914162, 2012.

127. **Nakaoka H, Perez DM, Baek KJ, Das T, Husain A, Misono K, Im MJ, and Graham RM.** Gh: a GTP-binding protein with transglutaminase activity and receptor signaling function. *Science* 264: 1593-1596, 1994.

128. **Nanda N, Iismaa SE, Owens WA, Husain A, Mackay F, and Graham RM.** Targeted inactivation of Gh/tissue transglutaminase II. *The Journal of biological chemistry* 276: 20673-20678, 2001.

129. **Nemes Z, Fesus L, Egerhazi A, Keszthelyi A, and Degrell IM.** N(epsilon)(gamma-glutamyl)lysine in cerebrospinal fluid marks Alzheimer type and vascular dementia. *Neurobiology of aging* 22: 403-406, 2001.

130. **Ni W, Geddes TJ, Priestley JR, Szasz T, Kuhn DM, and Watts SW.** The existence of a local 5-hydroxytryptaminergic system in peripheral arteries. *British journal of pharmacology* 154: 663-674, 2008.

131. **Ogden K, Thompson JM, Hickner Z, Huang T, Tang DD, and Watts SW.** A new signaling paradigm for serotonin: use of Crk-associated substrate in arterial contraction. *Am J Physiol Heart Circ Physiol* 291: H2857-2863, 2006.

132. **Ohura N, Yamamoto K, Ichioka S, Sokabe T, Nakatsuka H, Baba A, Shibata M, Nakatsuka T, Harii K, Wada Y, Kohro T, Kodama T, and Ando J.** Global analysis of shear stress-responsive genes in vascular endothelial cells. *Journal of atherosclerosis and thrombosis* 10: 304-313, 2003.

133. **Paulmann N, Grohmann M, Voigt JP, Bert B, Vowinckel J, Bader M, Skelin M, Jevsek M, Fink H, Rupnik M, and Walther DJ.** Intracellular serotonin modulates insulin secretion from pancreatic beta-cells by protein serotonylation. *PLoS biology* 7: e1000229, 2009.

134. **Perez-Rivera AA, Fink GD, and Galligan JJ.** Increased reactivity of murine mesenteric veins to adrenergic agonists: functional evidence supporting increased alpha1-adrenoceptor reserve in veins compared with arteries. *J Pharmacol Exp Ther* 308: 350-357, 2004.

135. **Perez-Rivera AA, Hlavacova A, Rosario-Colon LA, Fink GD, and Galligan JJ.** Differential contributions of alpha-1 and alpha-2 adrenoceptors to vasoconstriction in

mesenteric arteries and veins of normal and hypertensive mice. *Vascular pharmacology* 46: 373-382, 2007.

136. **Pietroni V, Di Giorgi S, Paradisi A, Ahvazi B, Candi E, and Melino G.** Inactive and highly active, proteolytically processed transglutaminase-5 in epithelial cells. *The Journal of investigative dermatology* 128: 2760-2766, 2008.

137. **Pinon M, Racotta IS, Ortiz-Butron R, and Racotta R.** Catecholamines in paraganglia associated with the hepatic branch of the vagus nerve: effects of 6-hydroxydopamine and reserpine. *J Auton Nerv Syst* 75: 131-135, 1999.

138. **Pistea A, Bakker EN, Spaan JA, Hardeman MR, van Rooijen N, and VanBavel E.** Small artery remodeling and erythrocyte deformability in L-NAME-induced hypertension: role of transglutaminases. *J Vasc Res* 45: 10-18, 2008.

139. **Qiao SW, Piper J, Haraldsen G, Oynebraten I, Fleckenstein B, Molberg O, Khosla C, and Sollid LM.** Tissue transglutaminase-mediated formation and cleavage of histamine-gliadin complexes: biological effects and implications for celiac disease. *Journal of immunology (Baltimore, Md : 1950)* 174: 1657-1663, 2005.

140. **Rasband WS.** ImageJ, 1997-2009.

141. **Romanic AM, Arleth AJ, Willette RN, and Ohlstein EH.** Factor XIIIa cross-links lipoprotein(a) with fibrinogen and is present in human atherosclerotic lesions. *Circ Res* 83: 264-269, 1998.

142. **Rondelli CM, Szasz IT, Kayal A, Thakali K, Watson RE, Rovner AS, Eddinger TJ, Fink GD, and Watts SW.** Preferential myosin heavy chain isoform B Expression may contribute to the faster velocity of contraction in veins versus arteries. *J Vasc Res* 44: 264-272, 2007.

143. **Rossi A, Catani MV, Candi E, Bernassola F, Puddu P, and Melino G.** Nitric oxide inhibits cornified envelope formation in human keratinocytes by inactivating transglutaminases and activating protein 1. *J Invest Dermatol* 115: 731-739, 2000.

144. **Rothe CF.** Physiology of venous return. An unappreciated boost to the heart. *Arch Intern Med* 146: 977-982, 1986.

145. **Russell LJ, DiGiovanna JJ, Rogers GR, Steinert PM, Hashem N, Compton JG, and Bale SJ.** Mutations in the gene for transglutaminase 1 in autosomal recessive lamellar ichthyosis. *Nat Genet* 9: 279-283, 1995.

146. **Russo L, Marsella C, Nardo G, Massignan T, Alessio M, Piermarini E, La Rosa S, Finzi G, Bonetto V, Bertuzzi F, Maechler P, and Massa O.** Transglutaminase 2 transamidation activity during first-phase insulin secretion: natural substrates in INS-1E. *Acta diabetologica*, 2012.

147. **Sakurada S, Takuwa N, Sugimoto N, Wang Y, Seto M, Sasaki Y, and Takuwa Y.** Ca2+-dependent activation of Rho and Rho kinase in membrane depolarization-induced and receptor stimulation-induced vascular smooth muscle contraction. *Circ Res* 93: 548-556, 2003.

148. **Sane DC, Kontos JL, and Greenberg CS.** Roles of transglutaminases in cardiac and vascular diseases. *Front Biosci* 12: 2530-2545, 2007.

149. **Schaertl S, Prime M, Wityak J, Dominguez C, Munoz-Sanjuan I, Pacifici RE, Courtney S, Scheel A, and Macdonald D.** A profiling platform for the characterization of transglutaminase 2 (TG2) inhibitors. *J Biomol Screen* 15: 478-487, 2010.

150. **Schauer IE, Knaub LA, Lloyd M, Watson PA, Gliwa C, Lewis KE, Chait A, Klemm DJ, Gunter JM, Bouchard R, McDonald TO, O'Brien KD, and Reusch JE.** CREB downregulation in vascular disease: a common response to cardiovascular risk. *Arteriosclerosis, thrombosis, and vascular biology* 30: 733-741, 2010.

151. **Schiffrin EL.** Remodeling of resistance arteries in essential hypertension and effects of antihypertensive treatment. *American journal of hypertension* 17: 1192-1200, 2004.

152. **Schmidt RE, Summerfield AL, and Hickey WF.** Ultrastructural and immunohistologic characterization of guanethidine-induced destruction of peripheral sympathetic neurons. *J Neuropathol Exp Neurol* 49: 150-167, 1990.

153. **Schomig E, Lazar A, and Grundemann D.** Extraneuronal monoamine transporter and organic cation transporters 1 and 2: a review of transport efficiency. *Handb Exp Pharmacol*: 151-180, 2006.

154. **Schuppan D, Dieterich W, Ehnis T, Bauer M, Donner P, Volta U, and Riecken EO.** Identification of the autoantigen of celiac disease. *Ann N Y Acad Sci* 859: 121-126, 1998.

155. **Siefring GE, Jr., Apostol AB, Velasco PT, and Lorand L.** Enzymatic basis for the Ca2+-induced cross-linking of membrane proteins in intact human erythrocytes. *Biochemistry* 17: 2598-2604, 1978.

156. **Singh US, Kunar MT, Kao YL, and Baker KM.** Role of transglutaminase II in retinoic acid-induced activation of RhoA-associated kinase-2. *EMBO J* 20: 2413-2423, 2001.

157. **Slaughter TF, Achyuthan KE, Lai TS, and Greenberg CS.** A microtiter plate transglutaminase assay utilizing 5-(biotinamido)pentylamine as substrate. *Anal Biochem* 205: 166-171, 1992.

158. **Smethurst PA and Griffin M.** Measurement of tissue transglutaminase activity in a permeabilized cell system: its regulation by Ca2+ and nucleotides. *The Biochemical journal* 313 (Pt 3): 803-808, 1996.

159. **Sorriento D, Santulli G, Del Giudice C, Anastasio A, Trimarco B, and Iaccarino G.** Endothelial cells are able to synthesize and release catecholamines both in vitro and in vivo. *Hypertension* 60: 129-136, 2012.

160. **Spina AM, Esposito C, Pagano M, Chiosi E, Mariniello L, Cozzolino A, Porta R, and Illiano G.** GTPase and transglutaminase are associated in the secretion of the rat anterior prostate. *Biochem Biophys Res Commun* 260: 351-356, 1999.

161. **Steinert PM, Chung SI, and Kim SY.** Inactive zymogen and highly active proteolytically processed membrane-bound forms of the transglutaminase 1 enzyme in human epidermal keratinocytes. *Biochem Biophys Res Commun* 221: 101-106, 1996.

162. **Stevenson AS, Cartin L, Wellman TL, Dick MH, Nelson MT, and Lounsbury KM.** Membrane depolarization mediates phosphorylation and nuclear translocation of CREB in vascular smooth muscle cells. *Exp Cell Res* 263: 118-130, 2001.

163. **Stjarne L.** Basic mechanisms and local modulation of nerve impulse-induced secretion of neurotransmitters from individual sympathetic nerve varicosities. *Reviews of physiology, biochemistry and pharmacology* 112: 1-137, 1989.

164. **Stjarne L and Stjarne E.** Geometry, kinetics and plasticity of release and clearance of ATP and noradrenaline as sympathetic cotransmitters: roles for the neurogenic contraction. *Prog Neurobiol* 47: 45-94, 1995.

165. **Sturniolo MT, Dashti SR, Deucher A, Rorke EA, Broome AM, Chandraratna RA, Keepers T, and Eckert RL.** A novel tumor suppressor protein promotes keratinocyte terminal differentiation via activation of type I transglutaminase. *J Biol Chem* 278: 48066-48073, 2003.

166. **Sugimura Y, Hosono M, Kitamura M, Tsuda T, Yamanishi K, Maki M, and Hitomi K.** Identification of preferred substrate sequences for transglutaminase 1--development of a novel peptide that can efficiently detect cross-linking enzyme activity in the skin. *The FEBS journal* 275: 5667-5677, 2008.

167. **Takashi R.** A novel actin label: a fluorescent probe at glutamine-41 and its consequences. *Biochemistry* 27: 938-943, 1988.

168. **Takeda H, Inazu M, and Matsumiya T.** Astroglial dopamine transport is mediated by norepinephrine transporter. *Naunyn-Schmiedeberg's archives of pharmacology* 366: 620-623, 2002.

169. **Tavernier G, Jimenez M, Giacobino JP, Hulo N, Lafontan M, Muzzin P, and Langin D.** Norepinephrine induces lipolysis in beta1/beta2/beta3-adrenoceptor knockout mice. *Molecular pharmacology* 68: 793-799, 2005.

170. **Thakali K, Fink GD, and Watts SW.** Arteries and veins desensitize differently to endothelin. *J Cardiovasc Pharmacol* 43: 387-393, 2004.

171. **Thomas H, Beck K, Adamczyk M, Aeschlimann P, Langley M, Oita RC, Thiebach L, Hils M, and Aeschlimann D.** Transglutaminase 6: a protein associated with central nervous system development and motor function. *Amino acids*, 2011.

172. **Thomazy V and Fesus L.** Differential expression of tissue transglutaminase in human cells. An immunohistochemical study. *Cell Tissue Res* 255: 215-224, 1989.

173. **Thyberg J, Nilsson J, Palmberg L, and Sjolund M.** Adult human arterial smooth muscle cells in primary culture. Modulation from contractile to synthetic phenotype. *Cell Tissue Res* 239: 69-74, 1985.

174. **Tseng HC, Lin HJ, Tang JB, Gandhi PS, Chang WC, and Chen YH.** Identification of the major TG4 cross-linking sites in the androgen-dependent SVS I exclusively expressed in mouse seminal vesicle. *J Cell Biochem* 107: 899-907, 2009.

175. **Tsuji M, Matsuoka Y, and Nakajima T.** Studies on formation of gamma-glutamylamines in rat brain and their synthetic and catabolic enzymes. *J Neurochem* 29: 633-638, 1977.

176. **Ueki S, Takagi J, and Saito Y.** Dual functions of transglutaminase in novel cell adhesion. *Journal of cell science* 109 (Pt 11): 2727-2735, 1996.

177. **Uemura N, Nakanishi Y, Kato H, Saito S, Nagino M, Hirohashi S, and Kondo T.** Transglutaminase 3 as a prognostic biomarker in esophageal cancer revealed by proteomics. *International journal of cancer Journal international du cancer* 124: 2106-2115, 2009.

178. **van de Wal Y, Kooy Y, van Veelen P, Pena S, Mearin L, Papadopoulos G, and Koning F.** Selective deamidation by tissue transglutaminase strongly enhances gliadin-specific T cell reactivity. *Journal of immunology (Baltimore, Md : 1950)* 161: 1585-1588, 1998.

179. **van den Akker J, VanBavel E, van Geel R, Matlung HL, Guvenc Tuna B, Janssen GM, van Veelen PA, Boelens WC, De Mey JG, and Bakker EN.** The redox state of transglutaminase 2 controls arterial remodeling. *PloS one* 6: e23067, 2011.

180. **Vanhoutte D, Schellings MW, Gotte M, Swinnen M, Herias V, Wild MK, Vestweber D, Chorianopoulos E, Cortes V, Rigotti A, Stepp MA, Van de Werf F, Carmeliet P, Pinto YM, and Heymans S.** Increased expression of syndecan-1 protects against cardiac dilatation and dysfunction after myocardial infarction. *Circulation* 115: 475-482, 2007.

181. **Vowinckel J, Stahlberg S, Paulmann N, Bluemlein K, Grohmann M, Ralser M, and Walther DJ.** Histaminylation of glutamine residues is a novel posttranslational modification implicated in G-protein signaling. *FEBS Lett*, 2012.

182. **Wajda I, Ginsburg M, and Waelsch H.** Incorporation of histamine into liver protein in vivo. *Nature* 191: 1204-1205, 1961.

183. **Wallace SM, Yasmin, McEniery CM, Maki-Petaja KM, Booth AD, Cockcroft JR, and Wilkinson IB.** Isolated systolic hypertension is characterized by increased aortic stiffness and endothelial dysfunction. *Hypertension* 50: 228-233, 2007.

184. **Walther DJ, Peter JU, Winter S, Holtje M, Paulmann N, Grohmann M, Vowinckel J, Alamo-Bethencourt V, Wilhelm CS, Ahnert-Hilger G, and Bader M.** Serotonylation of small GTPases is a signal transduction pathway that triggers platelet alpha-granule release. *Cell* 115: 851-862, 2003.

185. **Walther DJ, Stahlberg S, and Vowinckel J.** Novel roles for biogenic monoamines: from monoamines in transglutaminase-mediated post-translational protein modification to monoaminylation deregulation diseases. *The FEBS journal* 278: 4740-4755, 2011.

186. **Wang JL, Yang X, Xia K, Hu ZM, Weng L, Jin X, Jiang H, Zhang P, Shen L, Guo JF, Li N, Li YR, Lei LF, Zhou J, Du J, Zhou YF, Pan Q, Wang J, Wang J, Li RQ, and Tang BS.** TGM6 identified as a novel causative gene of spinocerebellar ataxias using exome sequencing. *Brain : a journal of neurology* 133: 3510-3518, 2010.

187. **Watson PA, Nesterova A, Burant CF, Klemm DJ, and Reusch JE.** Diabetes-related changes in cAMP response element-binding protein content enhance smooth muscle cell proliferation and migration. *The Journal of biological chemistry* 276: 46142-46150, 2001.

188. **Watts SW, Priestley JR, and Thompson JM.** Serotonylation of vascular proteins important to contraction. *PloS one* 4: e5682, 2009.

189. **Watts SW, Priestley JRC, and Thompson JM.** Serotonylation of vascular proteins important to contraction. *PLoS One* 4, 2009.

190. **Wei L, Warburton RR, Preston IR, Roberts KE, Comhair SA, Erzurum SC, Hill NS, and Fanburg BL.** Serotonylated fibronectin is elevated in pulmonary hypertension. *American journal of physiology Lung cellular and molecular physiology* 302: L1273-1279, 2012.

191. **Xin X, Yang N, Eckhart AD, and Faber JE.** Alpha1D-adrenergic receptors and mitogen-activated protein kinase mediate increased protein synthesis by arterial smooth muscle. *Molecular pharmacology* 51: 764-775, 1997.

192. **Yi SJ, Choi HJ, Yoo JO, Yuk JS, Jung HI, Lee SH, Han JA, Kim YM, and Ha KS.** Arachidonic acid activates tissue transglutaminase and stress fiber formation via intracellular reactive oxygen species. *Biochemical and biophysical research communications* 325: 819-826, 2004.

193. **Yin H, Li Q, Qian G, Wang Y, Li Y, Wu G, and Wang G.** Rab1 GTPase regulates phenotypic modulation of pulmonary artery smooth muscle cells by mediating the transport of angiotensin II type 1 receptor under hypoxia. *The international journal of biochemistry & cell biology* 43: 401-408, 2011.

194. **Yin H, Veer EV, Frontini MJ, Thibert V, O'Neil C, Watson A, Szasz P, Chu MW, and Pickering JG.** Intrinsic directionality of migrating vascular smooth muscle cells is regulated by NAD+ biosynthesis. *Journal of cell science*, 2012.

195. **Zhang H and Faber JE.** Trophic Effect of Norepinephrine on Arterial Intima-Media and Adventitia Is Augmented by Injury and Mediated by Different 1-Adrenoceptor Subtypes. *Circulation Research* 89: 815-822, 2001.

196. **Zhang H and Faber JE.** Trophic effect of norepinephrine on arterial intima-media and adventitia is augmented by injury and mediated by different alpha1-adrenoceptor subtypes. *Circ Res* 89: 815-822, 2001.

197. **Zhang H, Facemire CS, Banes AJ, and Faber JE.** Different alpha-adrenoceptors mediate migration of vascular smooth muscle cells and adventitial fibroblasts in vitro. *Am J Physiol Heart Circ Physiol* 282: H2364-2370, 2002.

198. **Zhang J, Lesort M, Guttmann RP, and Johnson GV.** Modulation of the in situ activity of tissue transglutaminase by calcium and GTP. *The Journal of biological chemistry* 273: 2288-2295, 1998.

199. **Zwart R, Verhaagh S, Buitelaar M, Popp-Snijders C, and Barlow DP.** Impaired activity of the extraneuronal monoamine transporter system known as uptake-2 in Orct3/Slc22a3-deficient mice. *Molecular and cellular biology* 21: 4188-4196, 2001.